Electronic Supplementary Material (ESI) for Dalton Transactions.

Supporting Information

Synthesis and Catalytic Activity of Single-Site Group V Alkoxide Complexes for the Ring-Opening Polymerization of ε-Caprolactone

Frank Peprah, Grace E. Tarantola, Alyson S. Plaman, Emily L. Vu, Alyssa B. Huynh, and Christopher B. Durr*

Department of Chemistry, Amherst College, 25 East Drive, Amherst, Massachusetts 01002, United States of America

Contents

Experimental Details

Some general experimental and analytical procedures in our lab have been reported previously.[1,2]

All manipulations of air-sensitive compounds and polymerizations were conducted in a nitrogen-filled MBraun glovebox. Glassware involved in air-sensitive manipulations was dried overnight in a 210 °C oven. Reagents were purchased from commercial sources (Sigma-Aldrich, STREM, Alfa-Aesar) and used as received without further purification. Anhydrous solvents were purchased from Thermo Fisher Scientific and Beantown Chemical and used as received. Deuterated chloroform ($CDCl_3$) was purchased from Beantown Chemical and dried over 4 Å activated molecular sieves, degassed under high-vacuum and stored in the glovebox. ε-Caprolactone was purchased from TCI America, degassed under high-vacuum, dried over 4 Å activated molecular sieves, and stored under nitrogen. CHN Elemental Analysis was conducted by Robertson Microlit Analytical Testing Lab. In some cases, despite multiple attempts, the carbon percentage diverges from the theoretical value, likely due to incomplete combustion or decomposition during shipping due to the highly air sensitive nature of the samples. Regardless, we report these data here as a measure of the best values found to date. NMR was performed with a Bruker Ascend 400 spectrometer.

GPC analysis was conducted on an Agilent PL 1260 Infinity II system and calibrated using narrow poly(styrene) standards. Samples for analysis were prepared by dissolving the polymer in 2 mL of HPCL grade THF overnight before filtering through 0.45 µm nylon filters. Separation was performed at 35 °C with a flow rate of 1 mL/minute in HPLC grade THF through two PLgel 5 µm Mixed-C 300 × 7.5 mm columns connected to a PLGel 50 × 7.5 mm guard column and the sample was detected by a refractive index detector. Data analysis was performed with Agilent OpenLAB Data Analysis Software. The resulting M_n was corrected by a factor of 0.56.[3]

Single Crystal X-ray Diffraction

Single crystals were grown either from a concentrated solution of THF or the slow diffusion of pentane into THF. In a typical experiment, crystals suitable for X-ray diffraction were isolated in a glovebox, submerged in fluorinated oil (Fomblin Y) and mounted on a MiTeGen MircoMount. The sample was then centered and cooled with an Oxford Cryosystem Cryostream 800 within a stream of dry nitrogen. Data was collected with a Rigaku Synergy Diffractometer (Cu Kα radiation) equipped with a HyPix3000 detector. Raw data was processed using CrysAlisPro[4]. Structural solutions were found using SHELXT[5] and structural refinement was conducted with SHELXL,[6] within the OLEX2 graphical user interface.[7]

The data associated with this work was deposited with the Cambridge Structural Database (Deposition Numbers: 2331117 – 2331124) and can be obtained free of charge at: www.ccdc.cam.ac.uk/structures.

To complement the reported tabulated values, full NMR spectral analysis (^{1}H, $^{13}C\{^{1}H\}$, COSY, HSQC and HMBC) for each compound can be found below.

Ligand Synthesis

Ligand synthesis was adapted from the literature.[8]

H_2L1 – Methylphenol ketoimine

2-amino-4-methylphenol (1.80 g, 14.6 mmol) was dissolved in ethanol (15 mL) in a 100 mL round bottom flask. Acetylacetone (1.46 g, 14.6 mmol) was then diluted with ethanol (15 mL) and added to the reaction flask. The reaction was heated at 80°C for 6 hours and cooled to room temperature before being placed in a –15 °C freezer overnight. The resulting crystals were then filtered and dried under vacuum. Yield (2.21 g, 10.7 mmol, 73%)

^{1}H NMR (400 MHz, $CDCl_3$) δ 12.03 (s, 1 -OH), 8.56 (s, 1 -NH), 6.98 – 6.96 (dd, J = 8 Hz, 2 Hz, $1H_e$), 6.90 – 6.88 (d, J = 8 Hz, $1H_f$), 6.81 (d, J = 2 Hz, $1H_g$) 5.13 (s, $1H_a$), 2.24 (s, $3H_b$), 2.05 (s, $3H_c$), 1.83 (s, $3H_d$)

H_2L2 – Chlorophenol ketoimine

2-amino-4-chlorophenol (2.00 g, 13.93 mmol) was dissolved in ethanol (15 mL) in a 100 mL round bottom flask. Acetylacetone (1.395 g, 13.93 mmol) was then diluted with ethanol (15 mL) and added to the reaction flask. The reaction was heated at 80°C for 6 hours and cooled to room temperature before being placed in a –15 °C freezer overnight. The resulting crystals were then filtered and dried under vacuum. Yield (1.99 g, 7.79 mmol, 56%)

^{1}H NMR (400 MHz, $CDCl_3$) δ 11.73 (s, 1 -OH), 9.44 (s, 1 – NH), 7.26, 7.13 - 7.11 (dd, J = 8 Hz, 2 Hz, $1H_d$), 7.03 - 7.02 (d, J= 2 Hz, $1H_f$), 6.95 - 6.93 (d, J = 8 Hz, $1H_e$), 5.17 (s, $1H_a$), 2.06 (s, $3H_b$), 1.88 (s, $3H_c$).

General Intermediate Synthesis

The desired metal alkoxide ($Nb(OEt)_5$ or $Ta(OEt)_5$) (0.705 g – 3.26 g, 2.215 mmol – 8.03 mmol) and ligand (**H_2L1** or **H_2L2**) (0.500 g – 1.65 g, 2.215 mmol – 8.03 mmol) were weighed separately into vials and dissolved in either THF or toluene. The ligand solution was added to the metal and the reaction was stirred overnight turning from yellow to orange in color. The solvent was removed under vacuum and the resulting solid was suspended in pentane. Pentane was likewise removed under vacuum to afford the product as a powder.

I-1. $Nb(OEt)_5$ (1.20 g, 3.77 mmol), **H_2L1** (0.774 g, 3.77 mmol). Yield (1.451 g, 3.36 mmol, 89%).

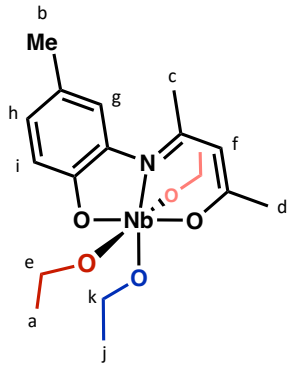

^{1}H NMR Labeling

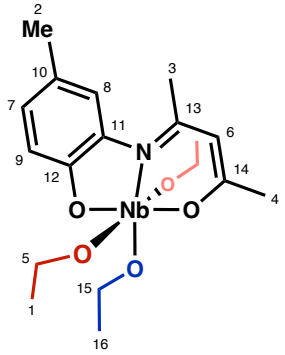

^{13}C NMR Labeling

^{1}H NMR (400 MHz, $CDCl_3$) δ 6.75 (m, $2H_{i,g}$), 6.56 (dd = broad, $1H_h$), 5.14 (s, $1H_f$), 4.39 (bs, $6H_{e,k}$), 2.34 (s, $3H_d$), 2.24 (s, $3H_b$), 1.99 (s, $3H_c$) , 1.11 (bs, $9H_{a,j}$). ^{13}C NMR (101 MHz, $CDCl_3$) δ 172.81(C_{14}), 166.31(C_{13}), 157.17(C_{12}), 138.26(C_{11}), 127.64(C_{10}), 127.18(C_9), 122.30(C_8), 115.17(C_7), 105.42(C_6), 72.11(C_{15}), 68.30(C_5), 24.21(C_4), 23.93(C_3), 21.06(C_2), 18.25($C_{1,16}$). Elemental Analysis: $C_{18}H_{28}NNbO_5$ (431.33 g/mol) Calculated: C, 50.12; H, 6.54; N, 3.25; Found: C, 49.14; H, 6.29; N, 3.25.

I-2. $Ta(OEt)_5$ (3.26 g, 8.03 mmol), **H_2L1** (1.65 g, 8.03 mmol). Yield (3.810 g, 7.336 mmol, 91%).

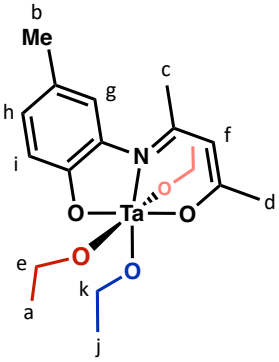

^{1}H NMR Labeling

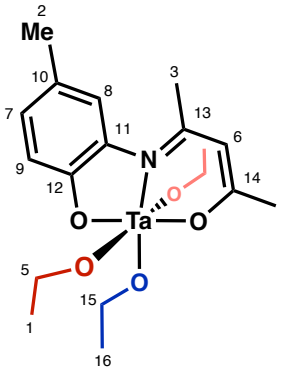

^{13}C NMR Labeling

^{1}H NMR (400 MHz, $CDCl_3$) δ 6.80 (m, $2H_{i,g}$), 6.61 (dd = broad, $1H_h$), 5.17 (s, $1H_f$), 4.43 (bs, $6H_{e,k}$), 2.35 (s, $3H_d$), 2.25 (s, $3H_b$), 2.00 (s, $3H_c$) , 1.16 (bs, $9H_{a,j}$). ^{13}C NMR (101 MHz, $CDCl_3$) δ 172.93(C_{14}), 167.50(C_{13}), 156.29(C_{12}), 138.20(C_{11}), 127.67(C_{10}), 127.57(C_9), 122.60(C_8), 116.44(C_7), 106.48(C_6), 70.13(C_{15}), 66.65(C_5), 24.28(C_4), 24.05(C_3), 21.03(C_2), 18.63($C_{1,16}$). Elemental Analysis: $C_{18}H_{28}NO_5Ta$ (519.37 g/mol) Calculated: C, 41.63; H, 5.43; N, 2.70; Found: C, 41.22; H, 5.36; N 2.70

I-3. $Nb(OEt)_5$ (0.705 g, 2.22 mmol), **H_2L2** (0.50 g, 2.22 mmol). Yield (0.995 g, 2.20 mmol, 99%)

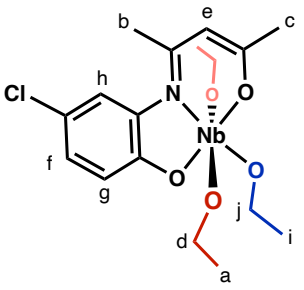

^{1}H NMR Labeling

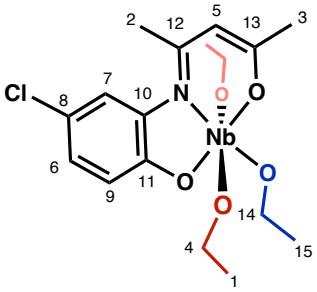

^{13}C NMR Labeling

^{1}H NMR (400 MHz, $CDCl_3$) δ 6.91 (m, $2H_{h,g}$), 6.61 (dd = broad, $1H_f$), 5.18 (s, $1H_e$), 4.39 (bs, $6H_{d,j}$), 2.34 (s, $3H_c$), 2.01 (s, $3H_b$) , 1.18 (bs, $9H_{a,i}$). ^{13}C NMR (101 MHz, $CDCl_3$) δ 174.12(C_{13}), 167.30(C_{12}), 158.19(C_{11}), 139.22(C_{10}), 126.23(C_9), 122.81(C_8), 121.48(C_7), 116.34(C_6), 105.60(C_5), 72.47(C_{14}), 68.45(C_4), 24.09(C_3), 24.05(C_2), 18.21($C_{1,15}$). Elemental Analysis: $C_{17}H_{25}ClNNbO_5$ (451.75 g/mol) Calculated: C, 45.20; H, 5.58; N, 3.10; Found: C, 41.57; H, 4.87; N, 3.09

I-4. $Ta(OEt)_5$ (0.900 g, 2.215 mmol), **H_2L2** (0.500 g, 2.215 mmol). Yield (0.833 g, 1.54 mmol, 70%)

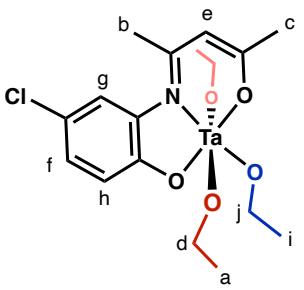

^{1}H NMR Labeling

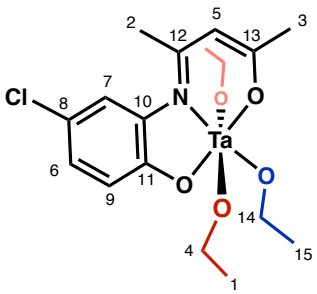

^{13}C NMR Labeling

^{1}H NMR (400 MHz, $CDCl_3$) δ 6.89 (m, $2H_{h,g}$), 6.57 (dd = broad, $1H_f$), 5.14 (s, $1H_e$), 4.40 (bs, $6H_{d,j}$), 2.28 (s, $3H_c$), 1.95 (s, $3H_b$) , 1.17 (bs, $9H_{a,i}$). ^{13}C NMR (101 MHz, $CDCl_3$) δ 174.26(C_{13}), 168.50(C_{12}), 157.37(C_{11}), 139.21(C_{10}), 126.61(C_9), 122.92(C_8), 121.83(C_7), 117.58(C_6), 106.65(C_5), 70.36(C_{14}), 66.81(C_4), 24.19($C_{2,3}$), 18.60($C_{1,15}$). Elemental Analysis: $C_{17}H_{25}ClNO_5Ta$ (539.79 g/mol) Calculated: C, 37.83; H, 4.67; N, 2.59; Found: C, 36.68; H, 4.42, N, 2.47.

General Catechol Derivative Synthesis

The desired intermediate (**I-1** – **I-4**) (0.100 g – 0.290 g, 0.231 mmol – 0.558 mmol) and catechol (0.02619 g – 0.084 g, 0.238 mmol – 0.600 mmol) were weighed separately into vials and dissolved in either THF or toluene. The catechol solution was added to the intermediate and the reaction was stirred overnight turning from orange to red in color. The solvent was removed under vacuum and the resulting solid was suspended in pentane. Pentane was likewise removed under vacuum to afford the product as a powder.

C-1. I-1 (0.1026 g, 0.238 mmol), catechol (0.02619 g, 0.238 mmol). Yield (0.086 g, 0.191 mmol, 80%)

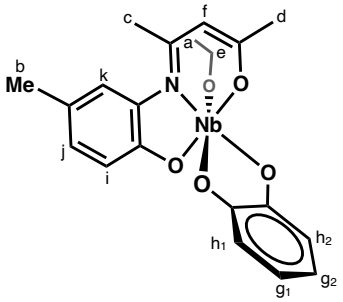

^{1}H NMR Labeling

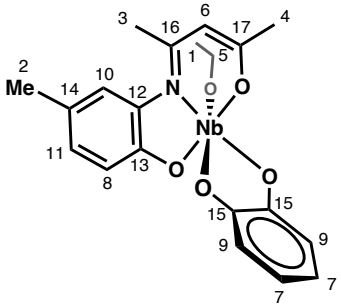

^{13}C NMR Labeling

^{1}H NMR (400 MHz, $CDCl_3$) δ 7.10 (d, J = 2 Hz, 1H_k), 7.01 (dd, J = 8 Hz, 2 Hz, 1H_j), 6.91 (d, J = 8 Hz, 1H_i), 6.60 (m, 2$H_{h1,2}$), 6.42 (m, 2$H_{g1,2}$), 5.95 (s, 1H_f), 4.84 (dq, J = 7 Hz, 2 Hz, 2H_e), 2.53 (s, 3H_d), 2.34 (s, 3H_b), 2.26 (s, 3H_c), 1.45 (t, J = 7 Hz, 3H_a). ^{13}C NMR (101 MHz, $CDCl_3$) δ 173.78(C_{17}), 168.12(C_{16}), 157.55(C_{15}), 155.26(C_{14}), 138.12(C_{13}), 129.59(C_{12}), 127.71(C_{11}), 122.17(C_{10}), 120.09(C_9), 115.54(C_8), 112.37(C_7), 111.23(C_6), 73.48(C_5), 25.37(C_4), 24.18(C_3), 21.37(C_2), 17.64(C_1). Elemental Analysis: $C_{20}H_{22}NNbO_5$ (449.30 g/mol) Calculated: C, 53.46; H, 4.94; N, 3.12; Found: C, 53.03; H, 4.87; N, 3.09

C-2. I-2 (0.290 g, 0.558 mmol), catechol (0.061 g, 0.558 mmol). Yield (0.255 g, 0.475 mmol, 85%)

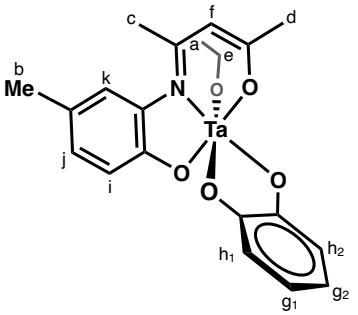

^{1}H NMR Labeling

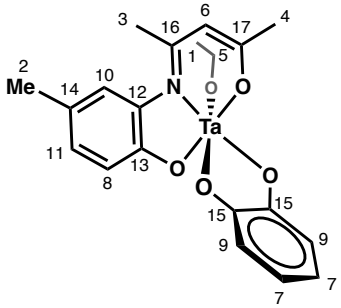

^{13}C NMR Labeling

^{1}H NMR (400 MHz, $CDCl_3$) δ 7.03 (d, J = 2 Hz, 1H_k), 6.99 (dd, J = 8 Hz, 2 Hz, 1H_j), 6.84 (d, J = 8 Hz, 1H_i), 6.63 (m, 2$H_{h1,2}$), 6.50 (m, 2$H_{g1,2}$), 5.83 (s, 1H_f), 4.86 (dq, J = 7 Hz, 1 Hz, 2H_e), 2.50 (s, 3H_d), 2.33 (s, 3H_b), 2.20 (s, 3H_c), 1.43 (t, J = 7, 3H_a). ^{13}C NMR (101 MHz, $CDCl_3$) δ 173.74(C_{17}), 170.17(C_{16}), 156.68(C_{15}), 154.14(C_{14}), 137.83(C_{13}), 129.30(C_{12}), 128.12(C_{11}), 122.70(C_{10}), 120.02(C_9), 116.50(C_8), 113.90(C_7), 111.14(C_6), 71.27(C_5), 25.45(C_4), 24.10(C_3), 21.25(C_2), 17.83(C_1). Elemental Analysis: $C_{20}H_{22}NO_5Ta$ (537.35 g/mol) Calculated: C, 44.70; H, 4.13; N, 2.61 Found: C, 43.29; H, 3.67; N, 2.48

C-3. I-3 (0.200 g, 0.443 mmol), catechol (0.0487 g, 0.443 mmol). Yield (0.2058 g, 0.438 mmol, 99%)

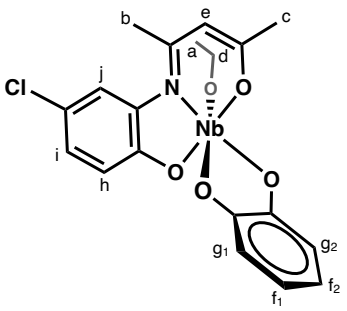

^{1}H NMR Labeling

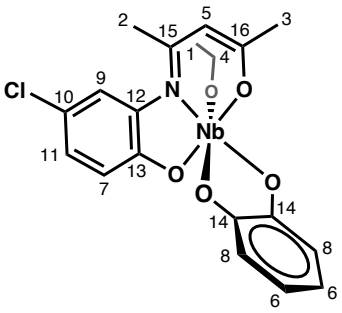

^{13}C NMR Labeling

^{1}H NMR (400 MHz, $CDCl_3$) δ 7.29 (d, J = 2 Hz, $1H_j$), 7.17 (dd, J = 8 Hz, 2 Hz, $1H_i$), 6.95 (d, J = 8 Hz, $1H_h$), 6.63 (m, $2H_{g1,2}$), 6.42 (m, $2H_{f1,2}$), 6.00 (s, $1H_e$), 4.85 (dq, J = 7 Hz, 2 Hz, $2H_d$), 2.53 (s, $3H_c$), 2.28 (s, $3H_b$), 1.48 (t, J = 7 Hz, $3H_a$). ^{13}C NMR (101 MHz, $CDCl_3$) δ 175.06(C_{16}), 169.04(C_{15}), 157.43(C_{14}), 156.18(C_{13}), 138.82(C_{12}), 126.77(C_{11}), 125.01(C_{10}), 121.52(C_9), 120.39(C_8), 116.77(C_7), 112.41(C_6), 111.54(C_5), 73.83(C_4), 25.31(C_3), 24.30(C_2), 17.60(C_1). Elemental Analysis: $C_{19}H_{19}ClNNbO_5$ (469.72 g/mol) Calculated: C, 48.58; H, 4.08; N, 2.98; Found: C, 42.31; H, 3.36; N, 2.67

C-4. I-4 (0.289 g, 0.537 mmol), catechol (0.0591 g, 0.537 mmol).

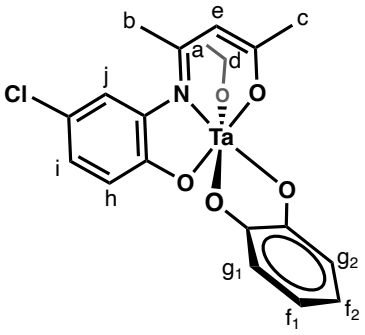

^{1}H NMR Labeling

^{1}H NMR (400 MHz, $CDCl_3$) δ 7.23 (d, J = 2 Hz, $1H_j$), 7.16 (dd, J = 8 Hz, 2 Hz, $1H_i$), 6.89 (d, J = 8 Hz, $1H_h$), 6.64(m, $2H_{g1,2}$), 6.50 (m, $2H_{f1,2}$), 5.88 (s, $1H_e$), 4.86 (q, J = 7 Hz, $2H_d$), 2.51(s, $3H_c$), 2.23 (s, $3H_b$), 1.44 (t, J = 7 Hz, $3H_a$). Yield and further NMR analyses are not reported due to impurities**

C-1tBu. I-1 (0.100 g, 0.231 mmol), 4-*tert*-butylcatechol (0.038 g, 0.231 mmol). Yield (0.114 g, 0.225 mmol, 97%)

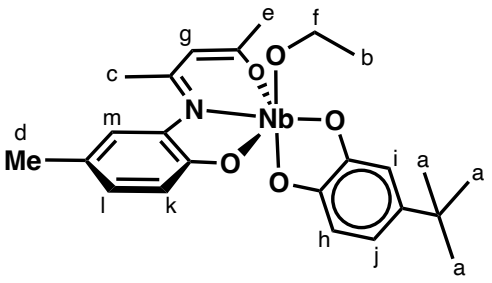

^{1}H NMR Labeling

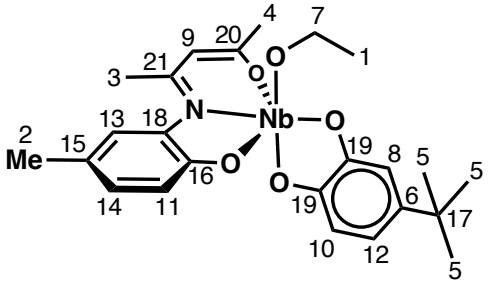

^{13}C NMR Labeling

^{1}H NMR (400 MHz, $CDCl_3$) δ 7.08 (d, J = 2 Hz, 1H_m), 6.98 (dd, J = 8 Hz, 2 Hz, 1H_l), 6.87 (d, J = 8 Hz, 1H_k), 6.64 (dd, J = 8 Hz, 2 Hz, 1H_j), 6.51 (d, J = 2 Hz, 1H_i), 6.35 (d, J = 8 Hz, 1H_h), 5.90 (s, 1H_g), 4.83 (m, 2H_f), 2.53 (s, 3H_e), 2.33 (s, 3H_d), 2.23 (s, 3H_c), 1.45 (t, J = 7 Hz, 3H_b), 1.21 (s, 9H_a). ^{13}C NMR (101 MHz, $CDCl_3$) δ 173.99 (C_{21}), 168.39 (C_{20}), 157.32 (C_{19}), 155.27 (C_{18}), 143.48 (C_{17}), 138.12 (C_{16}), 129.39 (C_{15}), 127.69 (C_{14}), 122.27 (C_{13}), 116.59 (C_{12}), 115.49 (C_{11}), 111.14 (C_{10}), 110.82 (C_9), 110.07 (C_8), 73.25 (C_7), 34.24 (C_6), 31.70 (C_5), 25.40 (C_4), 24.14 (C_3), 21.34 (C_2), 17.60 (C_1). Elemental Analysis: $C_{24}H_{30}NNbO_5$ (505.41 g/mol) Calculated: C, 57.04; H, 5.98; N, 2.77 Found: C, 57.01; H, 6.03; N, 2.57.

C-3OMe. I-3 (0.271 g, 0.600 mmol), 3-methoxycatechol (0.084 g, 0.600 mmol). Yield (0.260 g, 0.520 mmol, 87%)

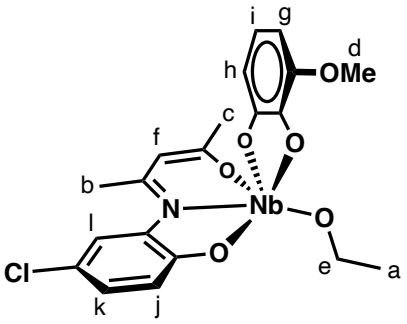

^{1}H NMR Labeling

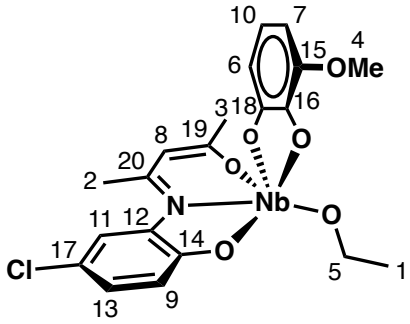

^{13}C NMR Labeling

^{1}H NMR (400 MHz, $CDCl_3$) δ 7.29 (dd, J = 2 Hz, 1H_l), 7.17 (dd, J = 8 Hz, 2 Hz, 1H_k), 6.95 (d, J = 8 Hz, 1H_j), 6.60 (t, J = 7 Hz, 1H_i), 6.34 (dd, J = 8 Hz, 2 Hz, 1H_h), 6.17 (dd, J = 8 Hz, 2 Hz, 1H_g), 5.99 (s, 1H_f), 4.88 (dq, J = 7 Hz, 2 Hz, 2H_e), 3.71 (s, 3H_d), 2.55 (s, 3H_c), 2.29 (s, 3H_b), 1.49 (t, J = 7 Hz, 3H_a). ^{13}C NMR (101 MHz, $CDCl_3$) δ 175.09 (C_{20}), 169.11 (C_{19}), 158.54 (C_{18}), 156.28 (C_{17}), 145.93 (C_{16}), 144.94 (C_{15}), 138.85 (C_{14}), 129.05 (C_{13}), 128.23 (C_{12}), 126.72 (C_{11}), 124.88 (C_{10}), 121.50 (C_9), 120.00 (C_8), 116.73 (C_9), 111.33 (C_8), 106.56 (C_7), 106.38 (C_6), 73.83 (C_5), 56.68 (C_4), 25.25 (C_3), 24.24 (C_2), 17.60 (C_1). Elemental Analysis: $C_{20}H_{21}ClNNbO_5$ (499.75 g/mol) Calculated: C, 48.07; H, 4.24; N, 2.80 Found: C, 46.01; H, 3.79; N, 2.60

Kinetic Studies

The desired amount of catalyst (0.0393 g – 0.0471 g, 0.08761 mmol) and ε-caprolactone (1.00 g, 8.761 mmol) were weighed into an oven-dried glass vial with a stir bar. The vial was then capped and added to an aluminum block preheated to 140 °C on a Heidolph Hei-Tec Hotplate and controlled by a PT1000 Temperature Sensor. Aliquots were removed at appropriate time intervals and dissolved in wet $CDCl_3$ for conversion analysis. After analysis these NMR samples were dried and subsequently redissolved in HPLC grade THF for subsequent GPC experiments.

Polymer Purification

Crude polymer was dissolved in a minimum of dichloromethane and precipitated from petroleum ether to afford the pure polymer as a pale orange solid. The polymer was isolated *via* vacuum filtration and dried before NMR analysis in $CDCl_3$.

NMR Spectra

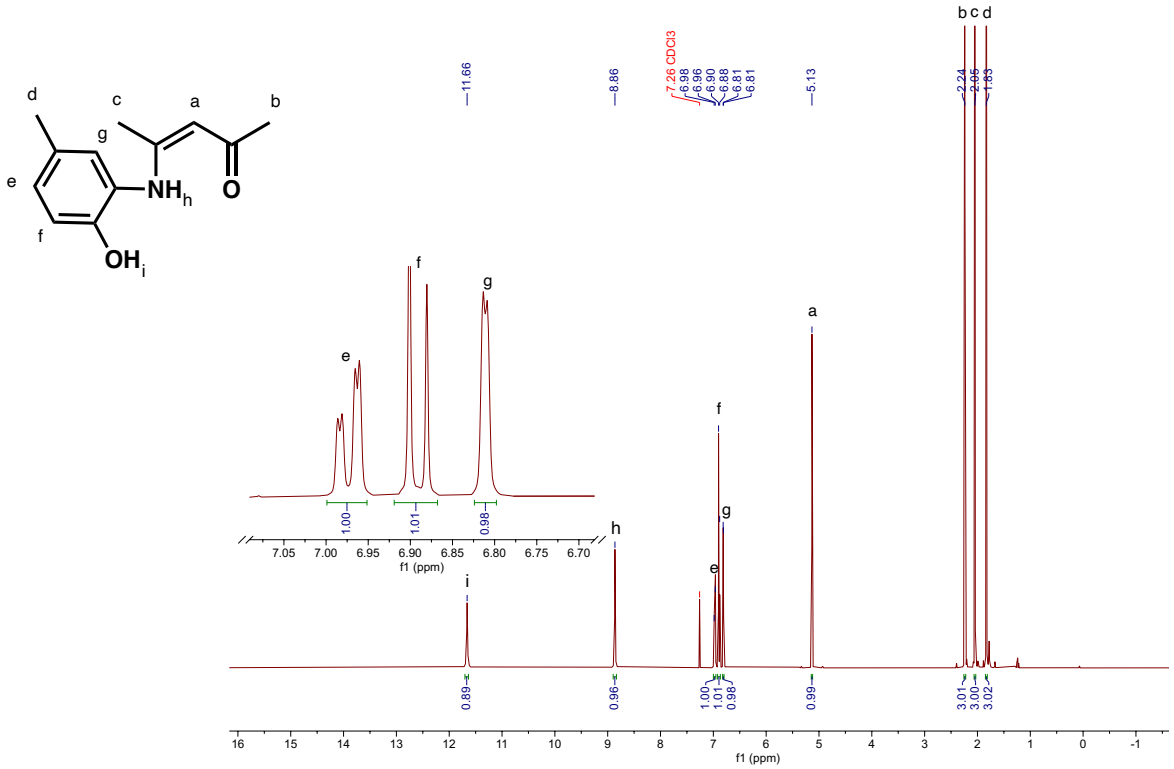

Figure S1. ^{1}H NMR (400 MHz, 293 K) spectrum of **H_2L1** in $CDCl_3$.

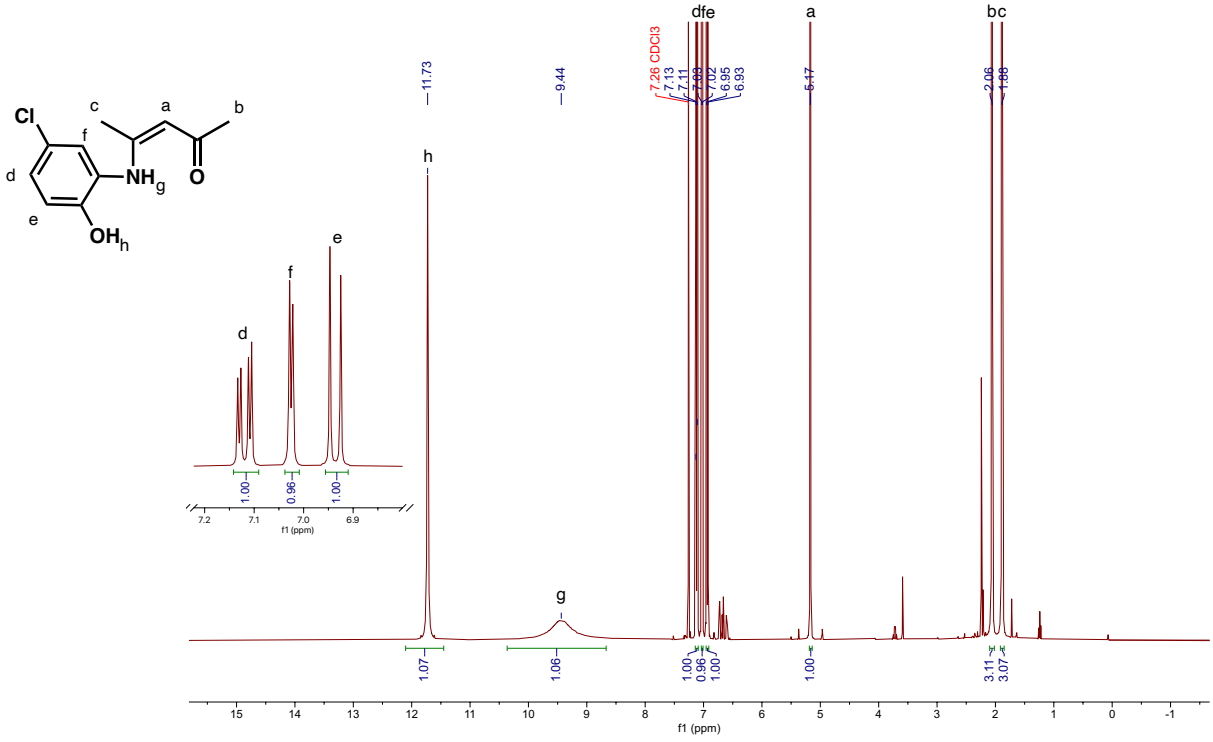

Figure S2. ^{1}H NMR (400 MHz, 293 K) spectrum of **H_2L2** in $CDCl_3$.

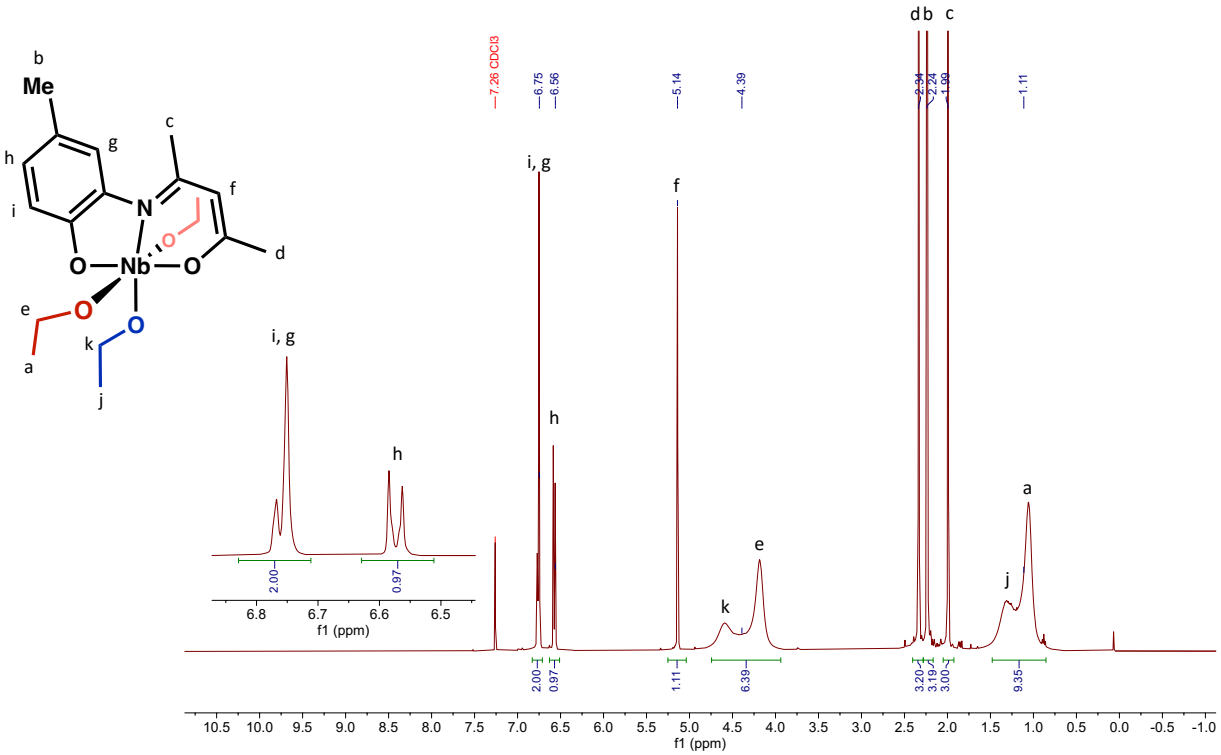

Figure S3. ^{1}H NMR (400 MHz, 293 K) spectrum of **I-1** in $CDCl_3$.

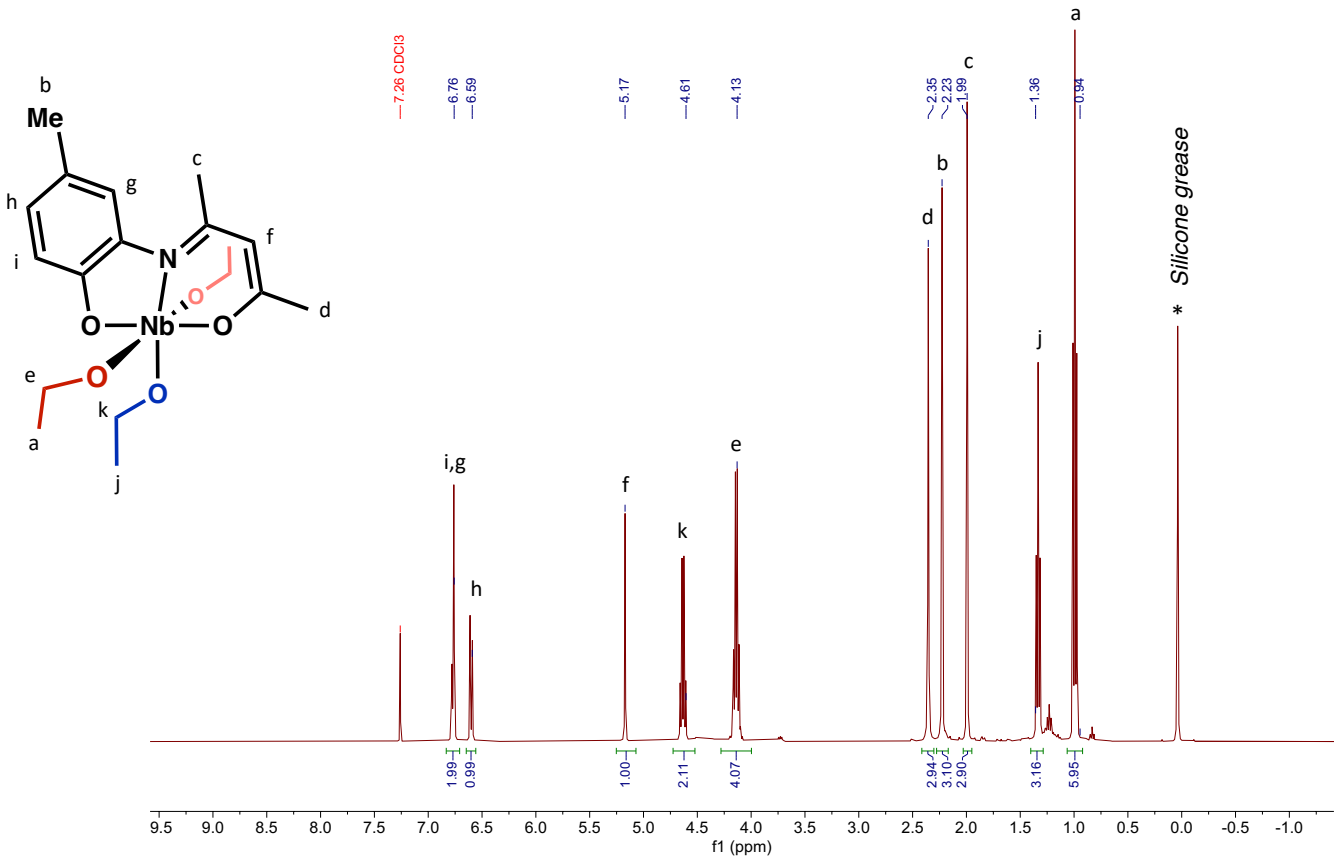

Figure S4. Low temperature ^{1}H NMR (400 MHz, 273 K) spectrum of **I-1** in $CDCl_3$.

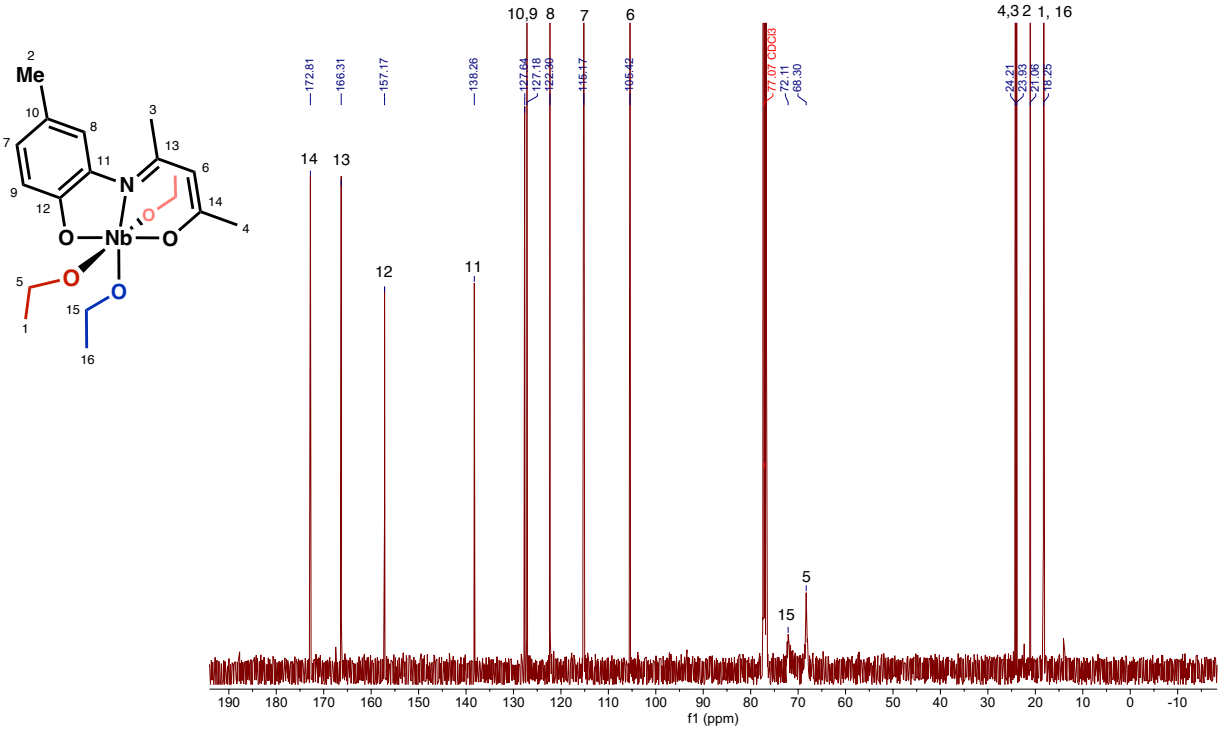

Figure S5. $^{13}C\{^{1}H\}$ NMR (101 MHz, 293 K) spectrum of **I-1** in $CDCl_3$.

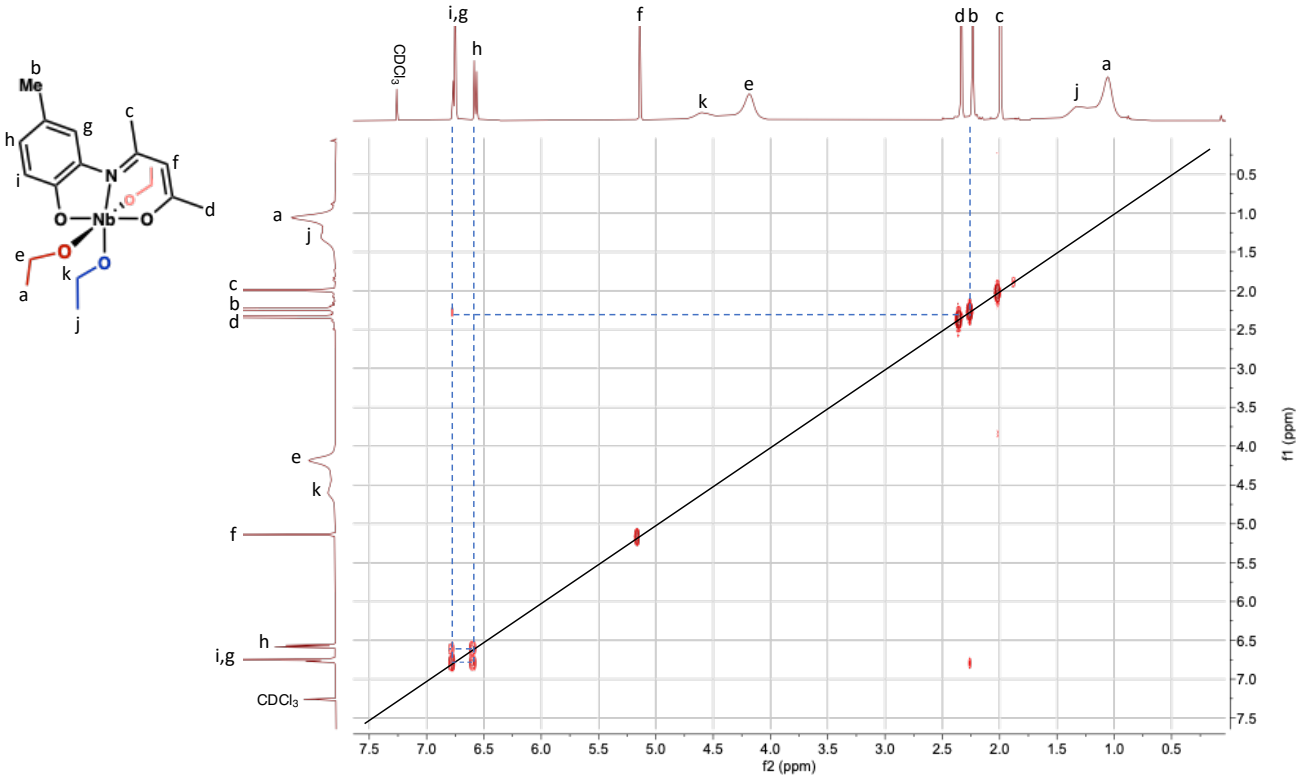

Figure S6. COSY NMR (293 K) spectrum of **I-1** in $CDCl_3$.

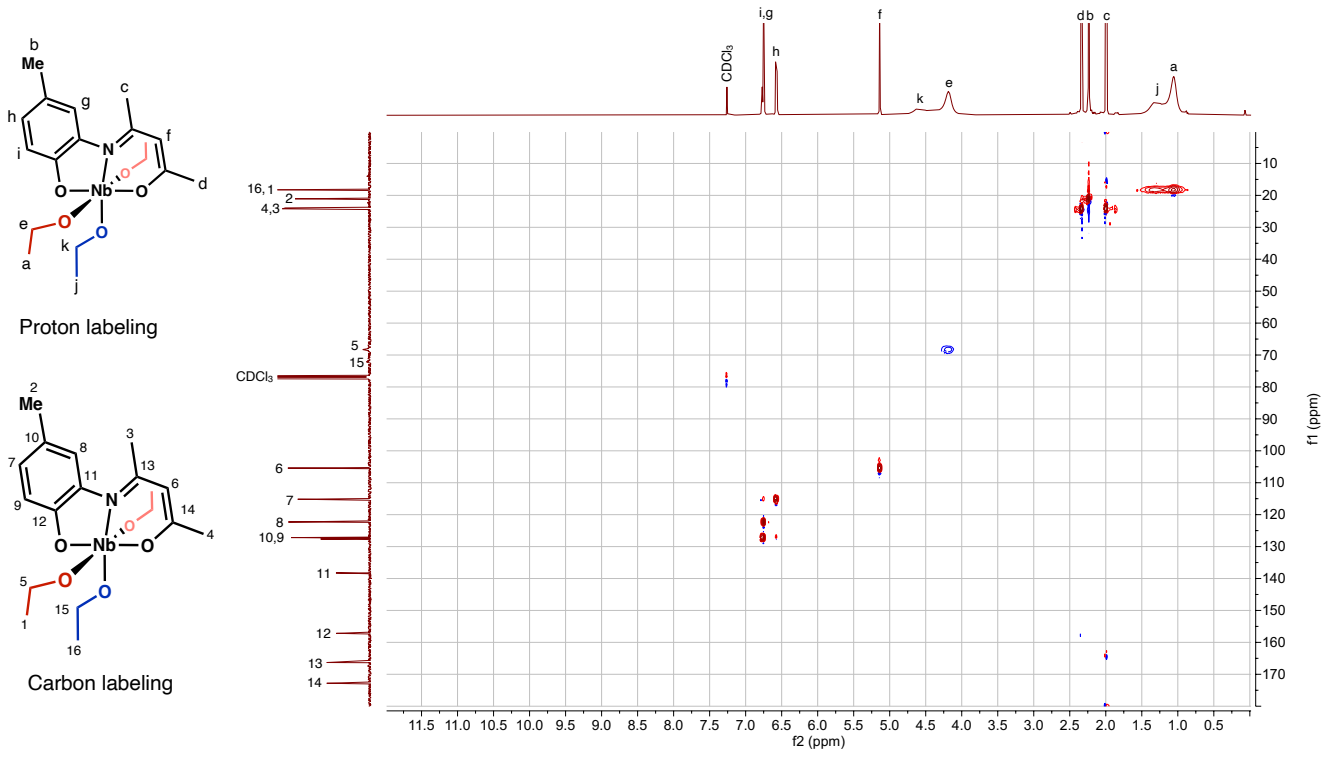

Figure S7. HSQC NMR (293 K) spectrum of **I-1** in $CDCl_3$.

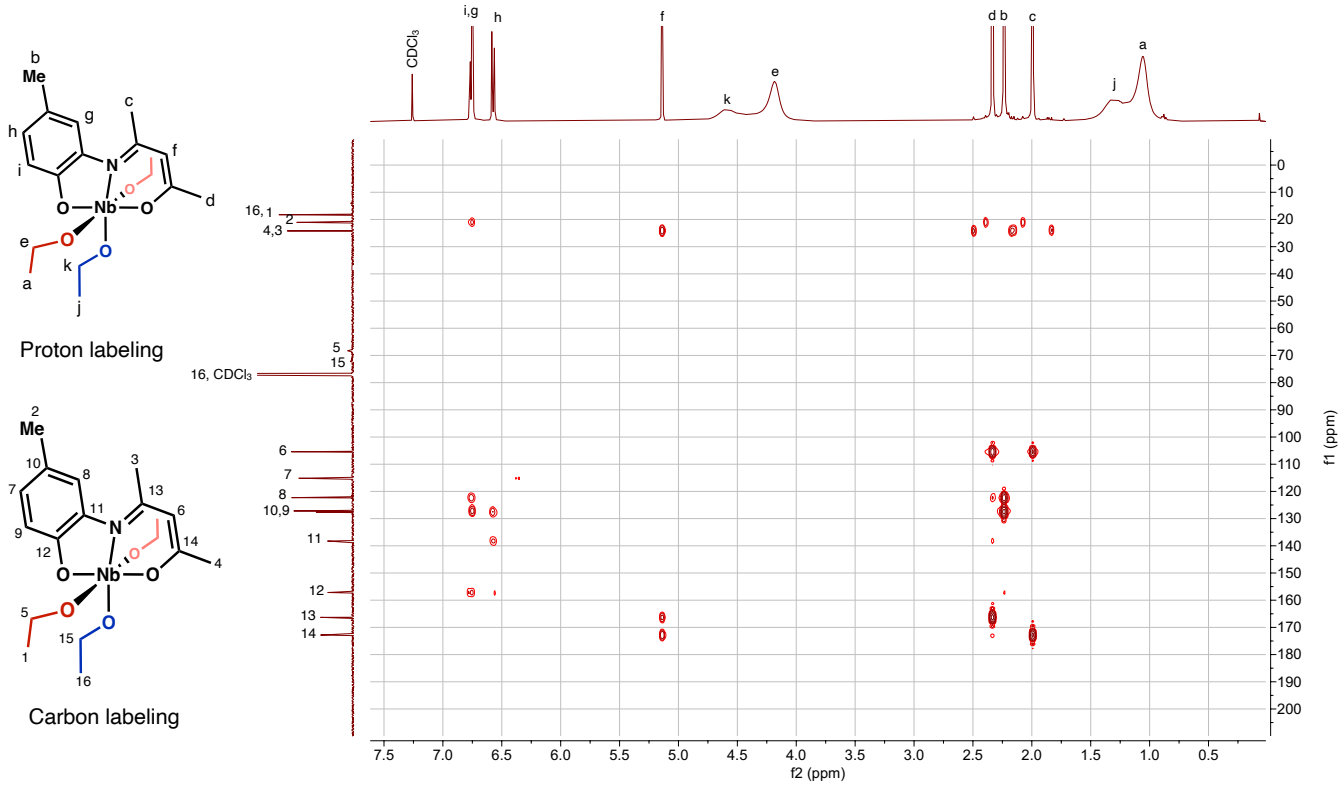

Figure S8. HMBC NMR (293 K) spectrum of **I-1** in $CDCl_3$.

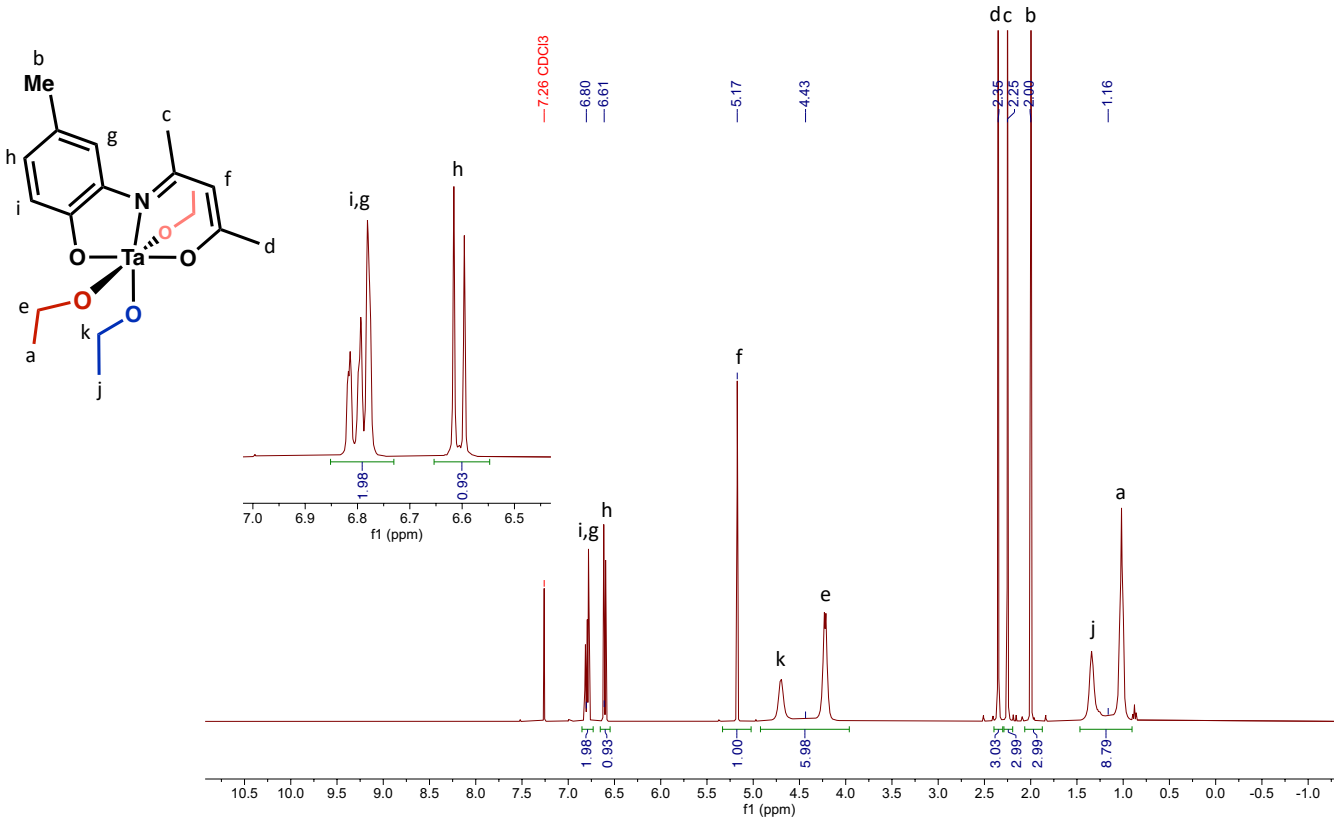

Figure S9. ^{1}H NMR (400 MHz, 293 K) spectrum of **I-2** in $CDCl_3$.

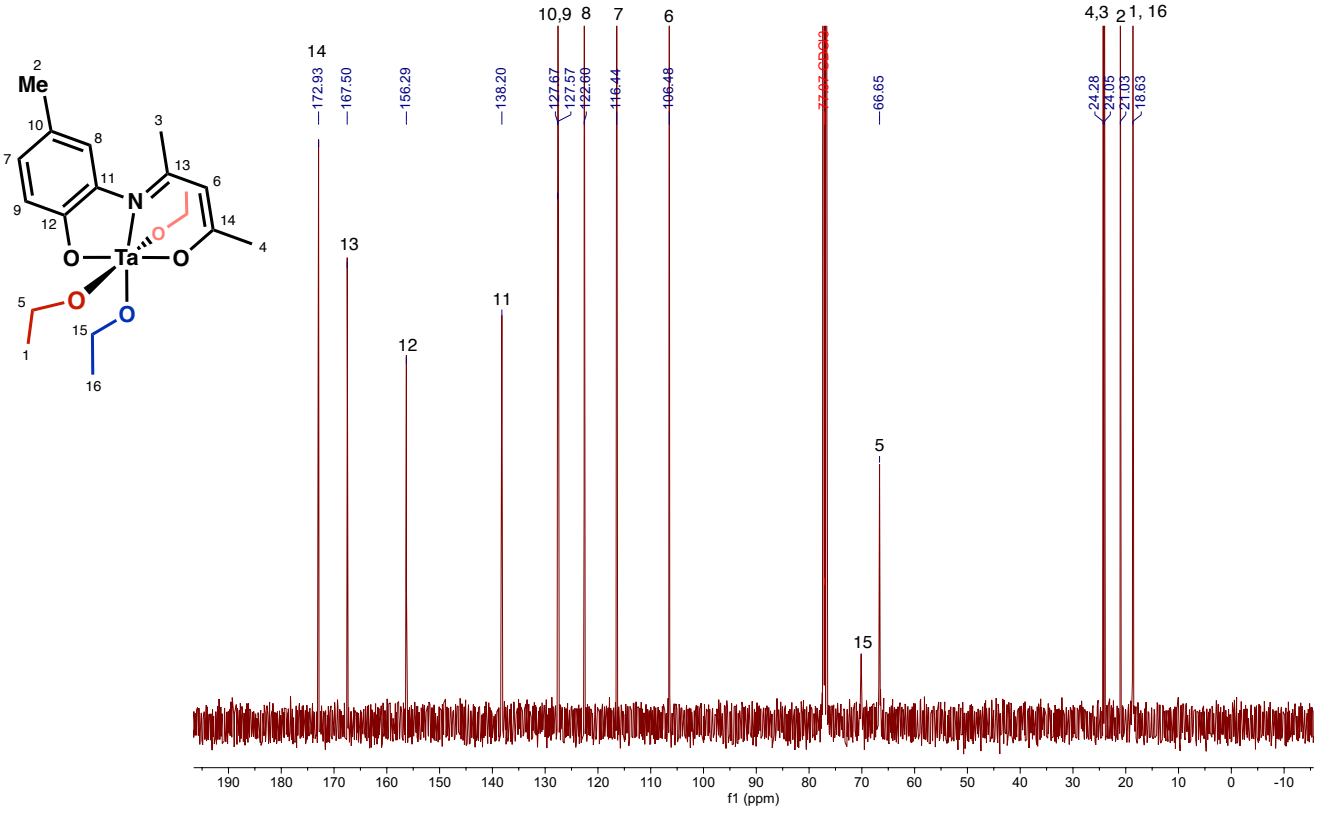

Figure S10. ^{13}C{^{1}H} NMR (101 MHz, 293 K) spectrum of **I-2** in $CDCl_3$.

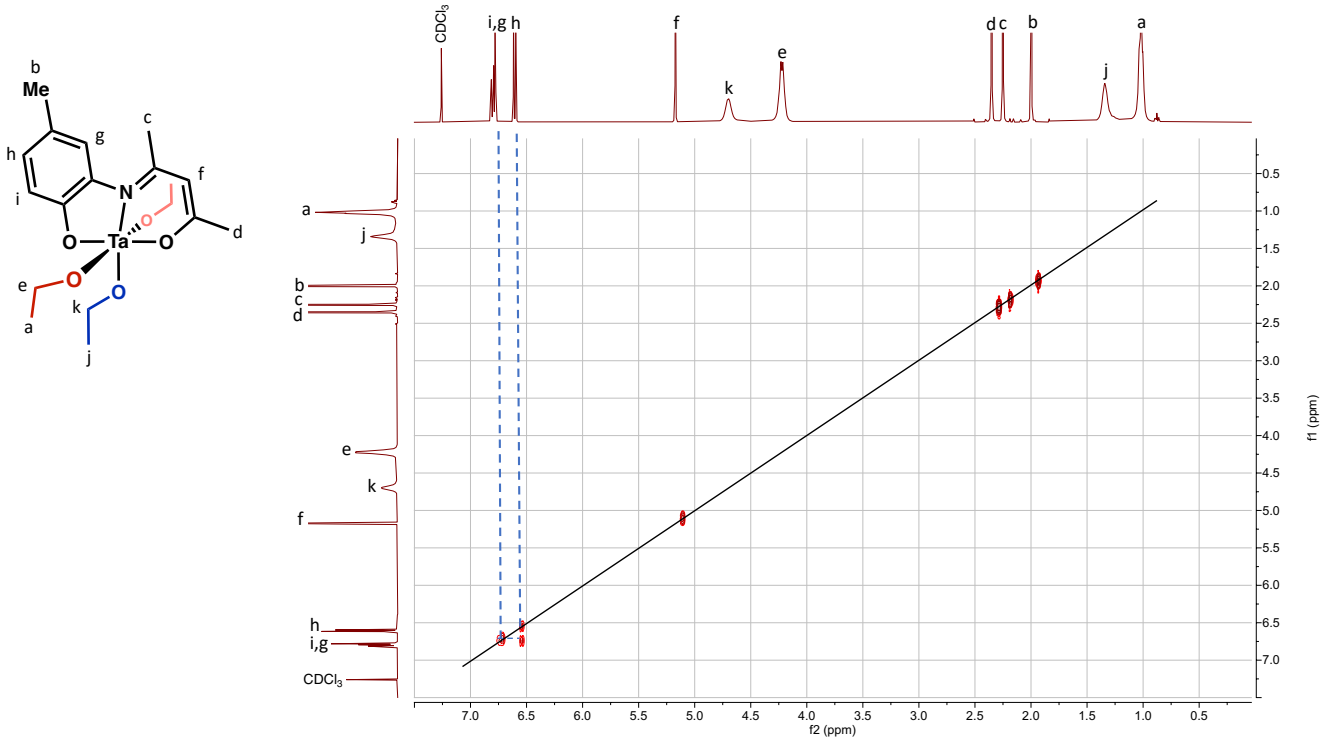

Figure S11. COSY NMR (293 K) spectrum of **I-2** in $CDCl_3$.

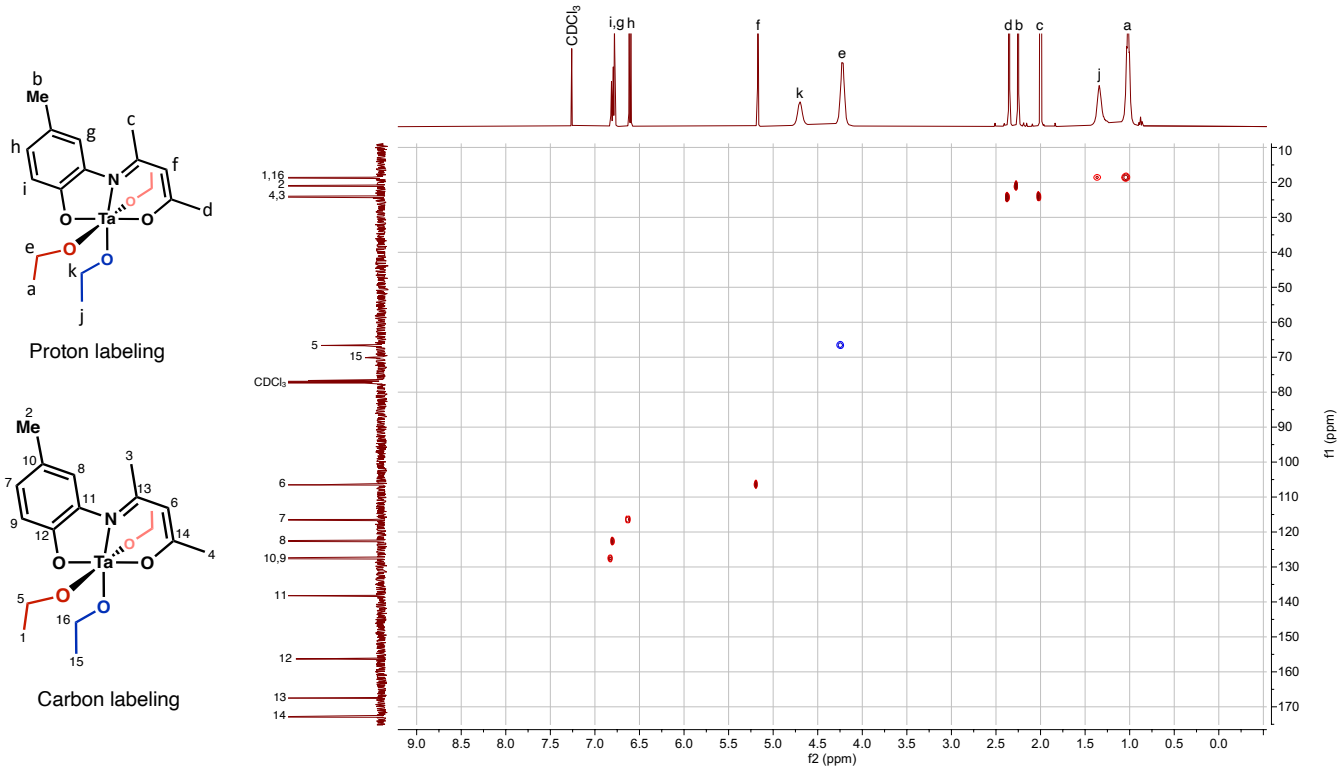

Figure S12. HSQC NMR (293 K) spectrum of **I-2** in $CDCl_3$.

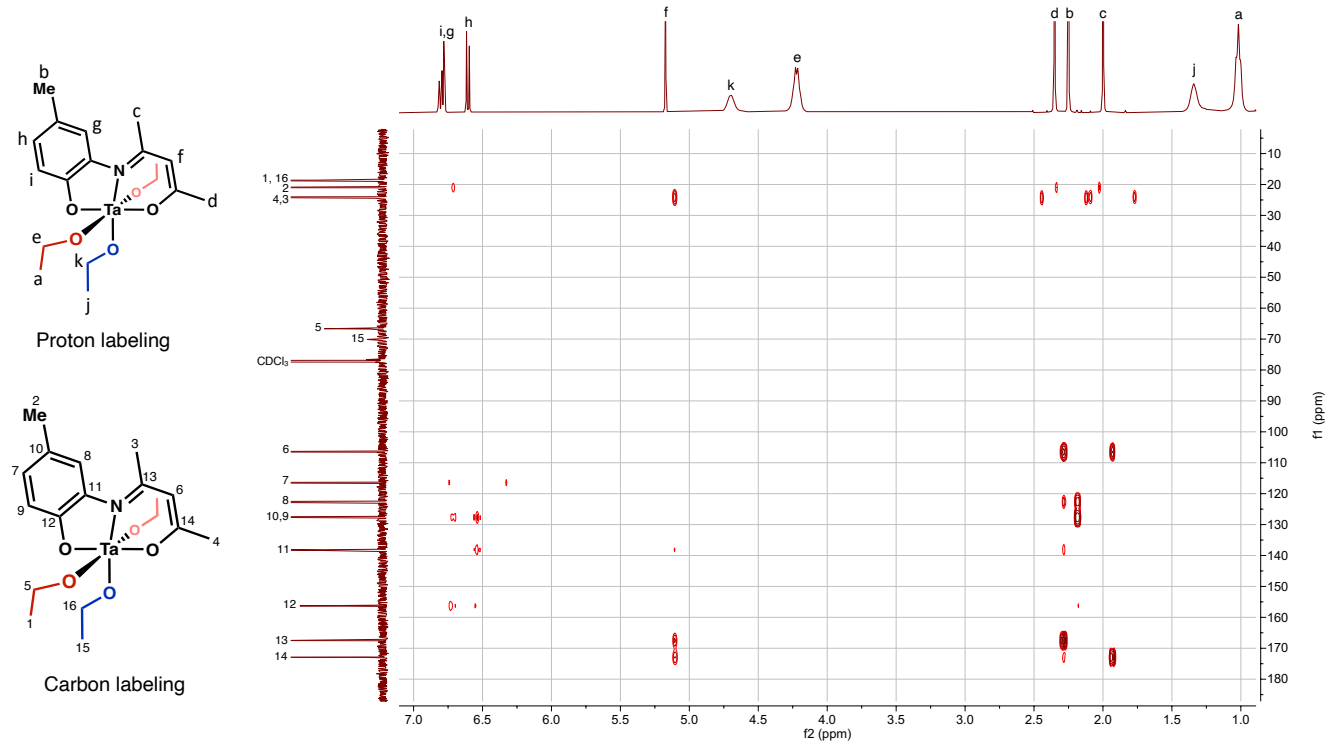

Figure S13. HMBC NMR (293 K) spectrum of **I-2** in $CDCl_3$.

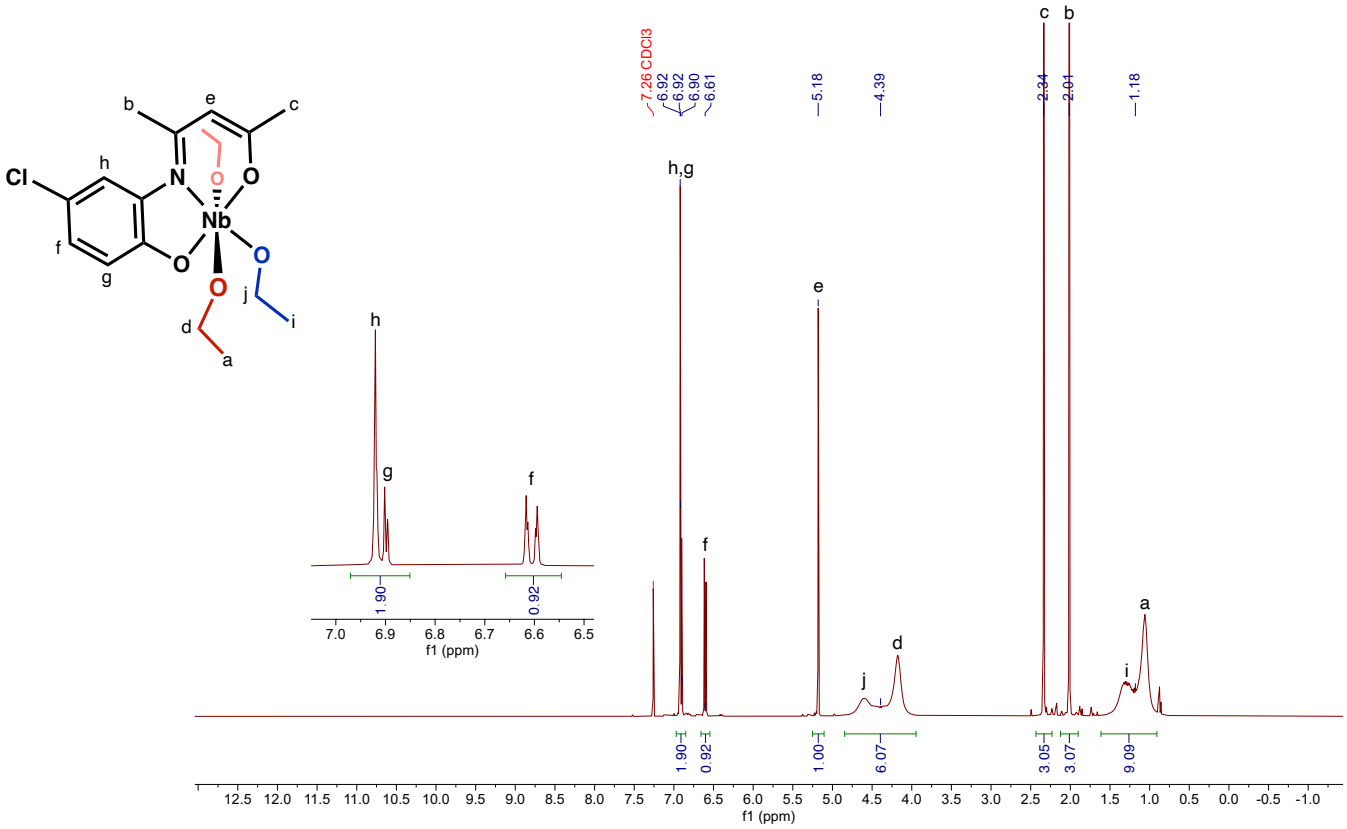

Figure S14. ^1H NMR (400 MHz, 293 K) spectrum of **I-3** in $CDCl_3$.

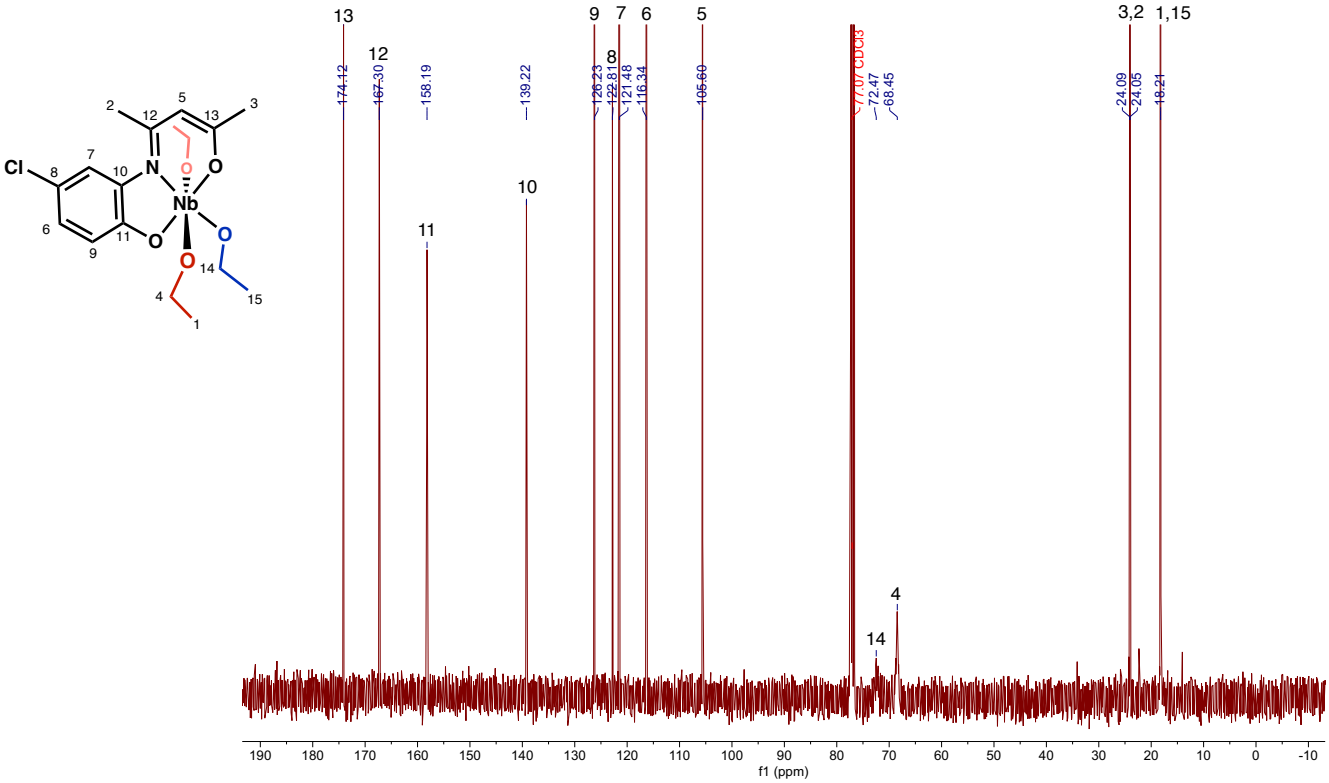

Figure S15. $^{13}C\{^{1}H\}$ NMR (101 MHz, 293 K) spectrum of **I-3** in $CDCl_3$.

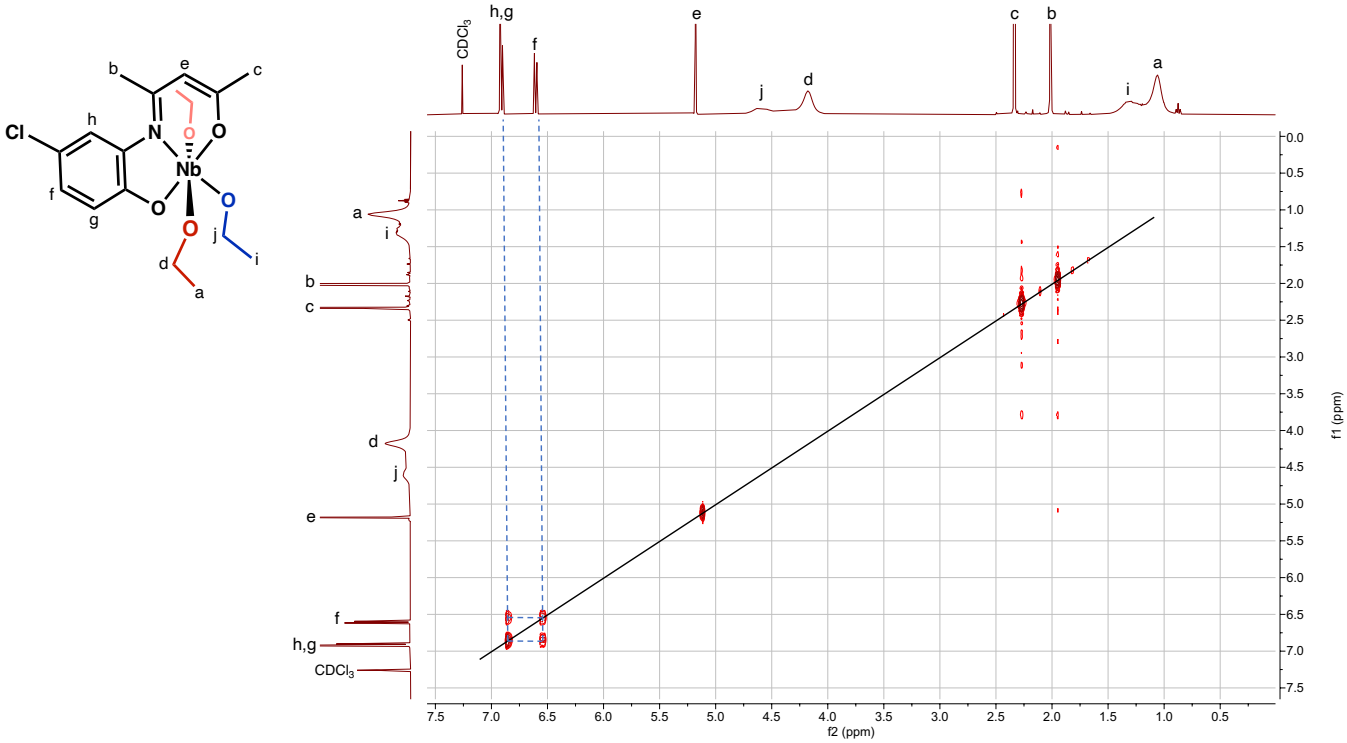

Figure S16. COSY NMR (293 K) spectrum of **I-3** in $CDCl_3$.

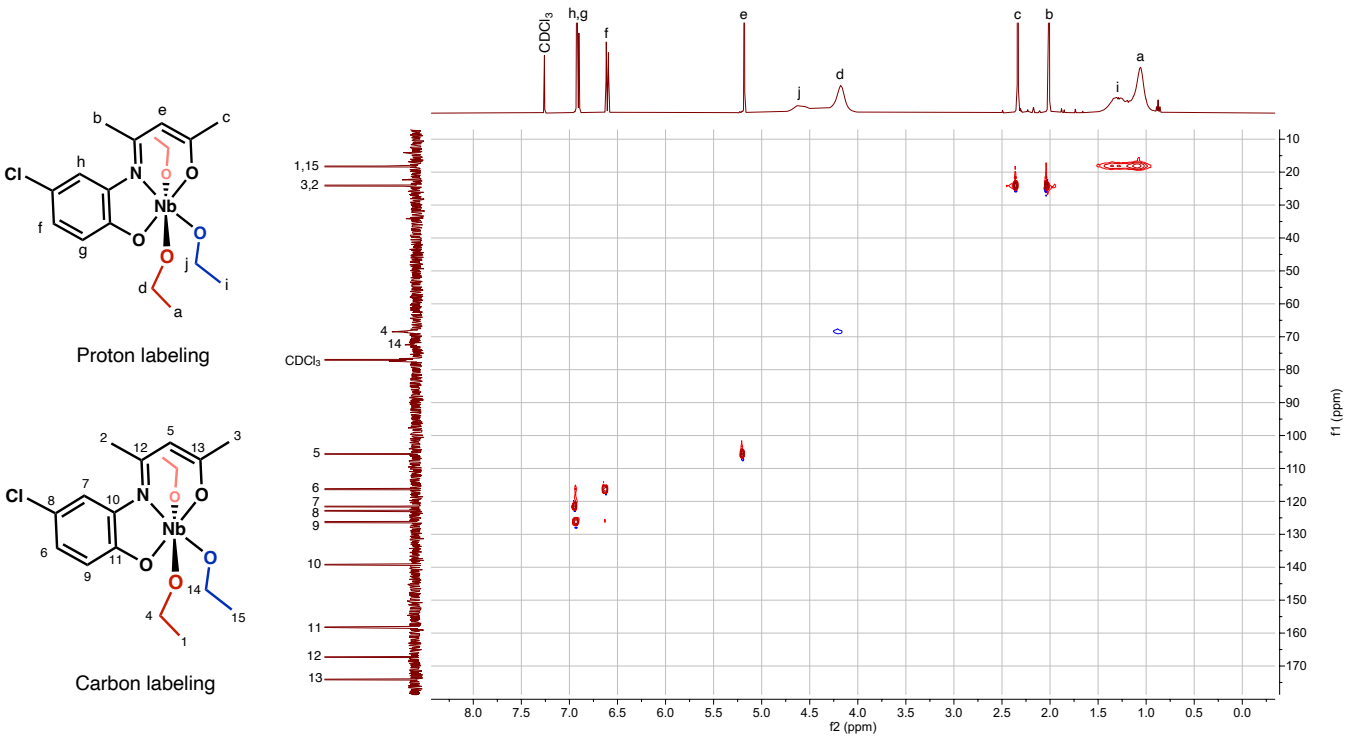

Figure S17. HSQC NMR (293 K) spectrum of **I-3** in $CDCl_3$.

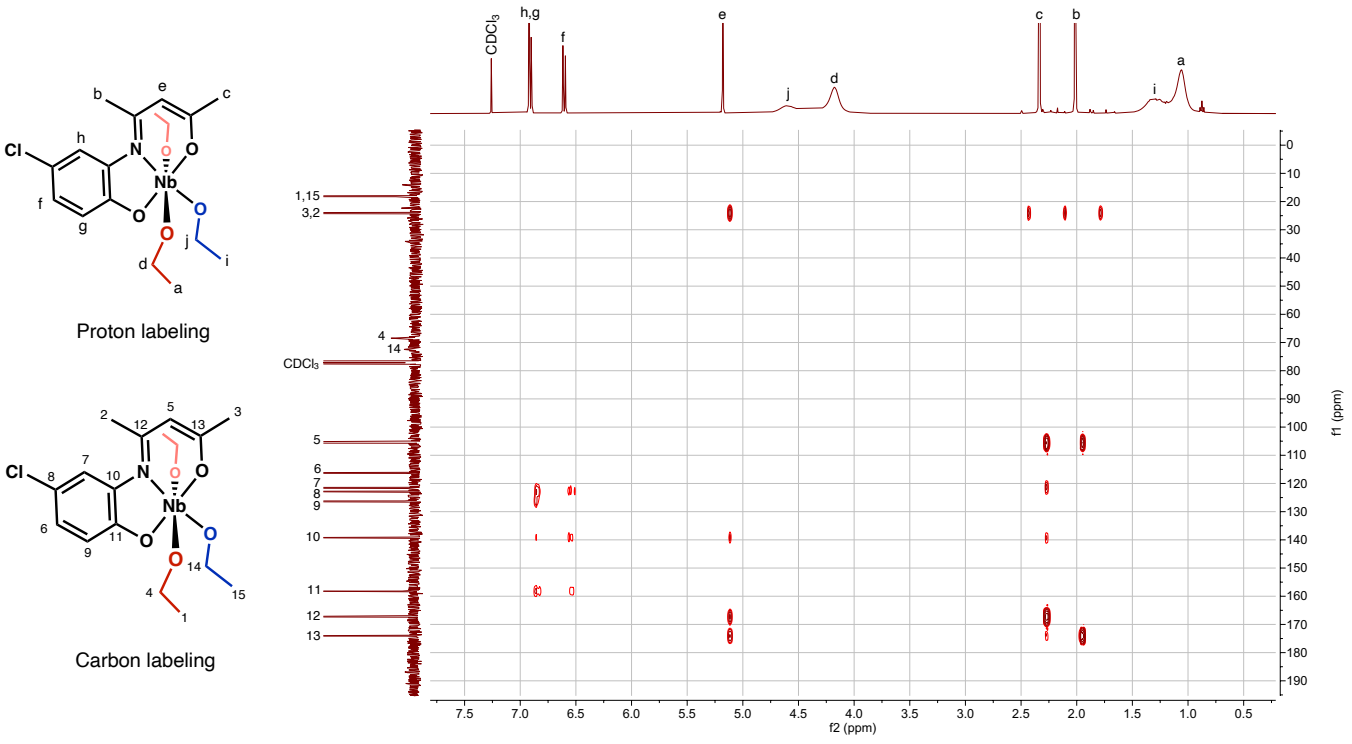

Figure S18. HMBC NMR (293 K) spectrum of **I-3** in $CDCl_3$.

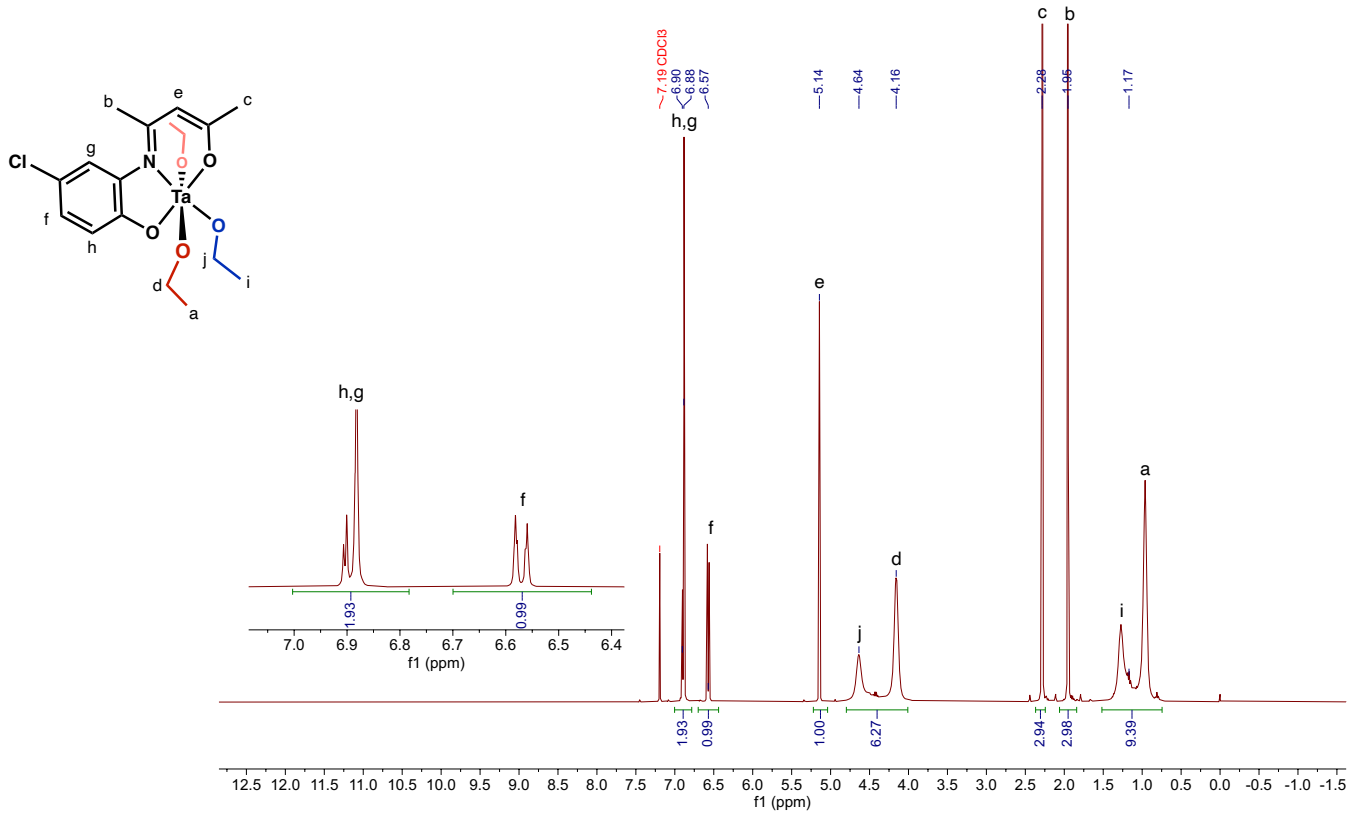

Figure S19. ^{1}H NMR (400 MHz, 293 K) spectrum of **I-4** in $CDCl_3$.

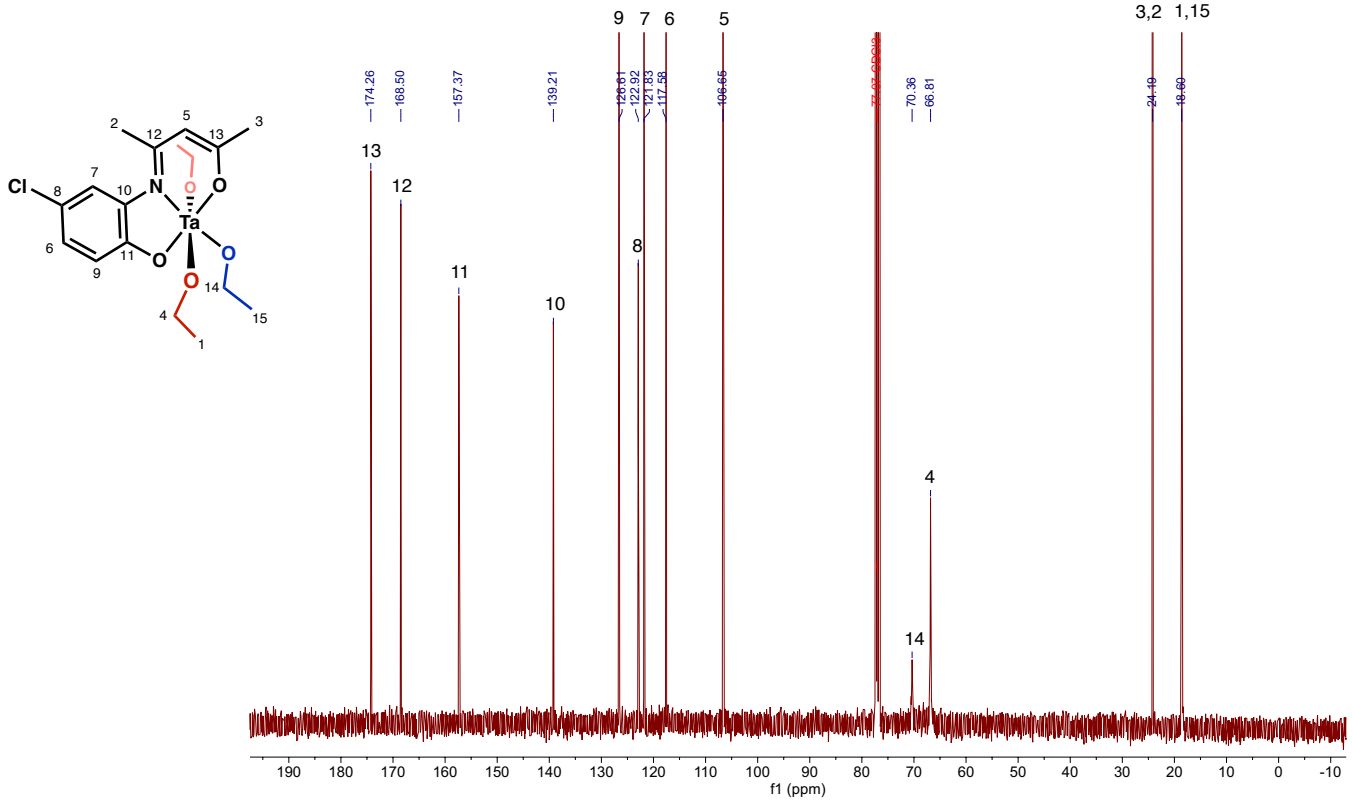

Figure S20. ^{13}C{^{1}H} NMR (101 MHz, 293 K) spectrum of **I-4** in $CDCl_3$.

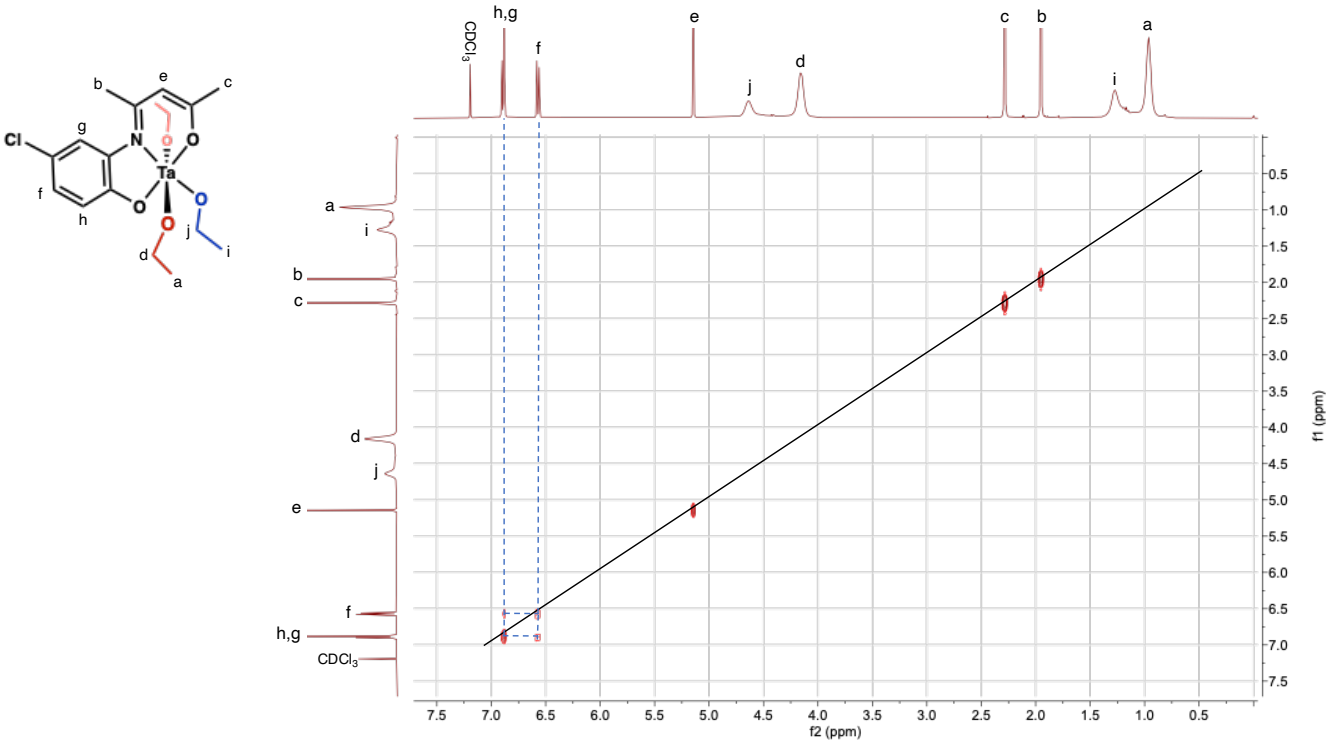

Figure S21. COSY NMR (293 K) spectrum of **I-4** in $CDCl_3$.

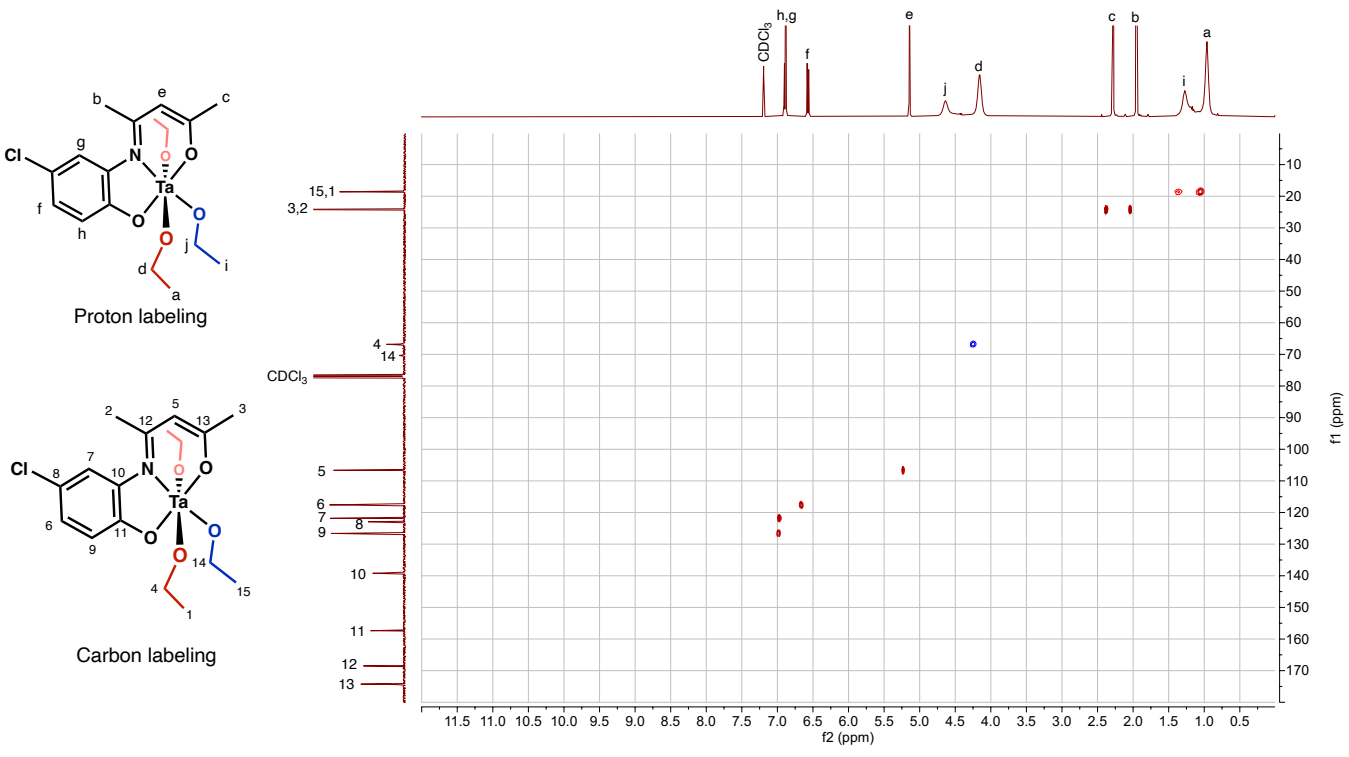

Figure S22. HSQC NMR (293 K) spectrum of **I-4** in $CDCl_3$.

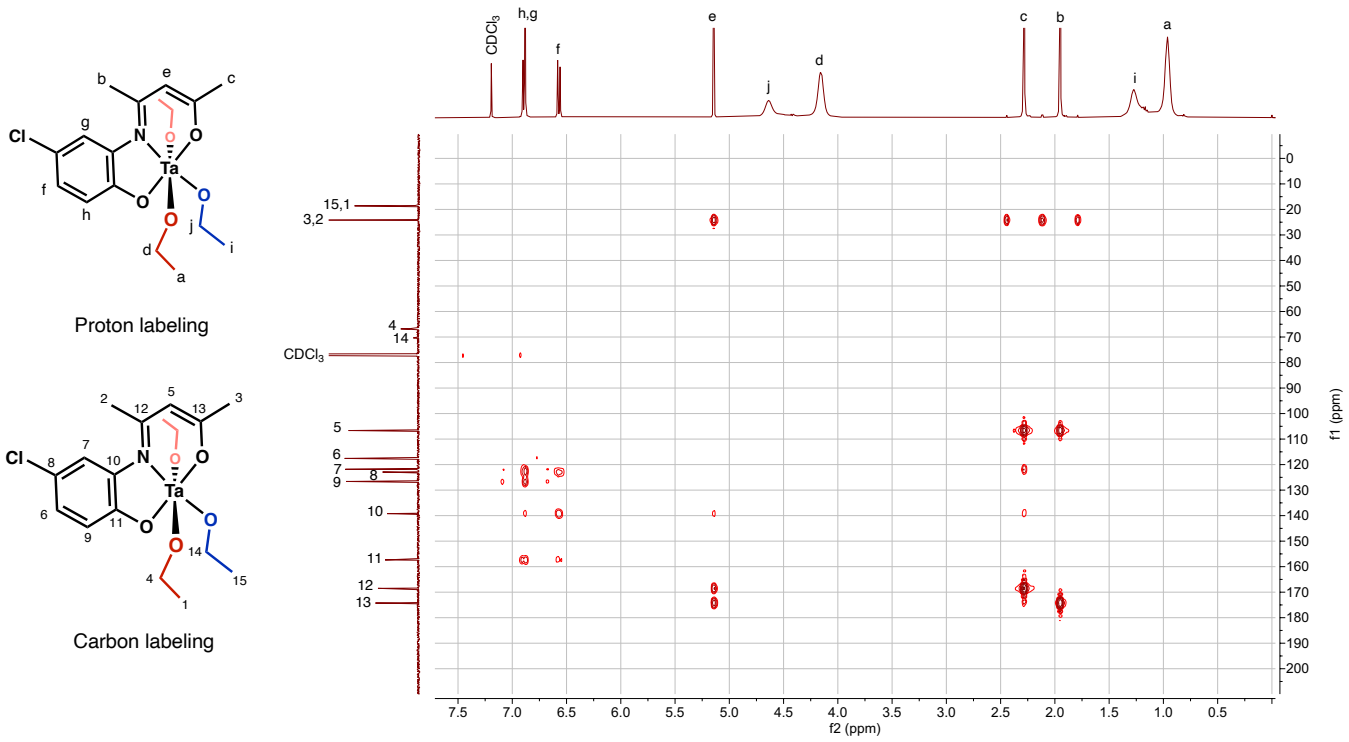

Figure S23. HMBC NMR (293 K) spectrum of **I-4** in $CDCl_3$.

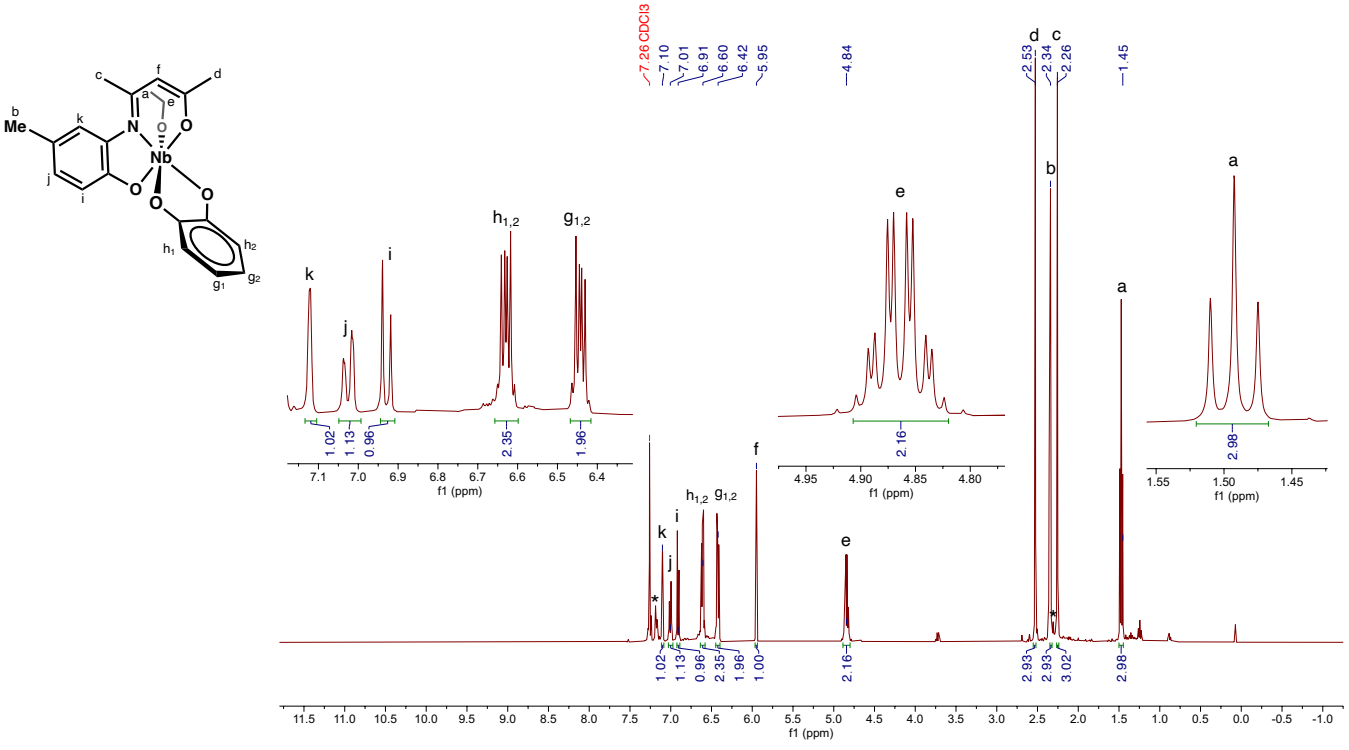

Figure S24. ^{1}H NMR (400 MHz, 293 K) spectrum of **C-1** in $CDCl_3$. *Trace toluene

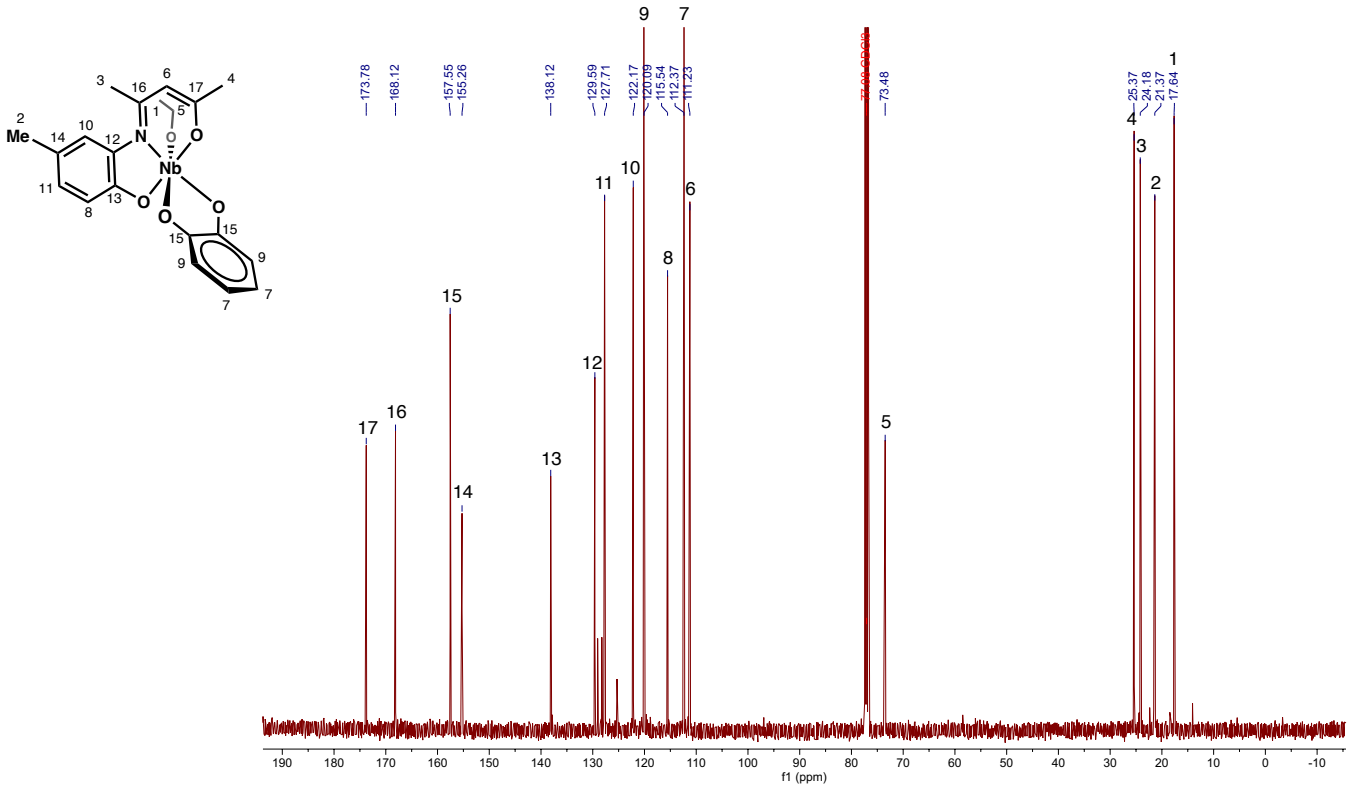

Figure S25. $^{13}C\{^{1}H\}$ NMR (101 MHz, 293 K) spectrum of **C-1** in $CDCl_3$.

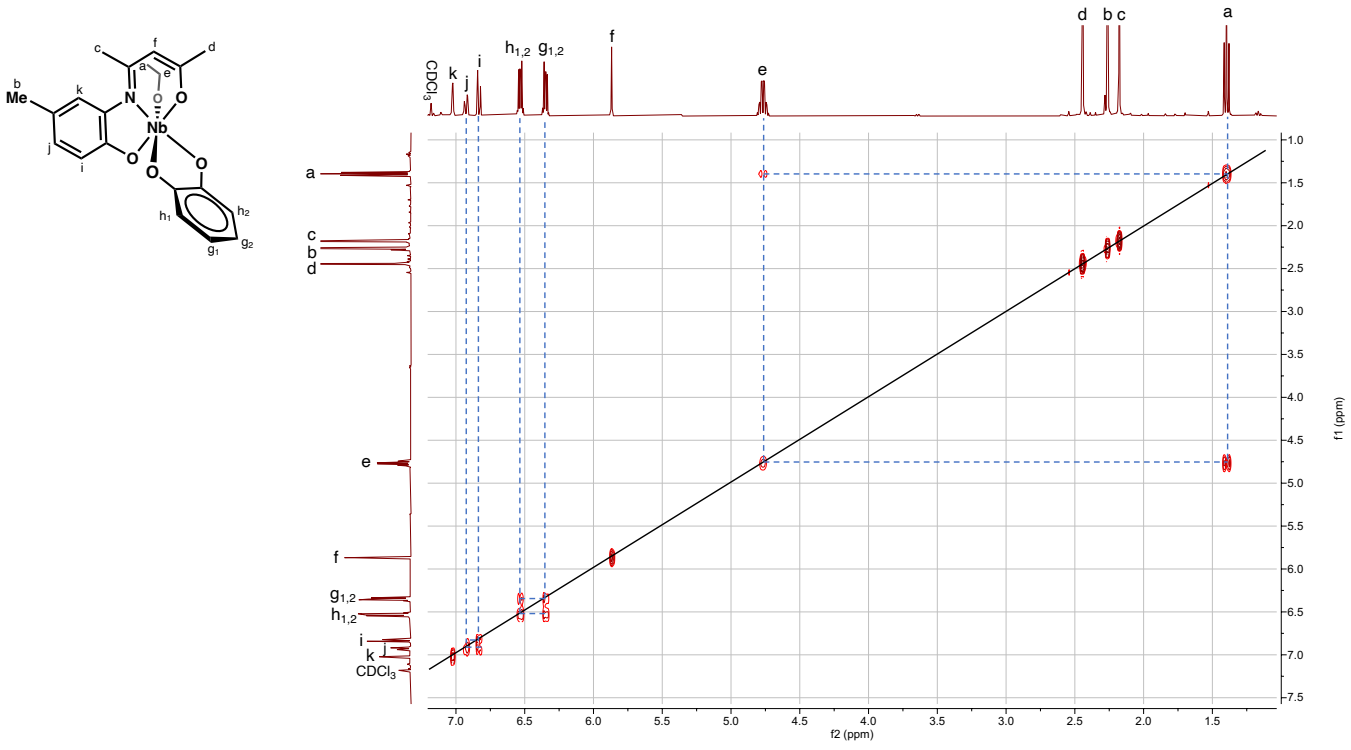

Figure S26. COSY NMR (293 K) spectrum of **C-1** in $CDCl_3$.

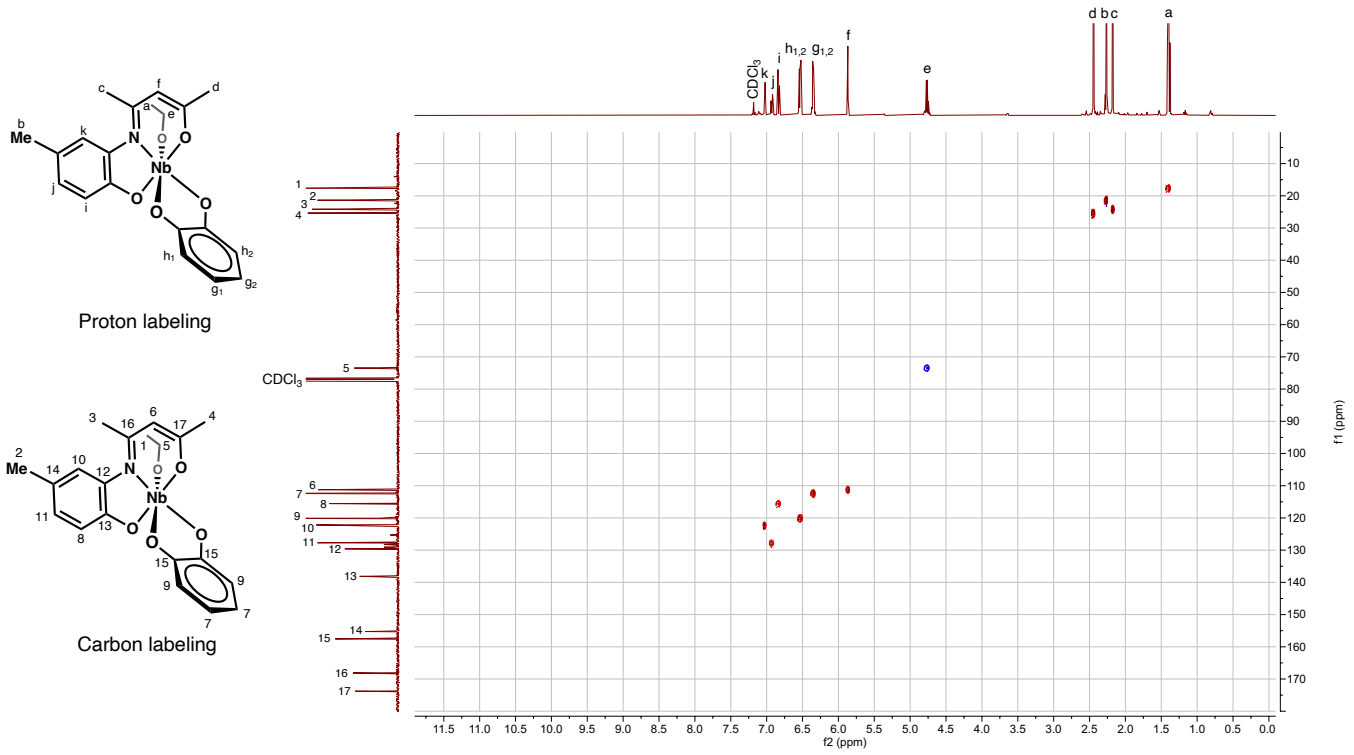

Figure S27. HSQC NMR (293 K) spectrum of **C-1** in $CDCl_3$.

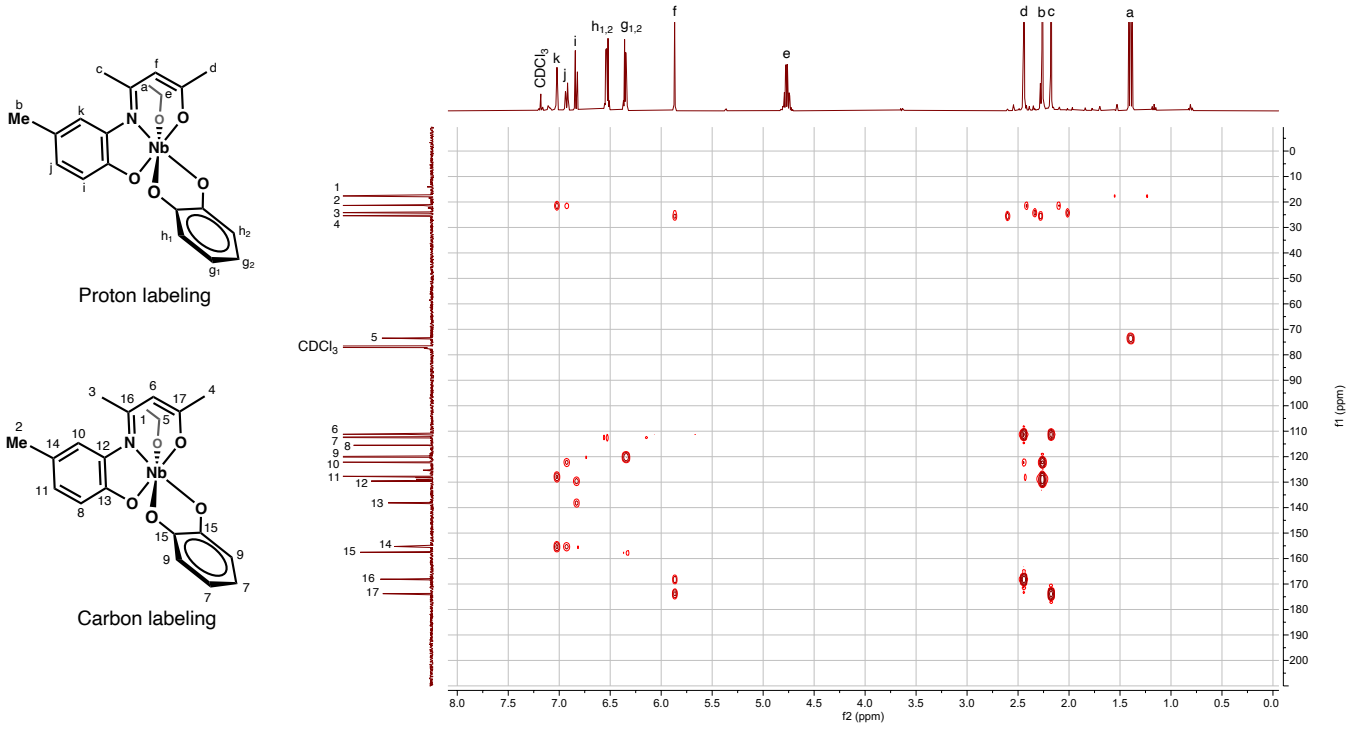

Figure S28. HMBC NMR (293 K) spectrum of **C-1** in $CDCl_3$.

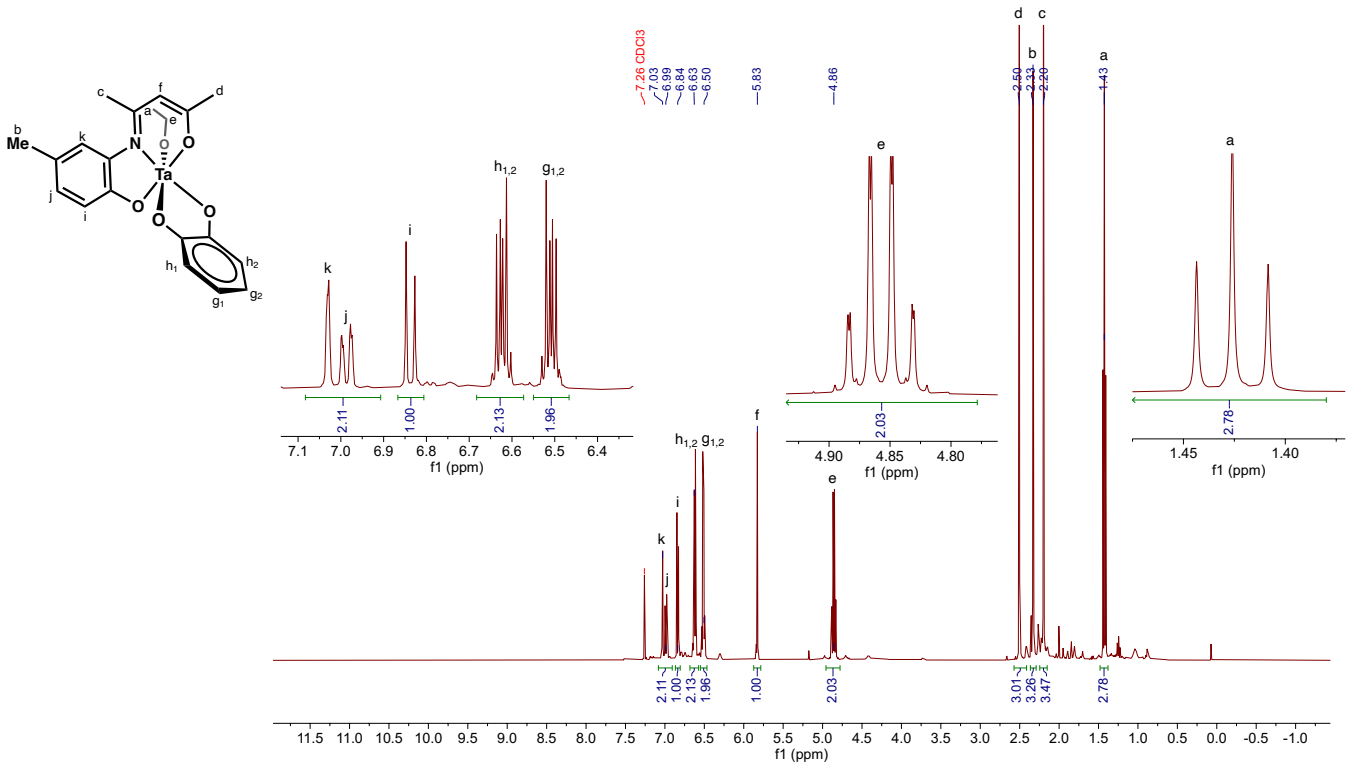

Figure S29. ^{1}H NMR (400 MHz, 293 K) spectrum of **C-2** in $CDCl_3$.

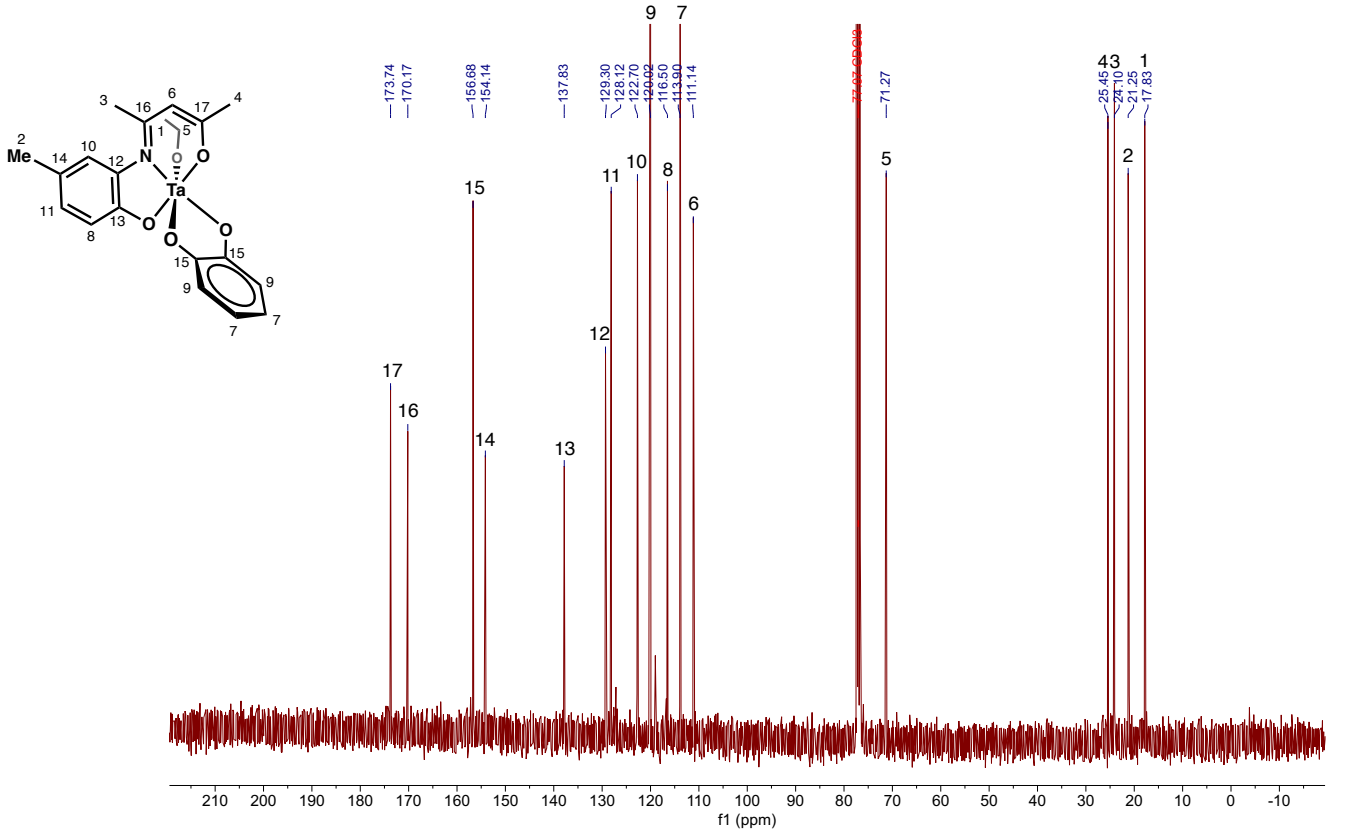

Figure S30. $^{13}C\{^{1}H\}$ NMR (101 MHz, 293 K) spectrum of **C-2** in $CDCl_3$.

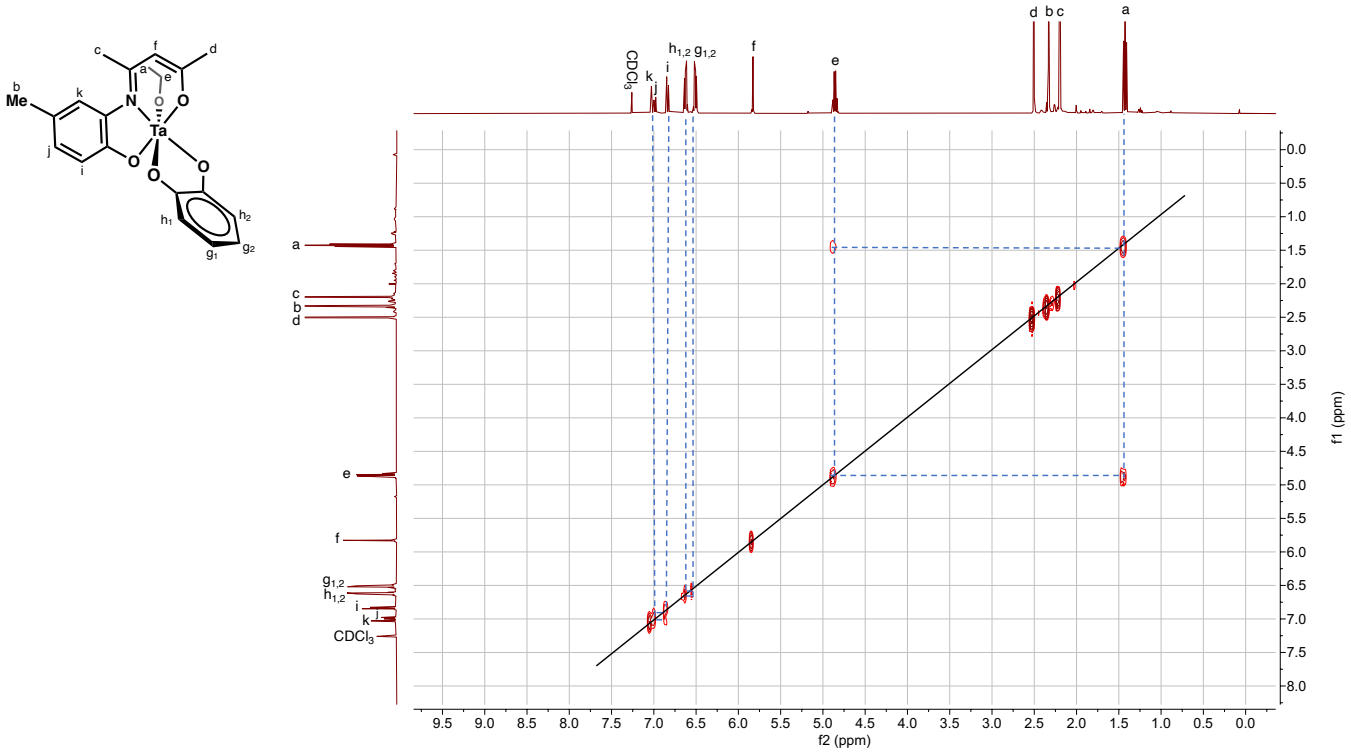

Figure S31. COSY NMR (293 K) spectrum of **C-2** in $CDCl_3$.

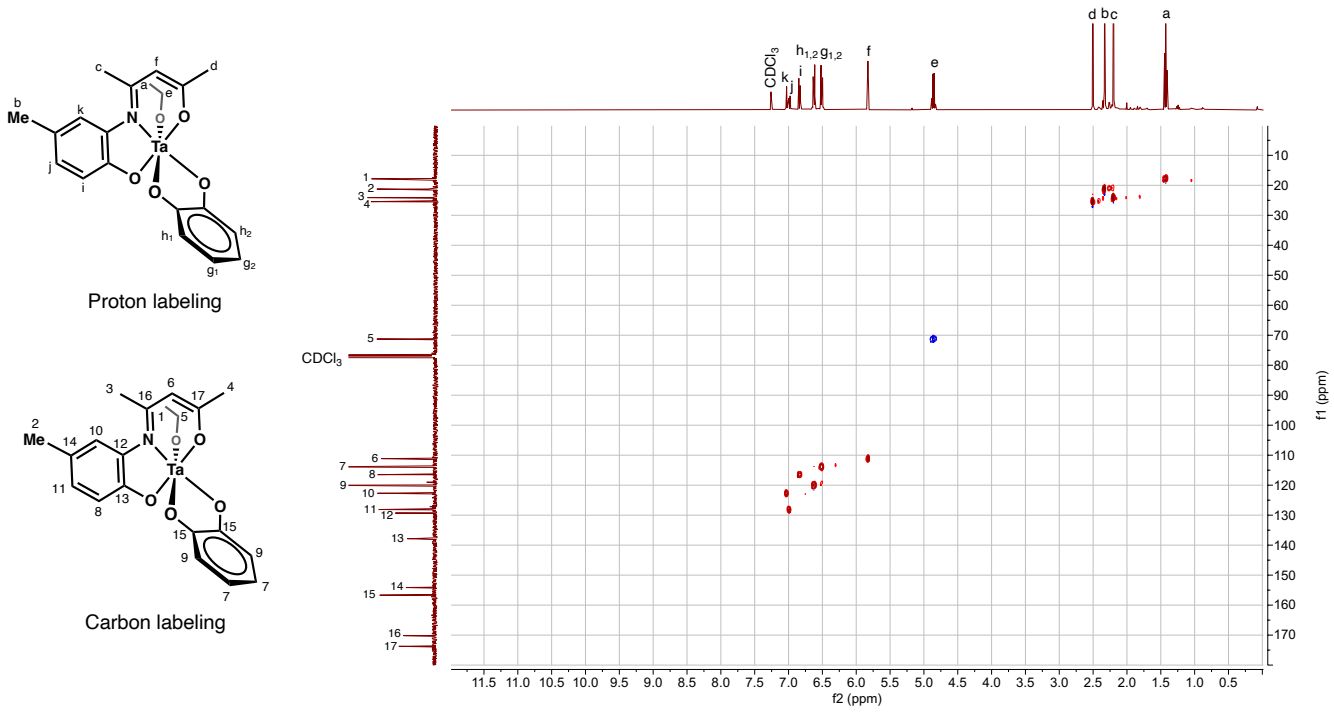

Figure S32. HSQC NMR (293 K) spectrum of **C-2** in $CDCl_3$.

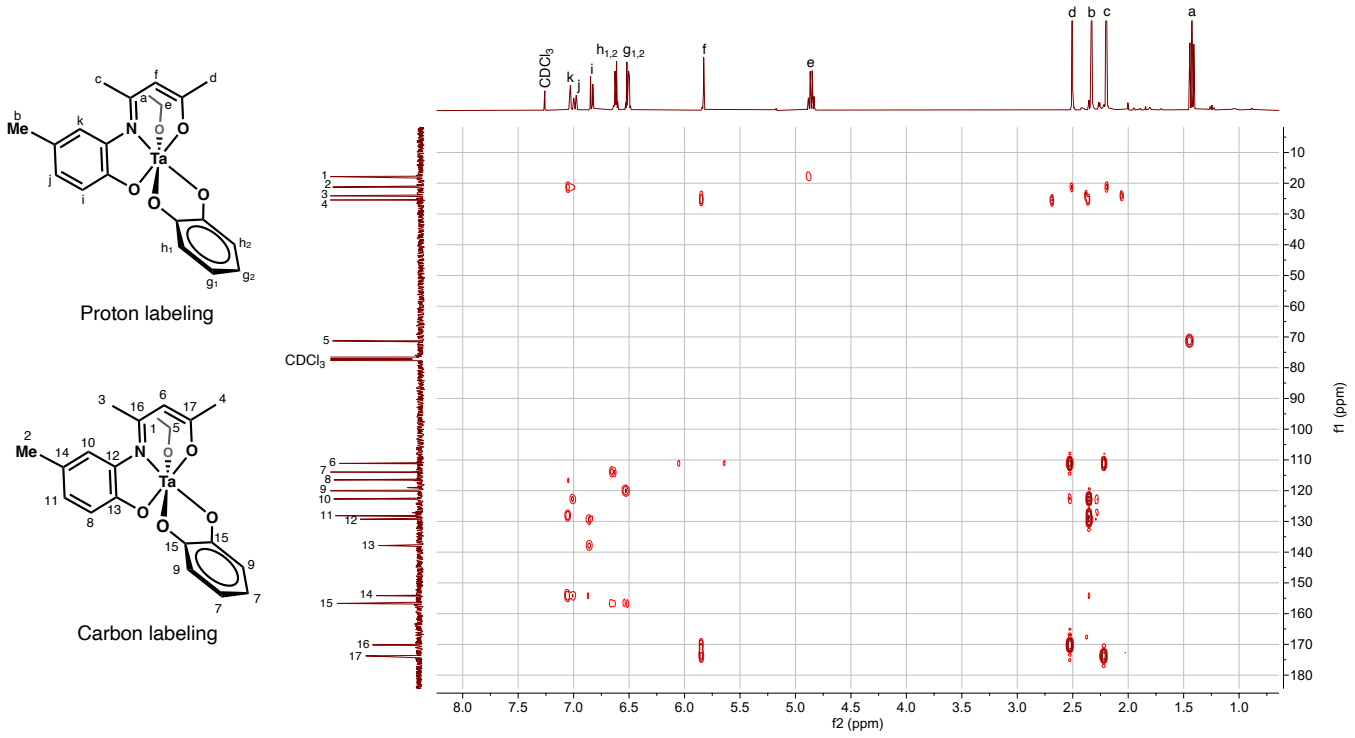

Figure S33. HMBC NMR (293 K) spectrum of **C-2** in $CDCl_3$.

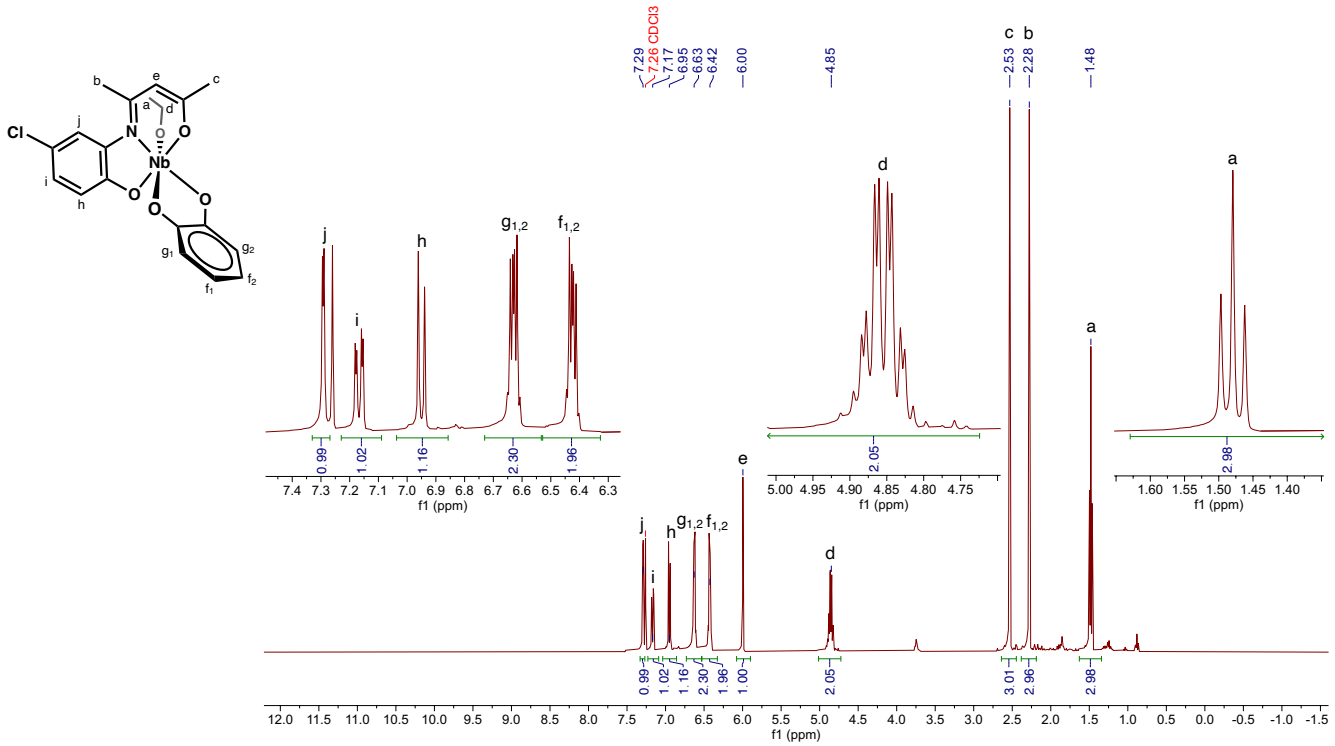

Figure S34. ^{1}H NMR (400 MHz, 293 K) spectrum of **C-3** in $CDCl_3$.

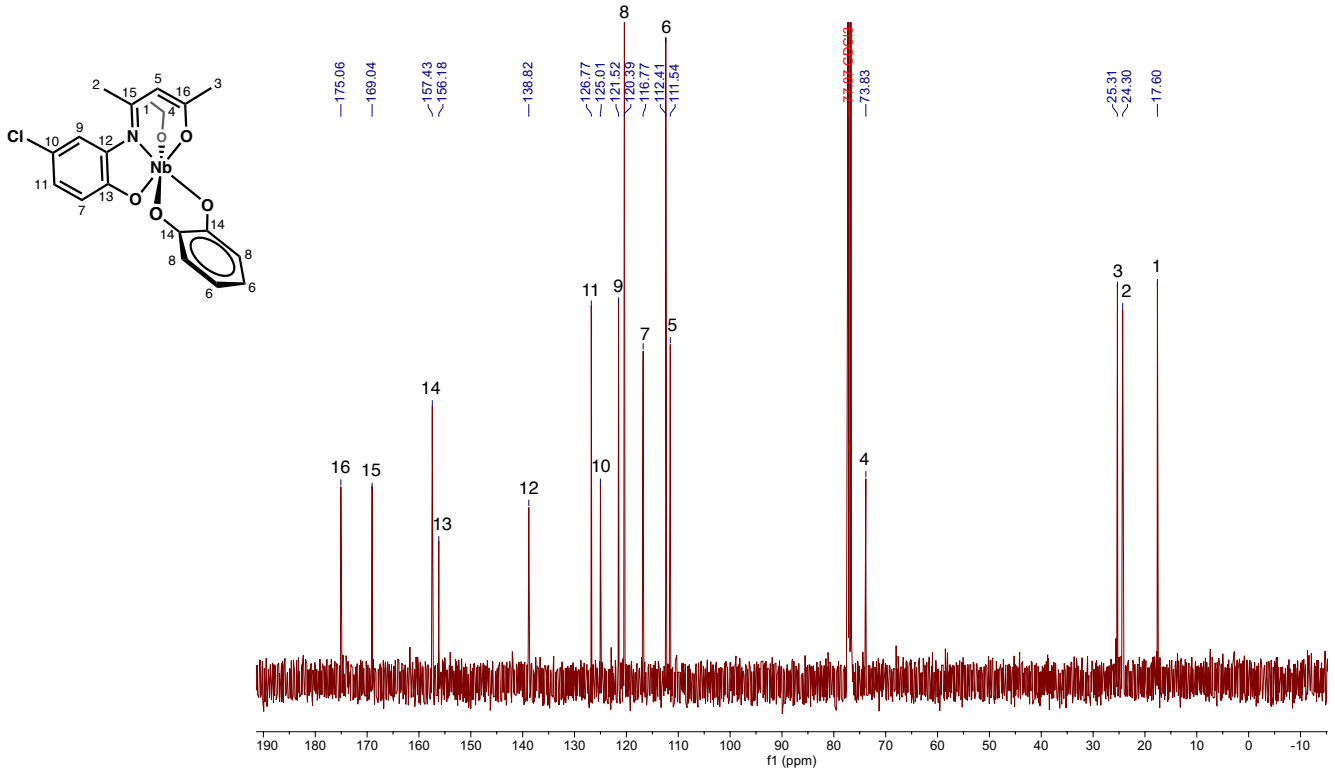

Figure S35. $^{13}C\{^{1}H\}$ NMR (101 MHz, 293 K) spectrum of **C-3** in $CDCl_3$.

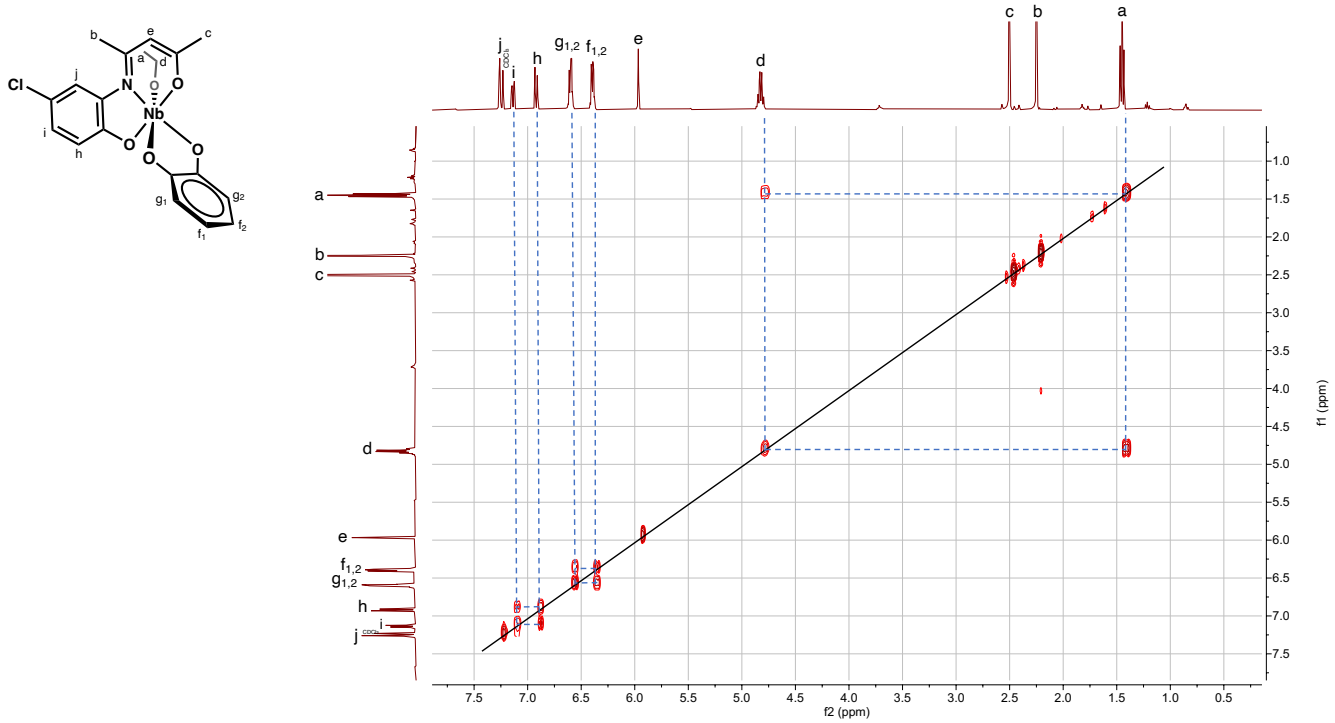

Figure S36. COSY NMR (293 K) spectrum of **C-3** in $CDCl_3$.

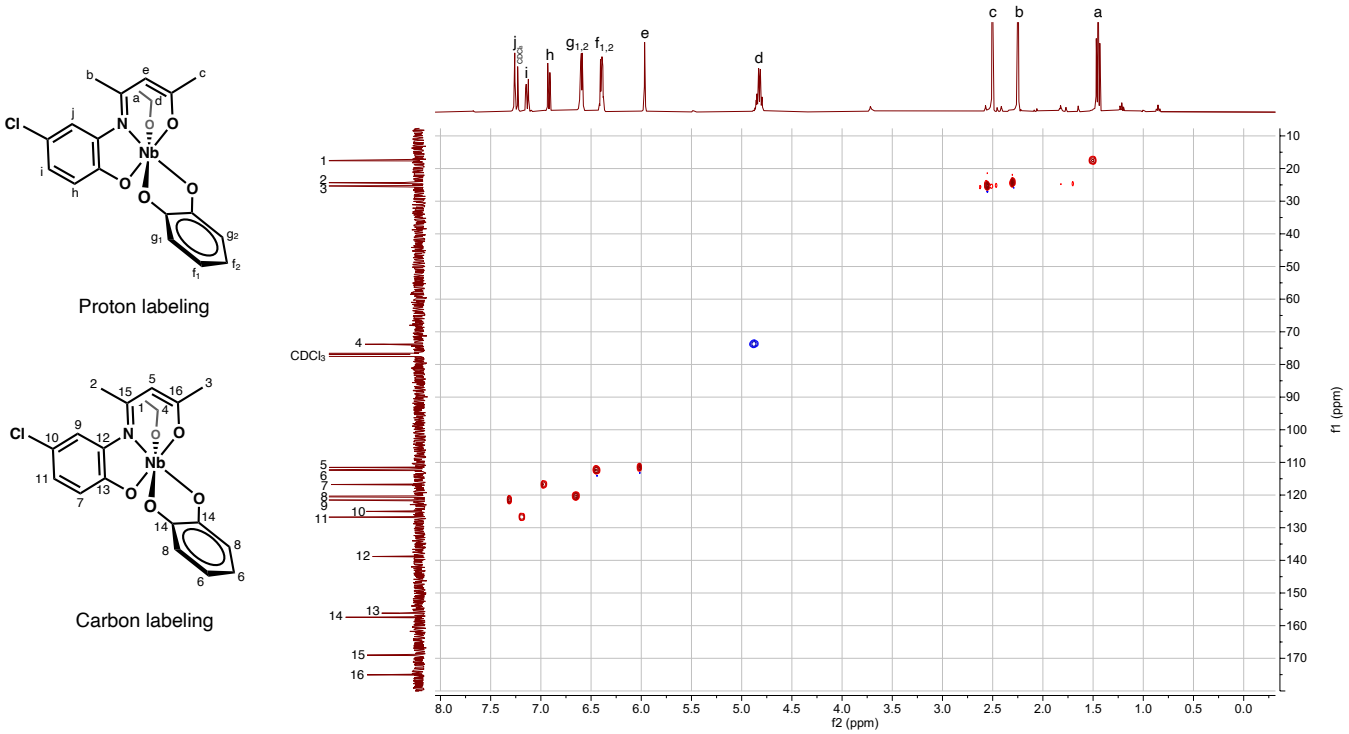

Figure S37. HSQC NMR (293 K) spectrum of **C-3** in $CDCl_3$.

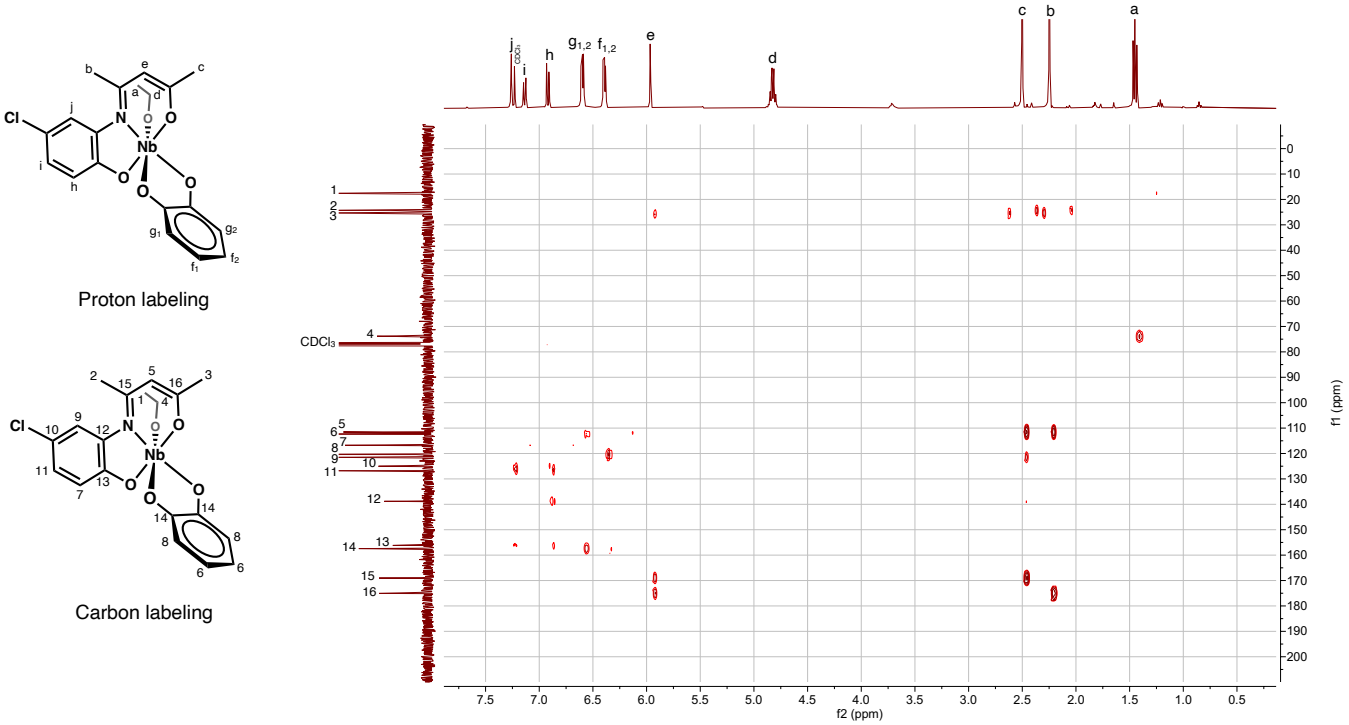

Figure S38. HMBC NMR (293 K) spectrum of **C-3** in $CDCl_3$.

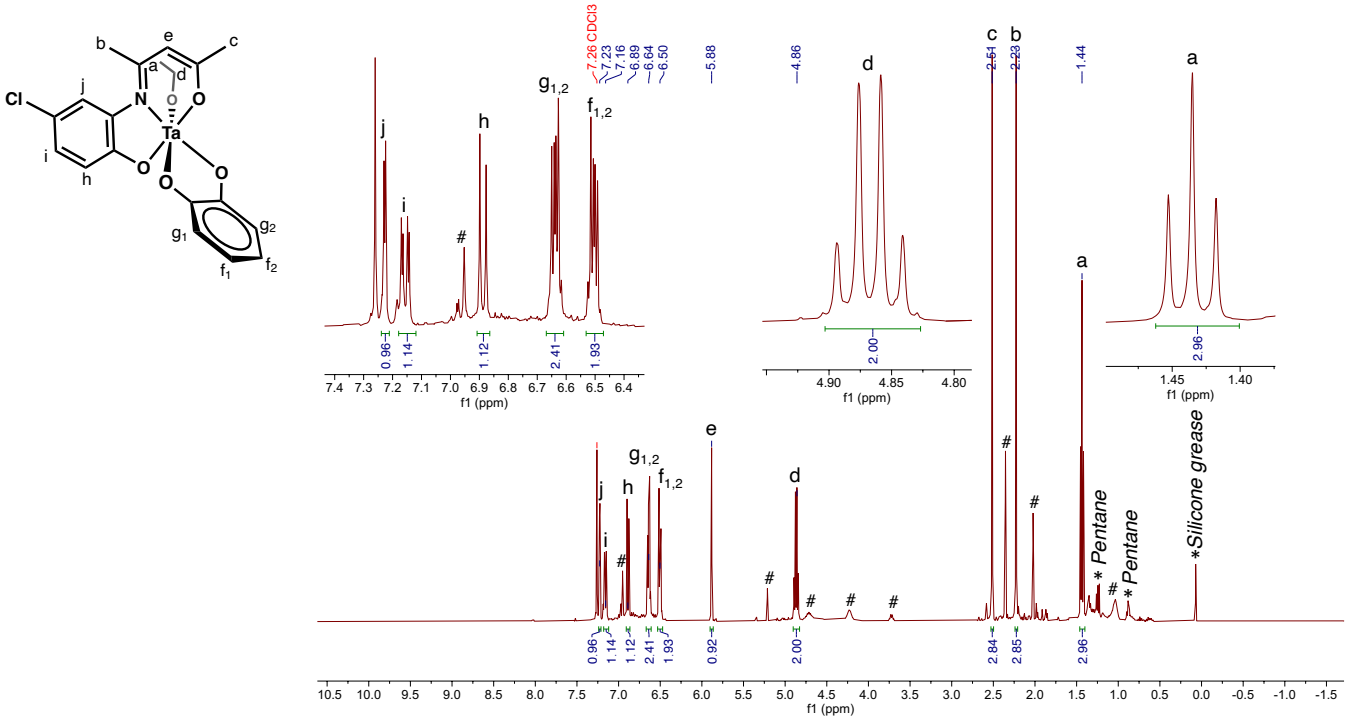

Figure S39. ^{1}H NMR (400 MHz, 293 K) spectrum of **C-4** in $CDCl_3$. #Unknown impurities

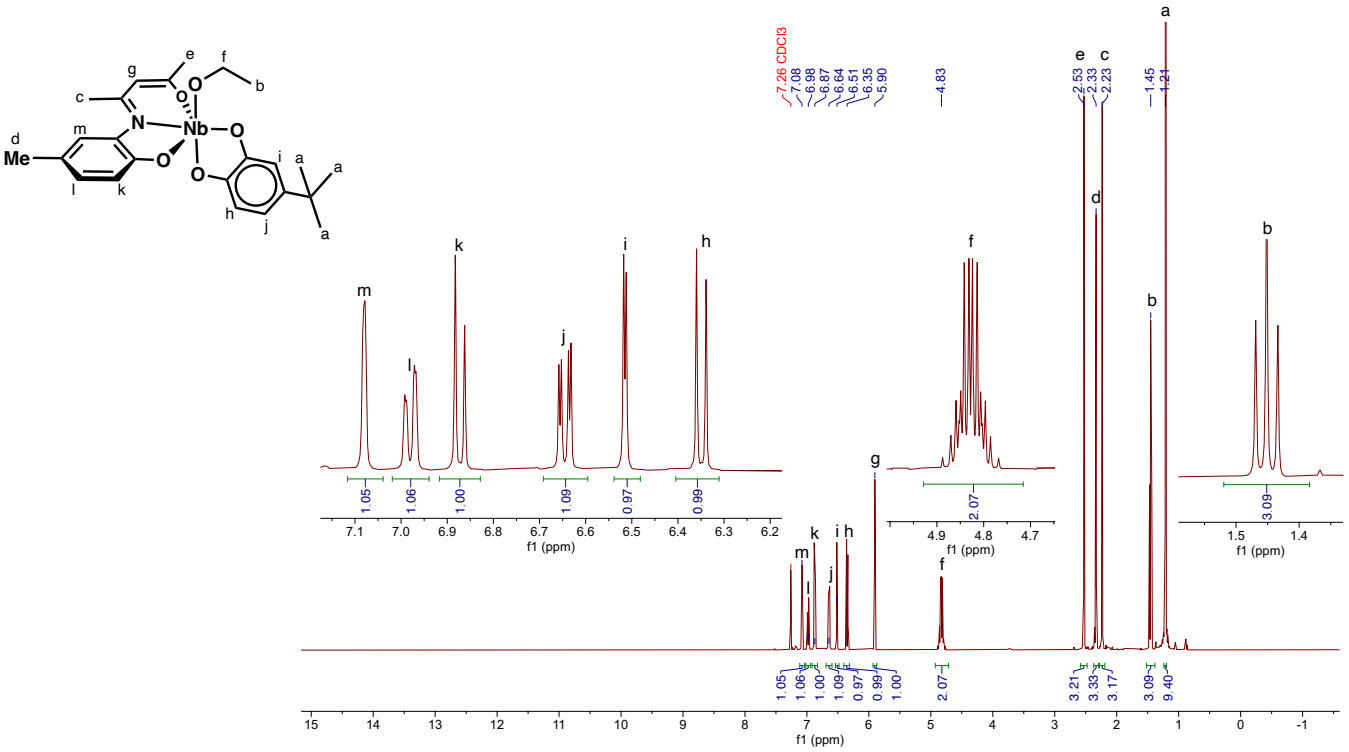

Figure S40. ^{1}H NMR (400 MHz, 293 K) spectrum of **C-1tBu** in $CDCl_3$.

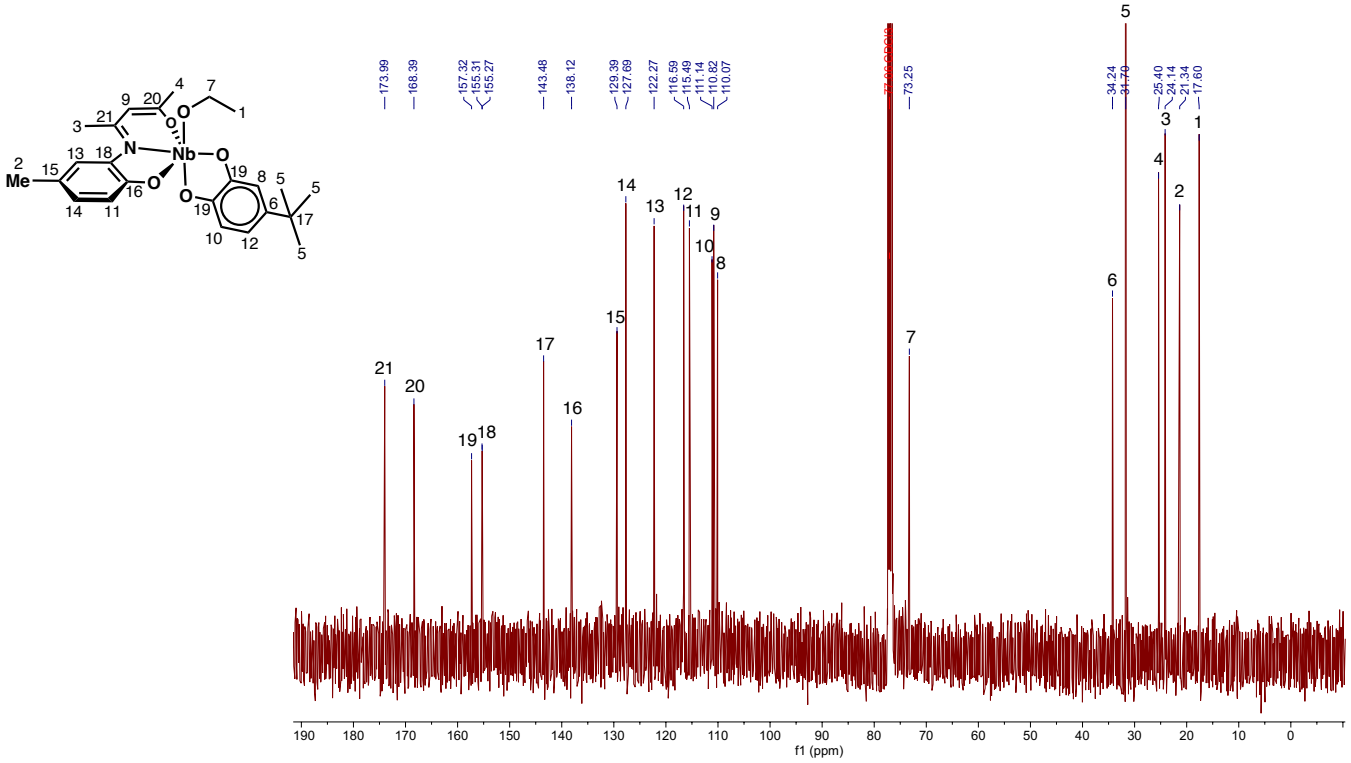

Figure S41. $^{13}C\{^{1}H\}$ NMR (101 MHz, 293 K) spectrum of **C-1tBu** in $CDCl_3$.

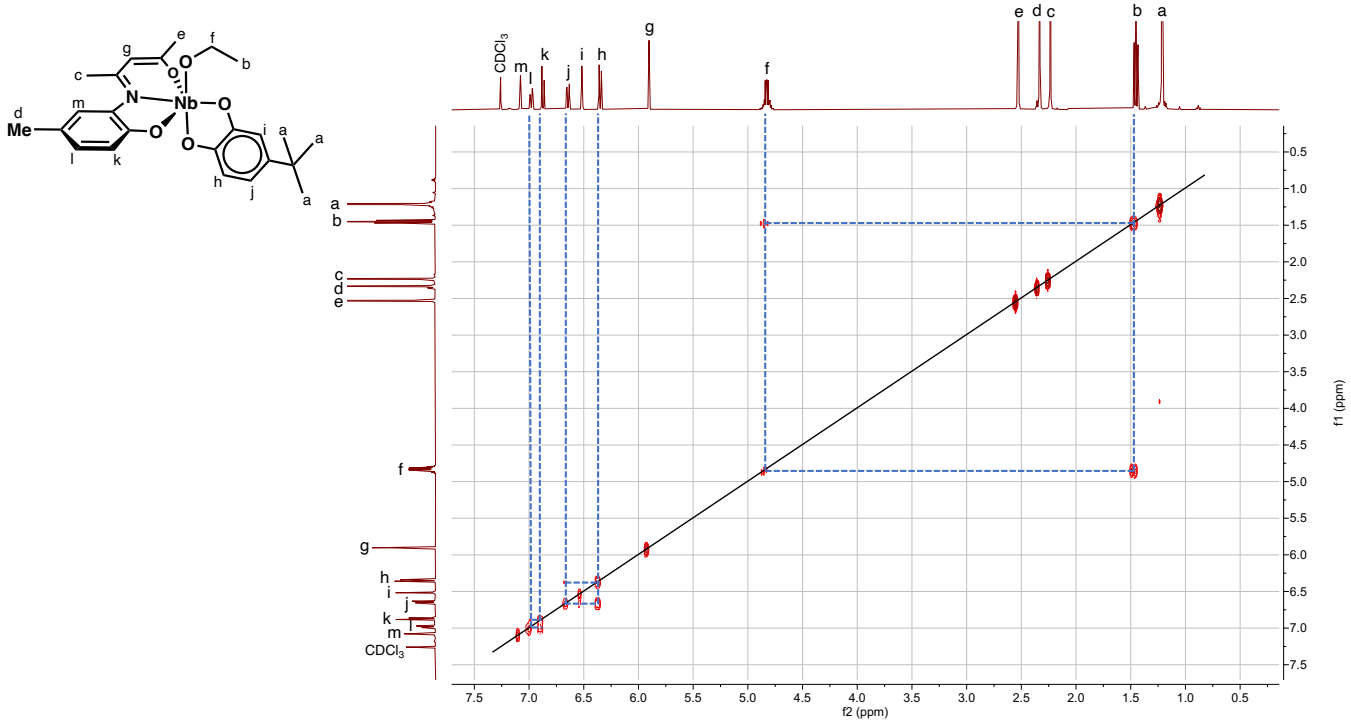

Figure S42. COSY NMR (293 K) spectrum of **C-1tBu** in $CDCl_3$.

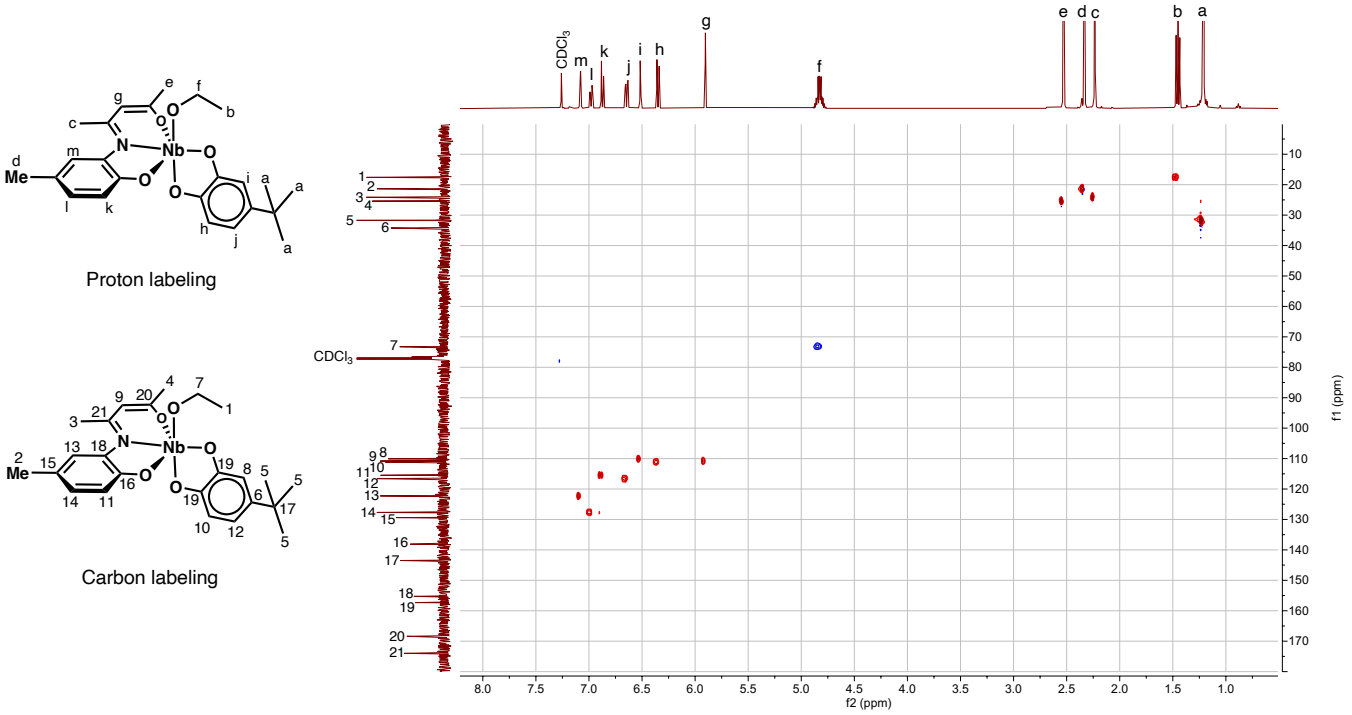

Figure S43. HSQC NMR (293 K) spectrum of **C-1tBu** in $CDCl_3$.

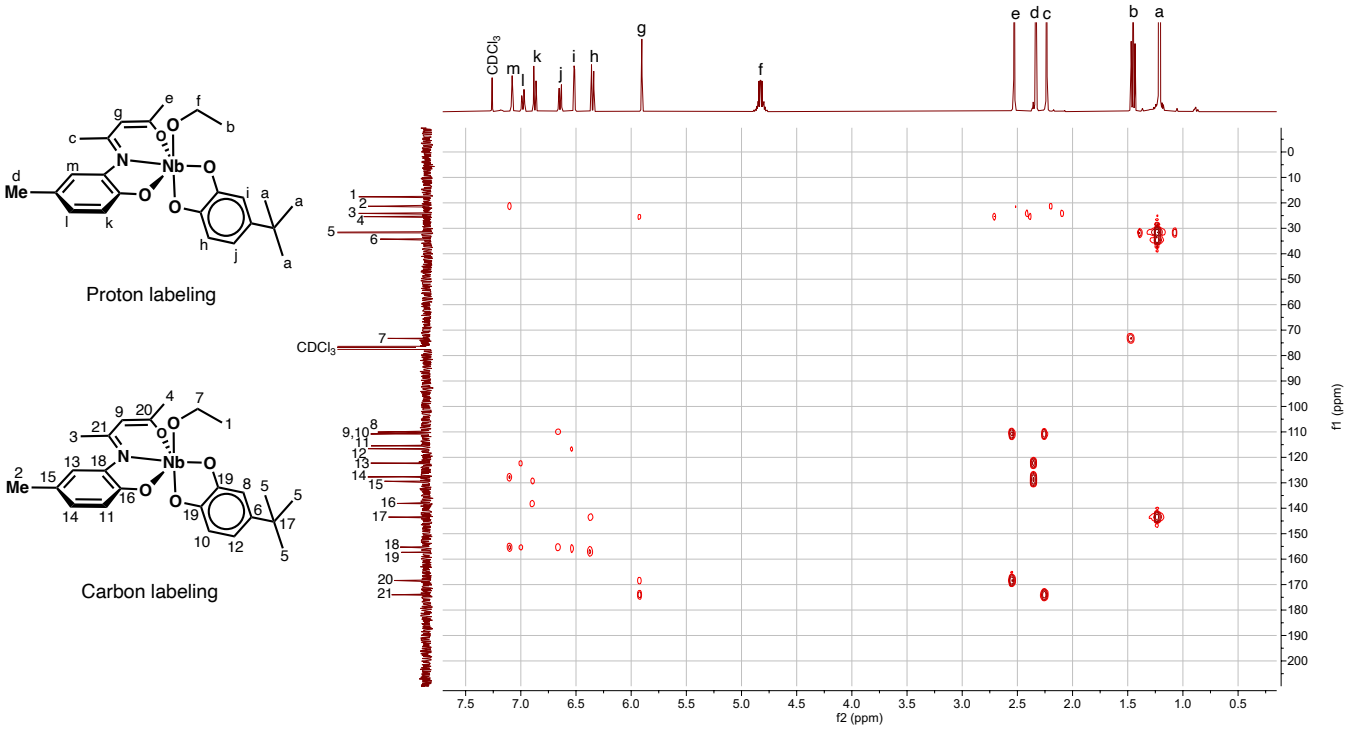

Figure S44. HMBC NMR (293 K) spectrum of **C-1tBu** in $CDCl_3$.

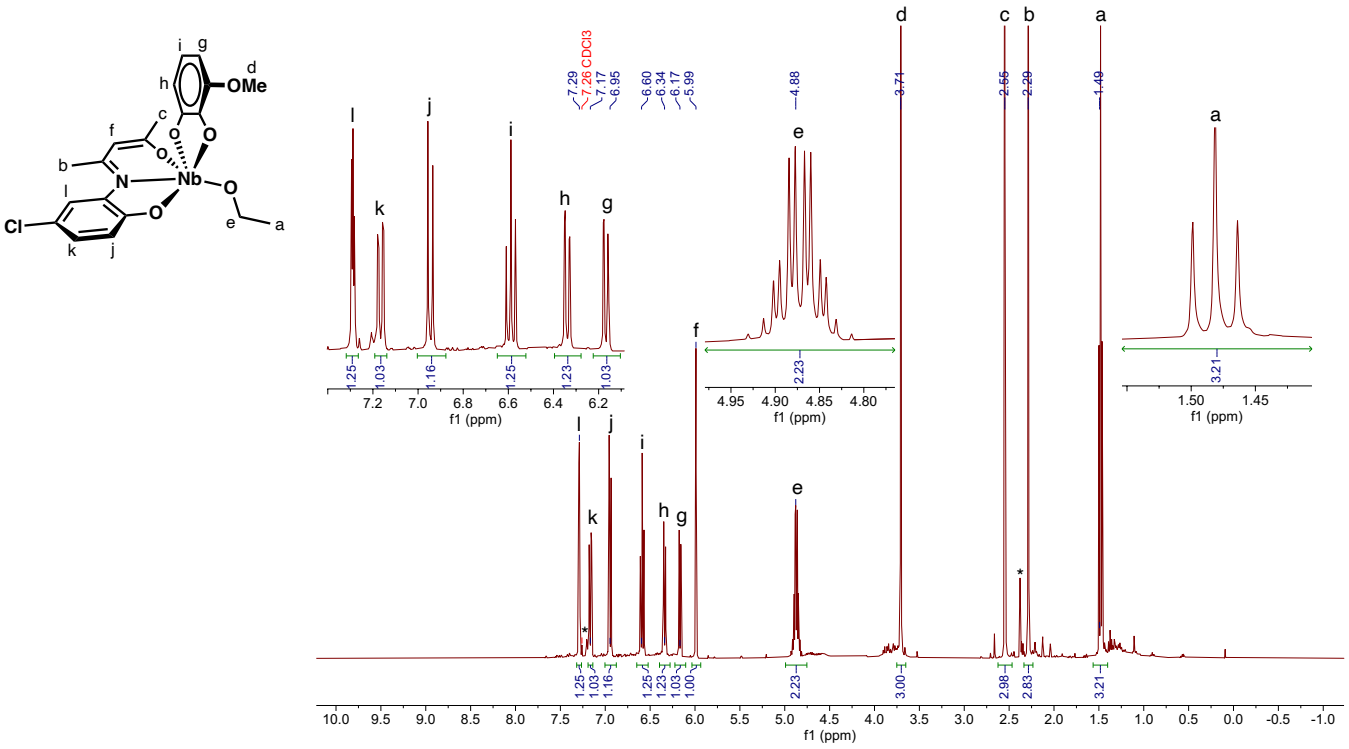

Figure S45. ^{1}H NMR (400 MHz, 293 K) spectrum of **C-3OMe** in $CDCl_3$. *Trace toluene.

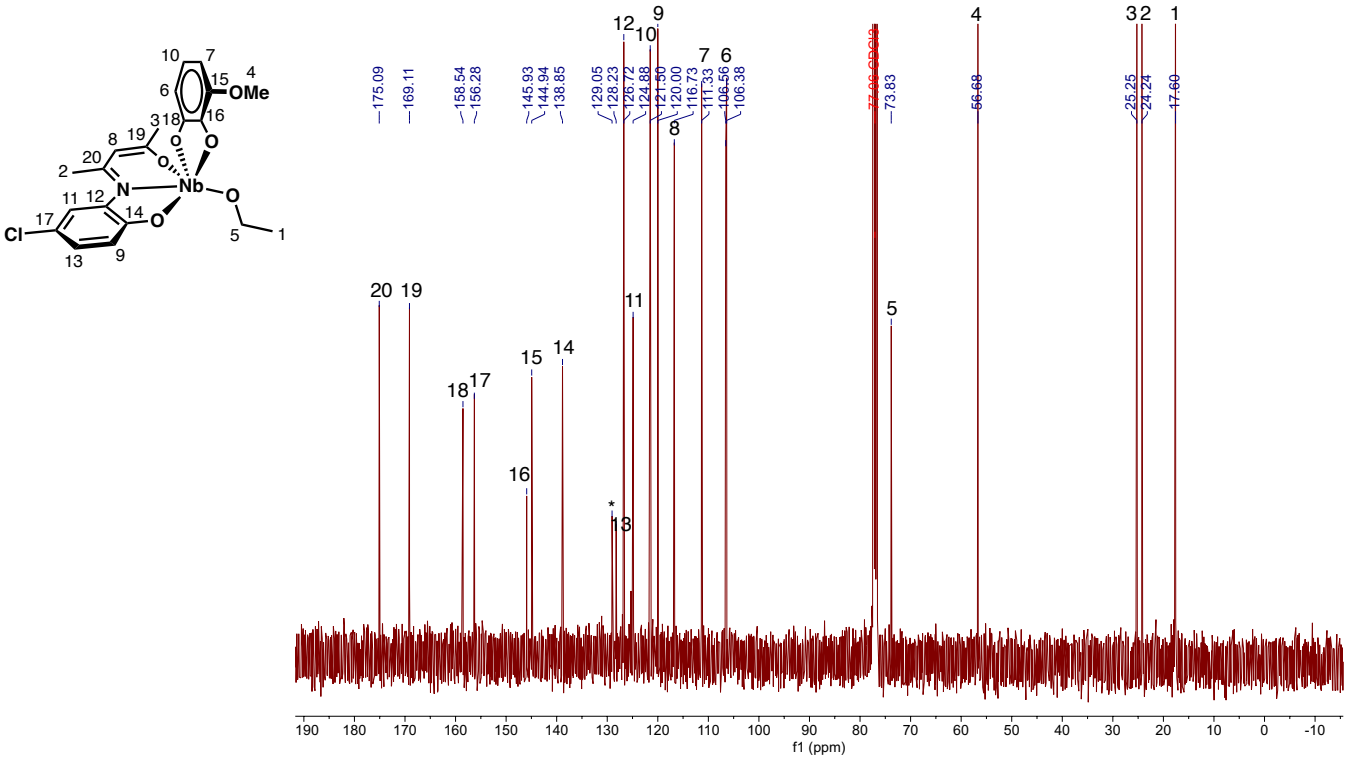

Figure S46. $^{13}C\{^{1}H\}$ NMR (101 MHz, 293 K) spectrum of **C-3OMe** in $CDCl_3$. *Trace toluene.

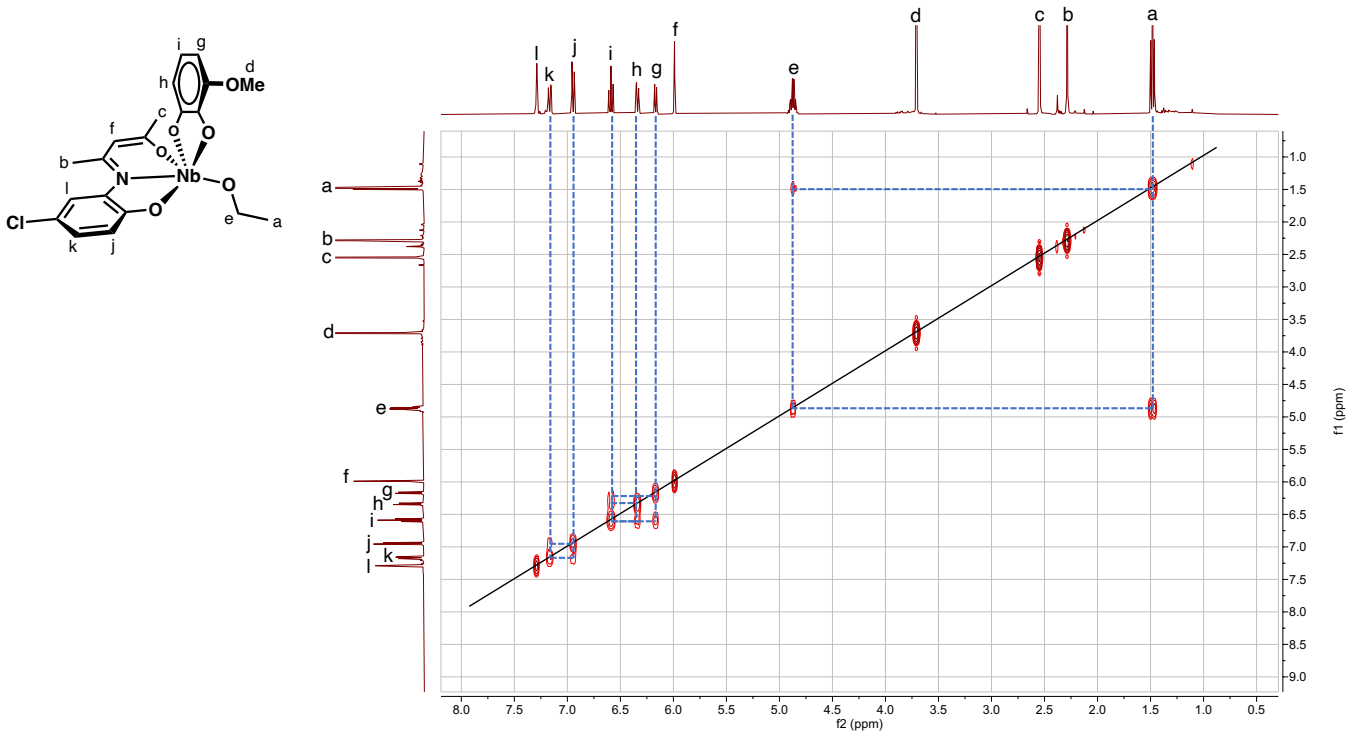

Figure S47. COSY NMR (293 K) spectrum of **C-3OMe** in $CDCl_3$.

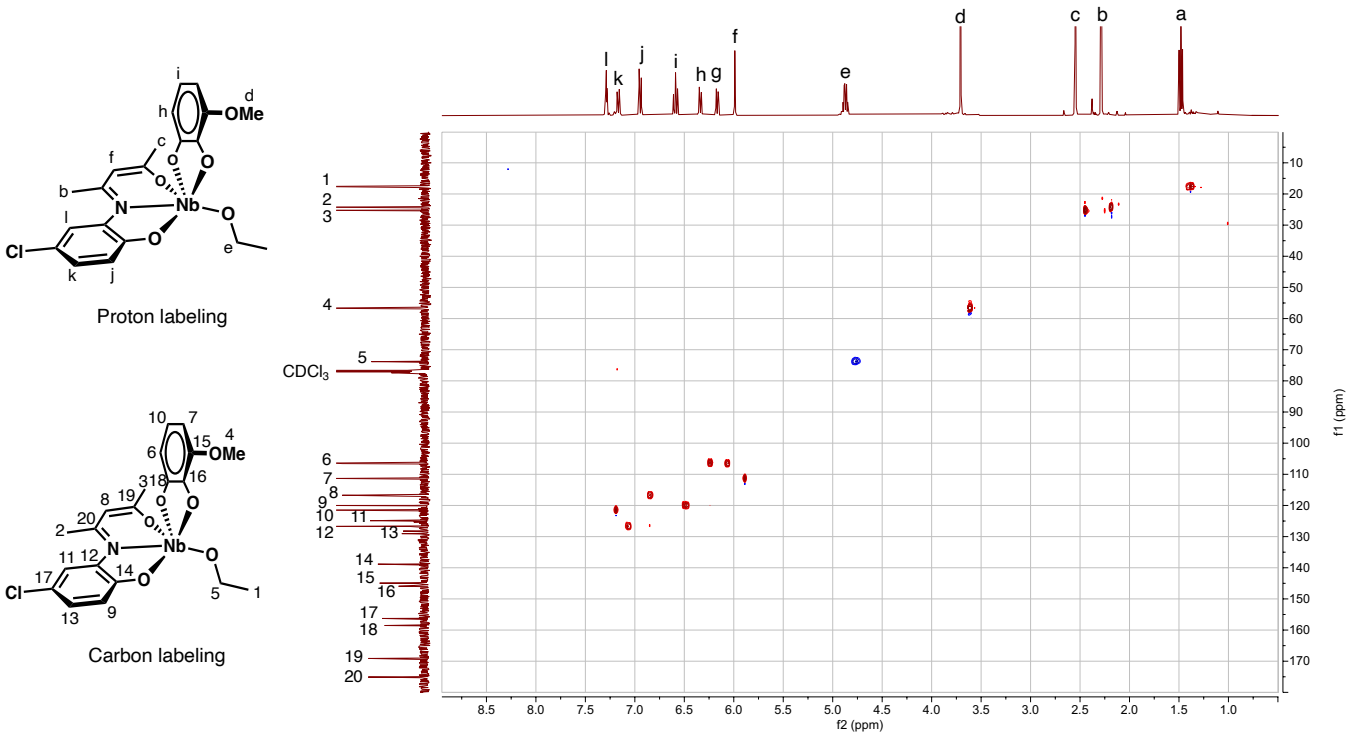

Figure S48. HSQC NMR (293 K) spectrum of **C-3OMe** in $CDCl_3$.

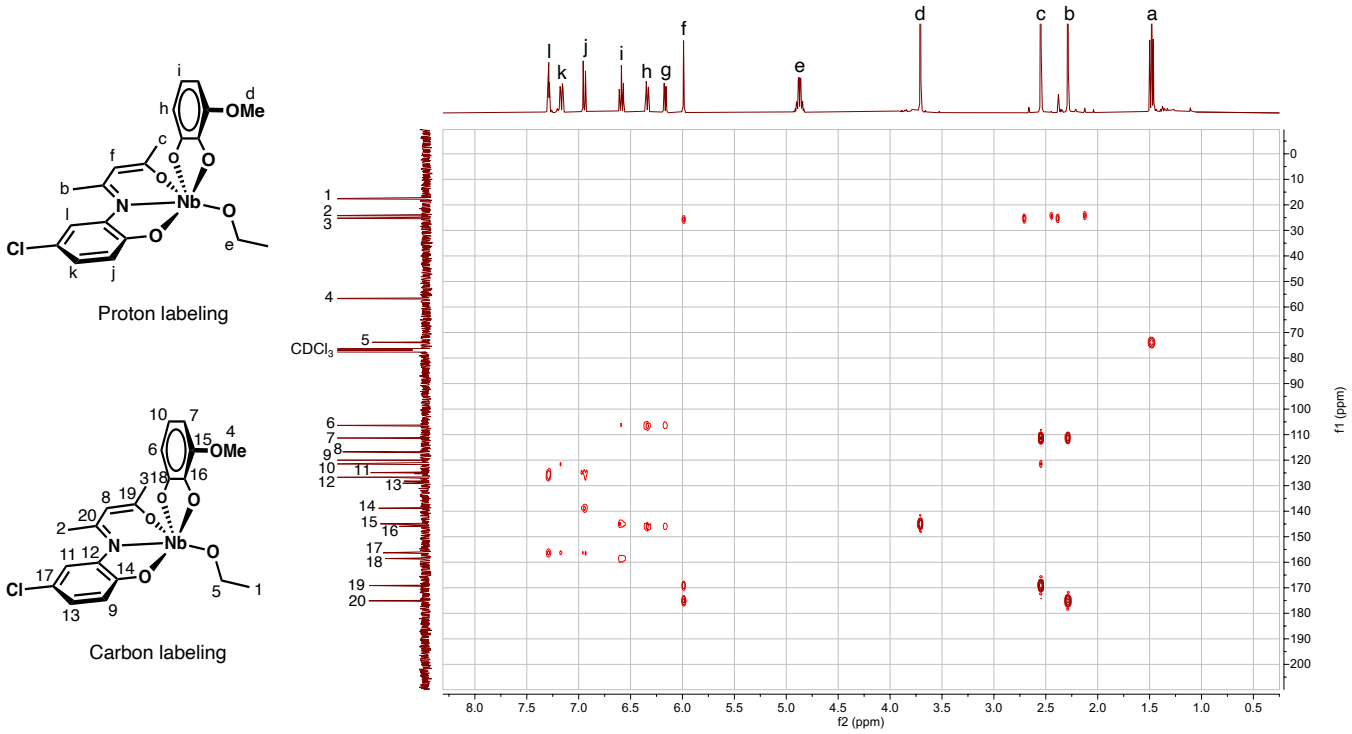

Figure S49. HMBC NMR (293 K) spectrum of **C-3OMe** in $CDCl_3$.

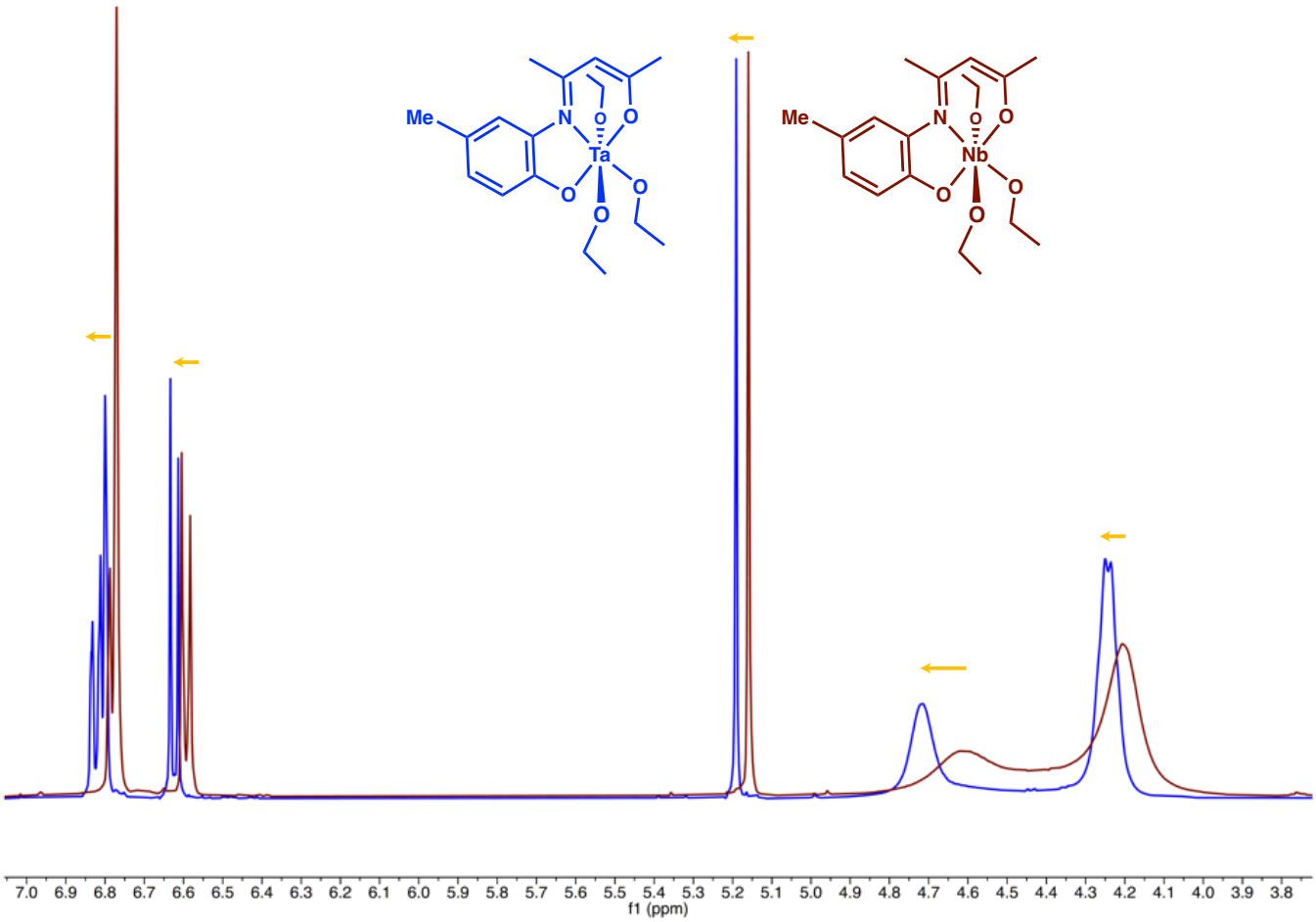

Figure S50. Selected region of ^{1}H NMR for **I-1** (red) and **I-2** (blue) showing a down field shift.

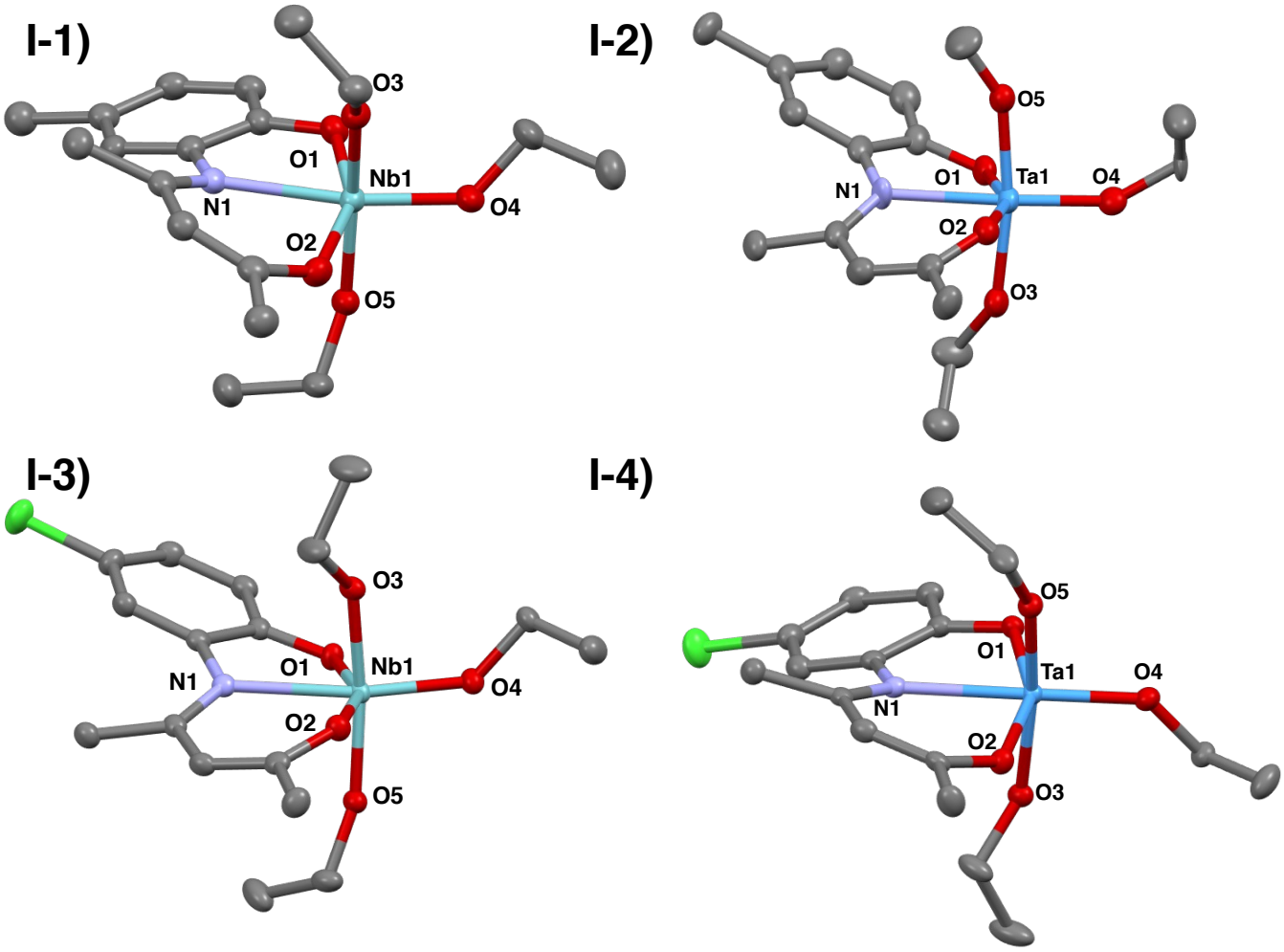

Figure S51. Thermal ellipsoid plots drawn at 50% probability of crystal structures **I-1** – **I-4**. In all cases only one of two molecules from the asymmetric unit are shown. Hydrogen atoms have been excluded for clarity. Niobium = teal, tantalum = bright blue, chlorine = green, nitrogen = dark blue, oxygen = scarlet, carbon = gray.

Bond	I-1		I-2		I-3		I-4	
Axial Ethoxide								
M–O_{Ax}	1.889(3)	1.901(4)	1.915(8)	1.899(7)	1.908(2)	1.909(2)	1.919(2)	1.883(2)
M–O_{Ax}	1.889(3)	1.897(4)	1.906(8)	1.905(8)	1.876(2)	1.878(2)	1.885(2)	1.917(2)
Equatorial Ethoxide								
M–O_{Eq}	1.918(3)	1.896(3)	1.883(7)	1.917(8)	1.901(2)	1.900(2)	1.904(2)	1.902(2)
KI Ligand								
M–N	2.293(3)	2.281(4)	2.273(8)	2.285(8)	2.291(2)	2.298(2)	2.277(2)	2.282(2)
M–O_{Ph}	1.961(4)	1.994(3)	1.988(7)	1.966(7)	1.980(2)	1.983(2)	1.978(2)	1.982(2)
M–O	2.038(4)	1.901(4)	1.998(7)	2.041(8)	2.023(2)	2.020(2)	2.016(2)	2.010(2)

Table S1. Selected metal-ligand bond distances (Å) for both molecules present in the asymmetric unit of **I-1** – **I-4**.

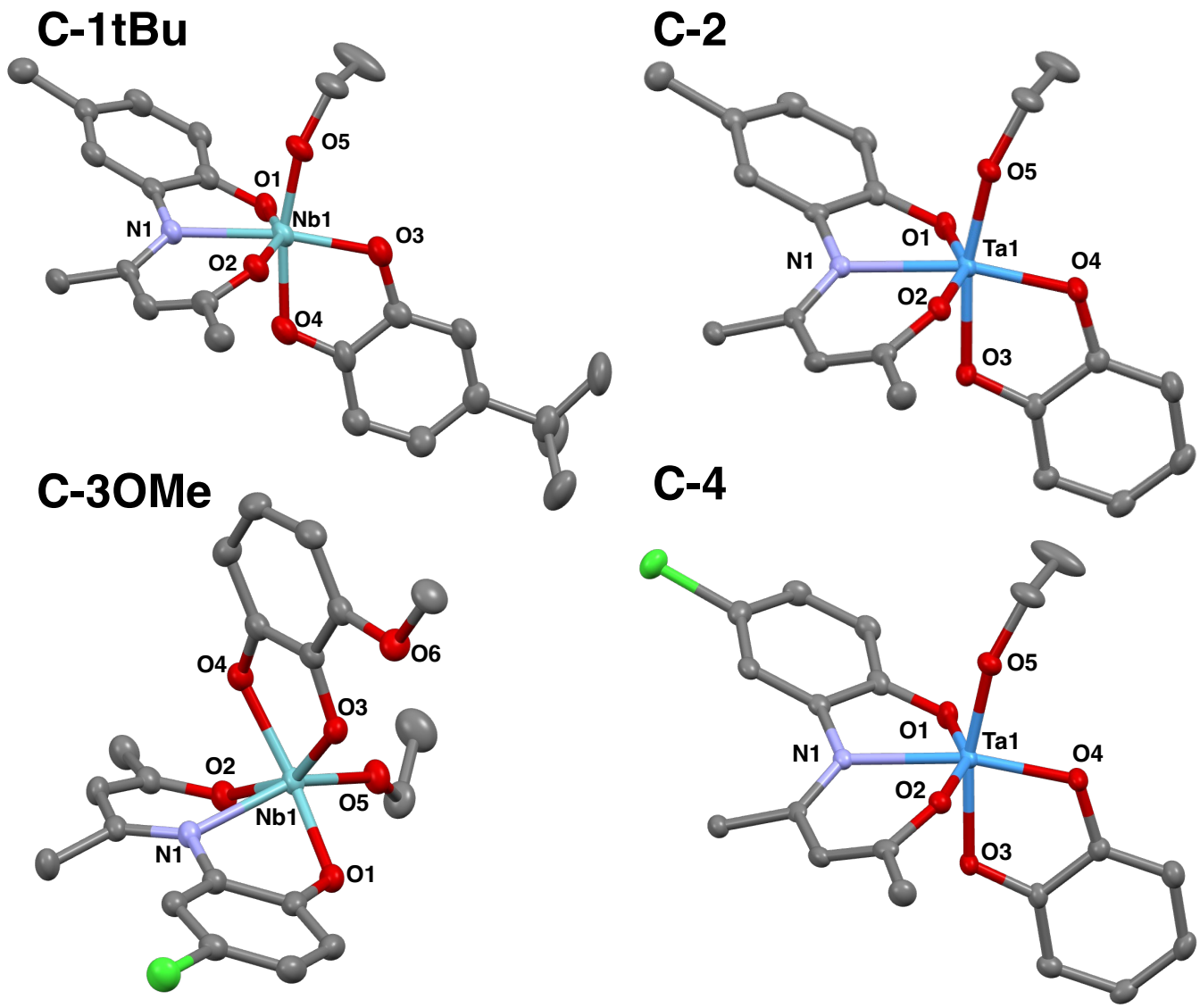

Figure S52. Thermal ellipsoid plots drawn at 50% probability of crystal structures **C-1tBu**, **C-2**, **C-3OMe**, and **C-4**. Hydrogen atoms have been excluded for clarity. Niobium = teal, tantalum = bright blue, green = chlorine, nitrogen = dark blue, oxygen = scarlet, carbon = gray.

Bond	C-1tBu	C-2	C-3OMe	C-4
		Catechol Phenoxides		
M–O_{Cat}	1.990(5)	1.976(2)	1.991(2)	1.971(2)
M–O_{Cat}	2.006(4)	2.011(2)	2.000(3)	2.007(2)
		Ethoxide		
M–O	1.843(4)	1.848(2)	1.867(2)	1.853(2)
		KI Ligand		
M–N	2.236(5)	2.218(2)	2.232(2)	2.220(2)
M–O_{Ph}	1.975(3)	1.968(2)	1.979(3)	1.977(2)
M–O	1.984(3)	1.977(2)	1.981(2)	1.974(2)

Table S2. Selected metal-ligand bond distances (Å) for **C-1tBu**, **C-2**, **C-3OMe**, and **C-4**.

Table S3: Crystallographic Details

	I-1	I-2	I-3	I-4
Chemical formula	$C_{18}H_{28}NNbO_5$	$C_{18}H_{28}NO_5Ta$	$C_{17}H_{25}ClNNbO_5$	$C_{17}H_{25}ClNO_5Ta$
M_r	431.32	519.36	451.74	539.78
Crystal system, space group	Monoclinic, *Cc*	Monoclinic, *Cc*	Monoclinic, $P2_1/n$	Monoclinic, $P2_1/n$
Temperature (K)	100	100	100	100
a (Å)	30.4282 (3)	30.4758 (4)	13.4876 (2)	13.5019 (1)
b (Å)	8.1140 (1)	8.1159 (1)	13.0436 (2)	13.0675 (2)
c (Å)	15.9970 (1)	16.0060 (3)	22.1841 (3)	22.1817 (2)
α (°)	90	90	90	90
β (°)	98.458 (1)	98.429 (1)	94.066 (1)	94.028 (1)
γ(°)	90	90	90	90
V (Å^3)	3906.61 (7)	3916.14 (10)	3892.96 (10)	3903.99 (8)
Z	8	8	8	8
Radiation type	Cu *K*a	Cu *K*a	Cu *K*a	Cu *K*a
μ (mm^{-1})	5.25	10.59	6.53	11.88
Crystal size (mm)	0.22 × 0.08 × 0.06	0.19 × 0.10 × 0.07	0.18 × 0.14 × 0.06	0.15 × 0.05 × 0.04
Diffractometer	XtaLAB Synergy, Single source at home/near, HyPix3000	XtaLAB Synergy, Single source at home/near, HyPix3000	XtaLAB Synergy, Single source at home/near, HyPix3000	XtaLAB Synergy, Single source at home/near, HyPix3000
Absorption correction[4]	Multi-scan *CrysAlis PRO* 1.171.41.110a	Multi-scan *CrysAlis PRO* 1.171.41.110a	Multi-scan *CrysAlis PRO* 1.171.41.110a	Multi-scan *CrysAlis PRO* 1.171.41.110a
T_{min}, T_{max}	0.742, 1.000	0.510, 1.000	0.634, 1.000	0.281, 1.000
No. of measured, independent and observed [$I > 2s(I)$] reflections	36703, 6259, 6106	35982, 6422, 6186	29938, 7048, 6137	64517, 7080, 6356
R_{int}	0.044	0.065	0.054	0.043
R [$F^2 > 2s(F^2)$], $wR(F^2)$, S	0.029, 0.074, 1.06	0.033, 0.085, 1.11	0.030, 0.080, 1.08	0.021, 0.054, 1.04
No. of reflections	6259	6422	7048	7080
No. of parameters	463	463	462	461
No. of constraints	2	2	0	0
H-atom treatment	H-atom parameters constrained	H-atom parameters constrained	H-atom parameters constrained	H-atom parameters constrained
$\Delta\rho_{max}$, $\Delta\rho_{min}$ (e Å^{-3})	0.68, -0.66	1.23, -0.72	0.64, -0.91	1.07, -1.02
Absolute Structure Parameter[9]	-0.033 (6)	-0.047 (11)	–	–

Tables have been adapted with the help of IUCr's online publishing tools.[10]

Table S4: Crystallographic Details

	C-1tBu	C-2	C-3OMe	C-4
Chemical formula	$C_{24}H_{30}NNbO_5$	$C_{20}H_{22}NO_5Ta$	$C_{20}H_{21}ClNNbO_6$	$C_{19}H_{19}ClNO_5Ta$
M_r	505.40	537.33	499.74	557.75
Crystal system, space group	Monoclinic, *I*2/*a*	Monoclinic, $P2_1/n$	Triclinic, *P*-1	Monoclinic, $P2_1/n$
Temperature (K)	100	100	120	111
a (Å)	20.5797 (4)	15.1648 (2)	7.93594 (17)	15.1854 (2)
b (Å)	7.4688 (2)	7.7301 (1)	11.4858 (2)	7.6946 (1)
c (Å)	31.9583 (9)	16.3269 (2)	12.4086 (2)	16.3573 (2)
α (°)	90	90	115.7499 (18)	90
β (°)	108.275 (3)	95.783 (1)	90.3226 (17)	95.785 (1)
γ(°)	90	90	91.8519 (16)	90
V (Å^3)	4664.4 (2)	1904.19 (4)	1017.95 (4)	1901.54 (4)
Z	8	4	2	4
Radiation type	Cu *K*a	Cu *K*a	Cu *K*a	Cu *K*a
μ (mm^{-1})	4.49	10.92	6.36	12.23
Crystal size (mm)	0.11 × 0.07 × 0.05	0.22 × 0.17 × 0.07	0.16 × 0.05 × 0.05	0.05 × 0.04 × 0.04
Diffractometer	XtaLAB Synergy, Single source at home/near, HyPix3000	XtaLAB Synergy, Single source at home/near, HyPix3000	XtaLAB Synergy, Single source at home/near, HyPix3000	XtaLAB Synergy, Single source at home/near, HyPix3000
Absorption correction[4]	Multi-scan *CrysAlis PRO* 1.171.41.110a	Multi-scan *CrysAlis PRO* 1.171.41.110a	Gaussian *CrysAlis PRO* 1.171.41.110a	Multi-scan *CrysAlis PRO* 1.171.41.110a
T_{min}, T_{max}	0.871, 1.000	0.401, 1.000	0.860, 1.000	0.860, 1.000
No. of measured, independent and observed [$I > 2s(I)$] reflections	15375, 4223, 3329	19529, 3443, 3278	19633, 3682, 3393	36004, 3459, 3215
R_{int}	0.061	0.037	0.056	0.045
$R[F^2 > 2s(F^2)]$, $wR(F^2)$, S	0.063, 0.172, 1.01	0.021, 0.050, 1.06	0.034, 0.093, 1.05	0.017, 0.040, 1.05
No. of reflections	4223	3443	3682	3459
No. of parameters	287	248	266	248
No. of constraints	0	0	0	0
H-atom treatment	H-atom parameters constrained	H-atom parameters constrained	H-atom parameters constrained	H-atom parameters constrained
$\Delta\rho_{max}$, $\Delta\rho_{min}$ (e Å^{-3})	3.17, -1.04	0.72, -0.87	0.95, -0.97	0.41, -0.56

Tables have been adapted with the help of IUCr's online publishing tools.[10]

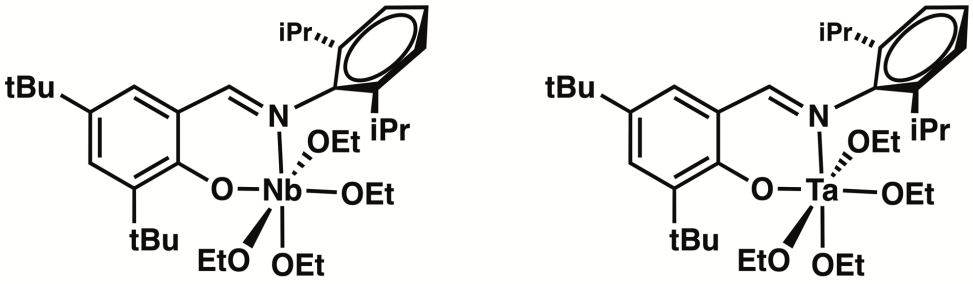

Catalyst I **Catalyst II**

Figure S53. Previously reported[2] catalyst structures used for comparison in Table 1.

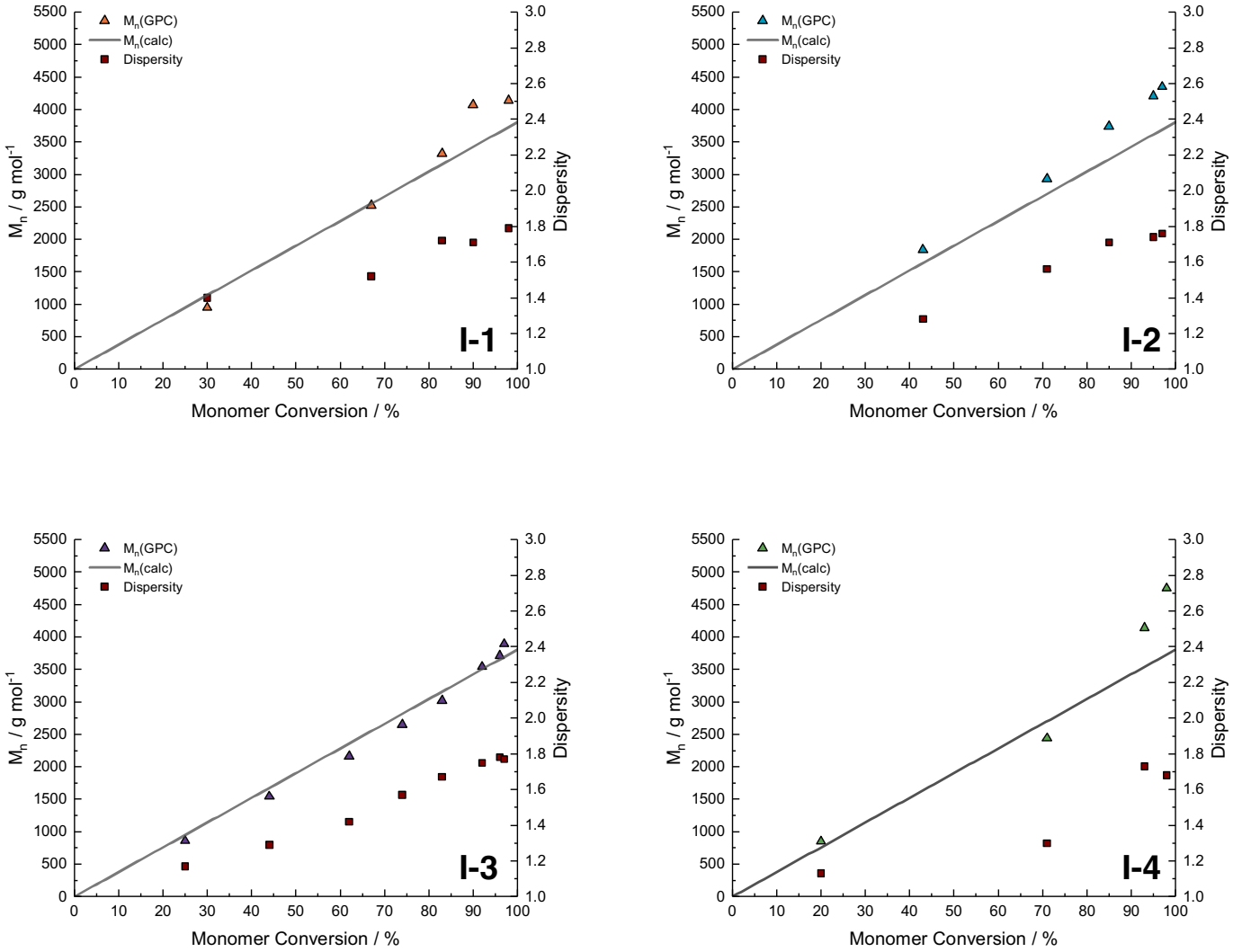

Figure S54. M_n(GPC), M_n(calc) for three initiators and dispersity vs monomer conversion. M_n(GPC) has been corrected by a factor of 0.56.[3]

$M_n(calc) = [114.14\ g\ mol^{-1} \times ([CL]/[catalyst]) \times (Conv\ \% / 100)]\ / 3\ Initiators$

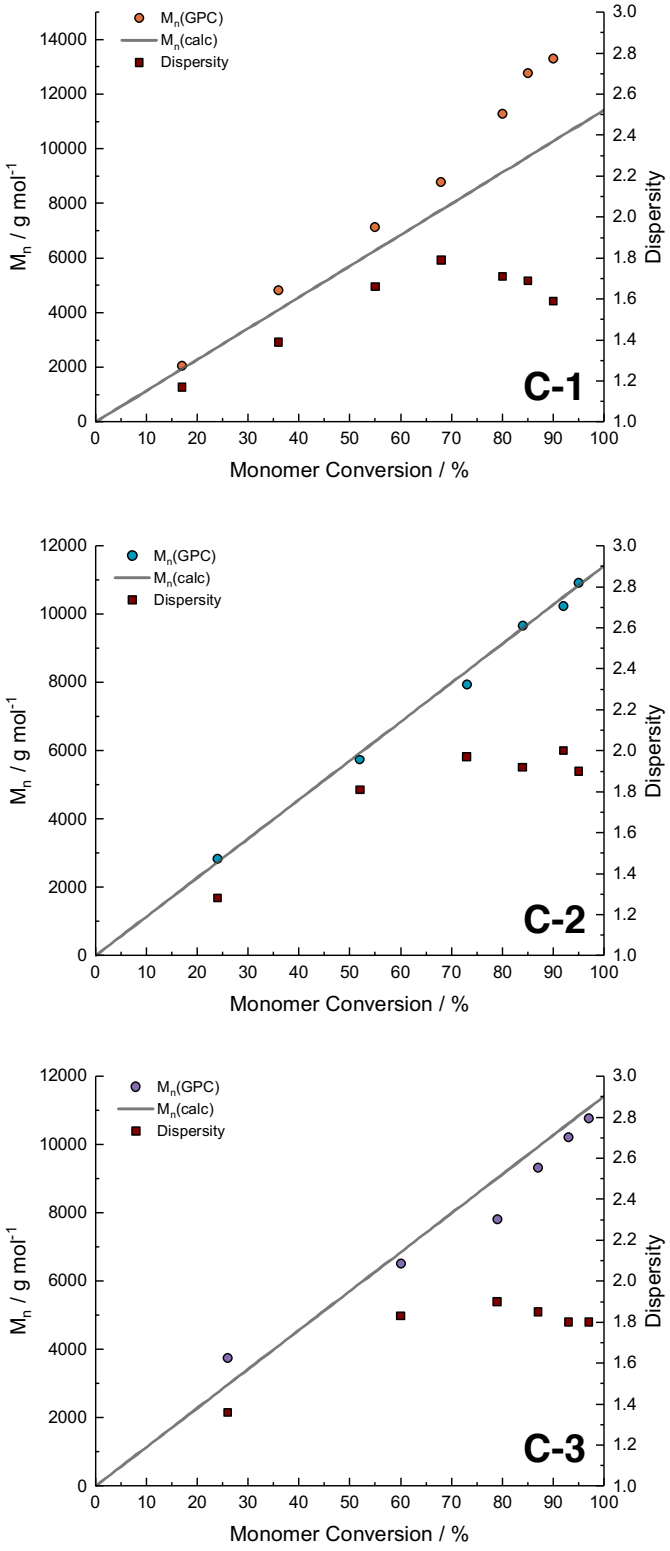

Figure S55. M_n(GPC), M_n(calc) for one initiator and dispersity vs monomer conversion. M_n(GPC) has been corrected by a factor of 0.56.[3]

$M_n(calc) = [114.14\ g\ mol^{-1} \times ([CL]/[catalyst]) \times (Conv\ \% / 100)]\ /\ 1\ Initiator$

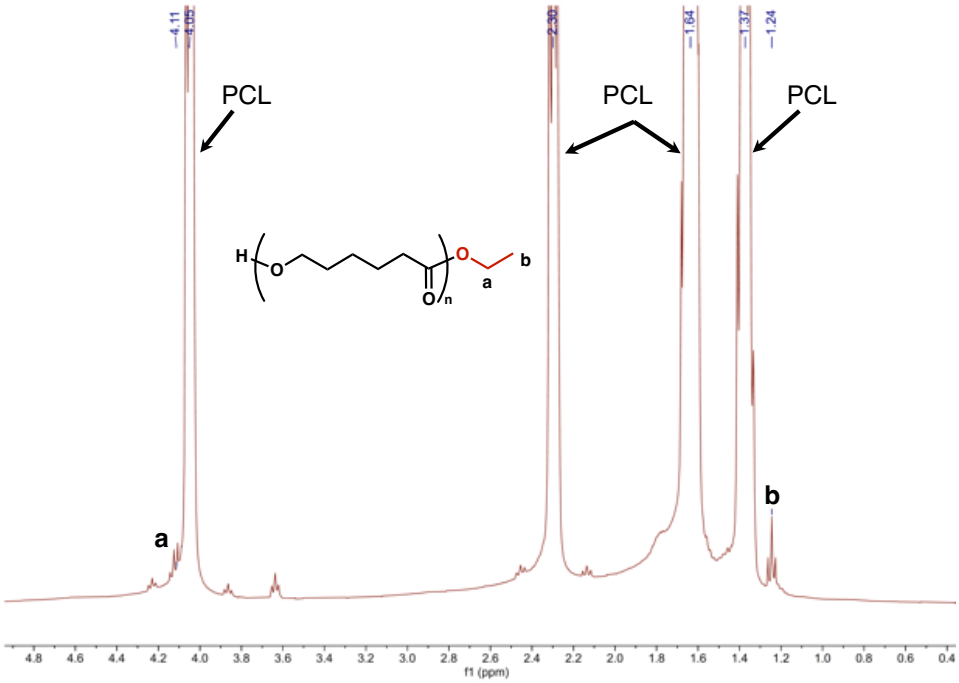

Figure S56. Selected region of a ^{1}H NMR showing the end group of purified PCL taken from the final kinetic timepoint of **C-3.**

References

1. C. C. Y. Seo, M. Ahmed, A. G. Oliver and C. B. Durr, *Inorg. Chem.*, 2021, **60**, 19336–19344.
2. A. S. Plaman and C. B. Durr, *ACS Omega*, 2022, **7**, 23995–24003.
3. M. Save, M. Schappacher and A. Soum, *Macromol. Chem. Phys.*, 2002, **203**, 889–899.
4. Oxford Diffraction, CrysAlisPRO Agilent Technologies UK Ltd, Yarnton, England.
5. G. M. Sheldrick, *Acta Crystallogr. Sect. Found. Adv.*, 2015, **71**, 3–8.
6. G. M. Sheldrick, *Acta Crystallogr. Sect. C Struct. Chem.*, 2015, **71**, 3–8.
7. O. V. Dolomanov, L. J. Bourhis, R. J. Gildea, J. a. K. Howard and H. Puschmann, *J. Appl. Crystallogr.*, 2009, **42**, 339–341.
8. H. Peng, Z. Zhang, R. Qi, Y. Yao, Y. Zhang, Q. Shen and Y. Cheng, *Inorg. Chem.*, 2008, **47**, 9828–9835.
9. S. Parsons, H. D. Flack and T. Wagner, *Acta Crystallogr. Sect. B Struct. Sci. Cryst. Eng. Mater.*, 2013, **69**, 249–259.
10. CIF publishing tools, https://publcif.iucr.org/publcif.php, (accessed March 17, 2022).